A SIMPLIFIED ANALYTICAL APPROACH FOR THE STRENGTH OF LONGITUDINALLY FRAMED VESSELS AND THEIR COMPONENTS.

MOHAMED BELKAID B.Sc

SUBMITTED AS A THESIS FOR THE DEGREE OF
MASTER OF SCIENCE
IN ENGINEERING

DEPARTMENT OF NAVAL ARCHITECTURE AND OCEAN ENGINEERING
UNIVERSITY OF GLASGOW

To my wife, mother, father, brothers and sisters.

Acknowledgements

This work was carried out at the Department of Naval Architecture and Ocean Engineering, University of Glasgow.

I would like to thank my supervisor Professor D. Faulkner, Head of the Department of Naval Architecture and Ocean Engineering, for his valuable guidance, help, advice and support throughout the project.

I would like also to thank Mr D.M. warwick, for his valuable help.

I would like to take this opportunity of acknowledging, with gratitude, the help and encouragement of Dr. R.M. Cameron.

In addition, thanks are due to members of ARE, and in particular Dr. C.S. Smith, in providing the finite element programs.

Finally, I would like to thank the Algerian Government who, through the Ministry of High Education, provided me with the financial support to complete this thesis.

M. Belkaid

July 1989

Author's statement:

All the material in this thesis is original except where reference is made to other sources.

CONTENTS

page No

Acknowledgements i
Contents ii
Notation v
List of figures viii
List of tables xi
Summary 1
Abstract 3
Introduction 4
CHAPTER ONE: REVIEW AND THEORY 5
1.1 Unstiffened panels 5
1.1.1 Introduction and Review 5
1.1.1.1 Theory 5
1.1.1.2 Tests 6
1.1.2 Buckling of plate elements 6
1.1.2.1 Effect of material and geometrical parameters 8
1.1.2.1.1 Residual stress 8
1.1.2.1.2 Initial distortion 8
1.1.2.1.3 Boundary conditions 8
1.1.2.1.4 Plate aspect ratio 8
1.2 Stiffened panels 9
1.2.1 Introduction and review 9
1.2.2 Tests 9
1.2.3 Stiffened plate model 10
1.2.3.1 Introduction 10
1.2.3.2 Beam-column approach 11
1.2.4 Effect of stiffened panel parameters 12
1.2.4.1 Plate slenderness 12
1.2.4.2 Initial plate deformation 12
1.2.4.3 Compressive residual stress 12
1.2.4.4 Column slenderness 12
1.2.4.5 Initial column deflection 12
1.2.4.6 Stiffener to plate area ratio 12
1.2.5 Failure modes 13

CHAPTER TWO : THE FINITE ELEMENT PROGRAM 16
2.1 General aspects of the program 16
2.2 Assumptions 17
2.3 Numerical procedure 17

CHAPTER THREE : PARAMETRIC STUDIES 21
3.1 Introduction 21
3.2 Stiffened panel parameters 21
3.2.1 Plate slenderness 21
3.2.2 Column slenderness 21
3.2.3 Plate residual stress and initial distortion 22
3.2.4 Stiffener initial distortion 22
3.2.5 Summary of parameters 22
3.3 Fixed load position 23
3.4 Effect of stiffened panel parameters 23
3.4.1 Effect of plate slenderness 23
3.4.2 Effect of column slenderness 24
3.4.3 Effect of residual stress and initial distortion 25
3.4.4 Effect of stiffener initial distortion 26
3.4.5 Effect of stiffener to plate area ratio 26
3.4.6 Effect of stiffener residual stress 27

CHAPTER FOUR : THE ANALYTICAL APPROACH 60
4.1 Introduction 60
4.2 Least squares technique 60
4.3 The analytical approach 61
4.3.1 Parametric analysis 61
4.3.2 The derived expressions for the ultimate strength 62
4.3.2.1 Effect of other parameters 64
4.3.2.2 Ultimate strain corresponding to maximum strength 65
4.3.3 Post-buckling modelling 67
4.3.3.1 Introduction 67
4.3.3.2 Unloading strength path 67
4.3.3.3 Loss of plate stiffness before collapse 68
4.4 Variables governing the modelling 70
4.4.1 Plate slenderness 70
4.4.2 Column slenderness 70
4.4.3 Plate residual stress and initial distortion 71
4.4.4 Stiffener initial distortion 72
4.4.5 Eccentricity of the applied load 72

CHAPTER FIVE : CORRELATION WITH TEST AND NUMERICAL RESULTS 78
5.1 Maximum load capacity 78
5.1.1 Correlation with test results 78
5.1.1.1 Manchester tests 78

5.1.1.2 RN College tests 79
5.1.1.3 Imperial college tests 79
5.1.1.4 ARE tests 80
5.2 Post-buckling strength 81
5.2.1 Test results 81
5.2.2 Numerical results 81
5.2.2.1 Correlation with finite element method 81
5.2.2.2 Correlation with dynamic relaxation technique 82

CHAPTER SIX : HULL GIRDER LONGITUDINAL STRENGTH 110

6.1 Introduction and review 110
6.2 Hull failure versus component failure 111
6.3 Failure modes 112
6.3.1 Plate instability 113
6.3.2 Inter-frame flexural buckling 113
6.3.3 Stiffener flexural tripping 114
6.3.4 Overall grillage instability 115
6.4 Numerical procedure 115
6.4.1 Introduction 115
6.4.2 Modelling of the cross-section 115
6.4.3 Incremental procedure 116
6.5 Results and comparison 117
6.5.1 Correlation with test results 117
6.5.1.1 Models of Dowling et al 117
6.5.1.2 Models of Reckling 118
6.5.2 Correlation with numerical results 119
6.5.2.1 ARE results 119
6.5.2.2 USAS finite element program results 120

CHAPTER SEVEN : CONCLUSIONS 137
7.1 General discussion and future developments 137

REFERENCES 140

NOTATION

b Plate width.

t Plate thickness.

b_f Flange width.

t_f Flange thickness.

h_w Web depth.

d Stiffener depth

t_w Web thickness.

A Cross-section of the plate-stiffener combination.

A_p Cross-section of the plating.

A_s Cross-section of the stiffener.

y_n Position of the neutral axis of the combined cross-section from the far surface of the plating.

L Length of the unsupported span

I Moment of inertia of the combined cross-section.

r Radius of gyration of the combined cross-section.

Δ_o Stiffener initial distortion.

Δ_{o+} Upward column initial distortion.

Δ_{o-} Downward column initial distortion.

δ_o Plate initial deformation.

μ_o Term representing magnitude of residual stress and initial distortion.

α Stiffener to plate area ratio ($\alpha = \frac{A_s}{b\,t}$)

w Flexural deformation.

u Extensional deformation.

$\{\delta\}$ Column matrix of incremental nodal displacements.

$\{R\}$ Column matrix representing applied loads.

$[K_G]$ Geometrical stiffness matrix representing the destabilising influence of axial forces in frame elements.

$[K]$ Stiffness matrix representing the axial and flexural stiffness of frame elements.

h_w/t_w Web slenderness.

K Non-dimensional plate initial distortion ($K = \frac{\delta_o}{t\ \beta^2}$)

W_o Non-dimensional stiffener initial distortion($W_o = \frac{\Delta_o}{L} 10^{+3}$)

E_c Eccentricity of the applied load.

K_{st} Tripping correction factor.

R_W Stiffener initial distortion correction factor.

R_α Stiffener to plate area ratio correction factor.

σ_{yp} Yield stress of the plating.

σ_{ys} Yield stress of the stiffener.

σ_e Combined yield stress :

$$\sigma_e = \frac{\sigma_{yp} A_p + \sigma_{ys} A_s}{A}$$

ε_y Yield strain.

σ_{cr} Euler critical buckling stress.

E Young modulus.

σ_r Compressive residual stress in the plating.

β Plate slenderness :

$$\beta = \frac{b}{t}\sqrt{\frac{\sigma_{yp}}{E}}$$

λ Column slenderness :

$$\lambda = \frac{L}{\pi r}\sqrt{\frac{\sigma_e}{E}}$$

σ_u Average ultimate stress.

ε_u Strain corresponding to ultimate stress.

Φ Ultimate load factor :

$$\Phi = \frac{\sigma_u}{\sigma_e}$$

Ψ Ultimate strain factor :

$$\Psi = \frac{\varepsilon_u}{\varepsilon_y}$$

E^- Non-dimensional post-ultimate tangentional stiffness.

Φ_r Non-dimensional residual strength.

Ψ_r Non-dimensional strain corresponding to residual strength.

Ψ_s Non-dimensional strain at which the panel starts to exhibit loss of stiffness.

k Factor defined as $k = \Psi_s / \Psi$

f Approximated function.

p_j Assumed polynomials for the approximation.

a_j Numerical coefficients

MP Number of assumed polynomials

N Number of sets of data.

φ_k Current cumulative curvature of the hull cross-section.

$\Delta\varphi_k$ Current incremental curvature

ε_{ik} Current cumulative strain of the i^{th} component of the hull cross-section.

$\Delta\varepsilon_{ik}$ Current incremental strain of the i^{th} component of the hull cross-section.

σ_{ik} Current cumulative stress of the i^{th} component of the hull cross-section.

$\Delta\sigma_{ik}$ Current incremental stress of the i^{th} component of the hull cross-section.

A_i The area of the i^{th} component of the hull cross-section.

Z_i Distance from the centroid of the i^{th} component to the base axis.

Z_{Nk} Distance from the instantinious neutral axis of the hull cross-section to the base axis.

$(EI)_{Hk}$ Current rigidity of the hull cross-section.

M_k Current cumulative vertical moment of the hull girder.

ΔM_k Current incremental vertical moment of the hull girder.

M_P Fully plastic vertical moment of the hull girder.

M_u Ultimate longitudinal moment.

NE Number of elements of the hull cross-section

List of figures:

Figure No	Title	Page No
1.1	Load-shortening curves for square plates under uni-axial compression	14
1.2	Load-shortening curves for rectangular plates under uni-axial compression	15
2.1	Beam-column modelling	19
2.2	Residual stress modelling	20
3.1.a	Ultimate load-slenderness curves: Shifting of the applied load	27
3.1.b	Ultimate load-slenderness curves: Shifting of the applied load	28
3.1.c	Ultimate load-slenderness curves: Shifting of the applied load	29
3.1.d	Ultimate load-slenderness curves: Shifting of the applied load	30
3.2.a	Ultimate strength-slenderness curves	31
3.2.b	Ultimate strength-slenderness curves	32
3.2.c	Effect of column slenderness	33
3.3.a	Ultimate strength-slenderness curves: Effect of residual stress and initial distortion	34
3.3.b	Ultimate strength-slenderness curves: Effect of residual stress and initial distortion	35
3.4	Effect of column initial distortion	36
3.5.a	Ultimate load-slenderness curves: Effect of stiffener to plate area ratio	37
3.5.b	Ultimate load-slenderness curves: Effect of stiffener to plate area ratio	38
3.5.c	Ultimate load-slenderness curves: Effect of stiffener to plate area ratio	39
3.6.a	Load-shortening curves: Effect of residual stress and initial distortion	40
3.6.b	Load-shortening curves: Effect of residual stress and initial distortion	41
3.6.c	Load-shortening curves: Effect of residual stress and initial distortion	42
3.6.d	Load-shortening curves: Effect of residual stress and initial distortion	43
3.6.e	Load-shortening curves: Effect of residual stress and initial distortion	44
3.6.f	Load-shortening curves: Effect of residual stress and initial distortion	45

3.7.a Stress-strain curves :
Effect of stiffener to plate area ratio 46
3.7.b Stress-strain curves :
Effect of stiffener to plate area ratio 47
3.8.a Stress-strain curves :
Effect of stiffener to plate area ratio 48
3.8.b Stress-strain curves :
Effect of stiffener to plate area ratio 49
3.9.a Stress-strain curves :
Effect of stiffener to plate area ratio 50
3.9.b Stress-strain curves :
Effect of stiffener to plate area ratio 51
3.10.a Stress-strain curves :
Effect of stiffener to plate area ratio 52
3.10.b Stress-strain curves :
Effect of stiffener to plate area ratio 53
3.10.c Stress-strain curves :
Effect of stiffener to plate area ratio 54
3.10.d Stress-strain curves :
Effect of stiffener to plate area ratio 55
3.11.a Stress-strain curves :
Effect of stiffener to plate area ratio 56
3.11.b Stress-strain curves :
Effect of stiffener to plate area ratio 57
3.12.a Stress-strain curves :
Effect of stiffener to plate area ratio 58
3.12.b Stress-strain curves :
Effect of stiffener to plate area ratio 59
4.1 Linear modelling of the stress-strain curves 75
4.2.a Stiffness of the combined plate-stiffener during post-buckling 76
4.4 Probability density distribution of plate slenderness in frigates and tankers 77
5.1.a Percentage error of results for 75 tests 98
5.1.b Percentage error of results for 75 tests 99
5.1.c Correlation with test results 100
5.2.a Unloading curves for test models:
Correlation with test results 101
5.2.b Unloading curves for test models:
Correlation with test results 102

5.2.c Unloading curves for test models:
Correlation with test results 103
5.3.a Unloading curves for stiffened panels:
Correlation with numerical results 104
5.3.b Unloading curves for stiffened panels:
Correlation with numerical results 105
5.3.c Unloading curves for stiffened panels:
Correlation with numerical results 106
5.3.d Unloading curves for stiffened panels:
Correlation with numerical results 107
5.4.a Unloading curves for stiffened panels :
Correlation with numerical results 108
5.4.b Unloading curves for stiffened panels:
Correlation with numerical results 109
6.1 Hull girder subdivision into elements 121
6.2 Models of Dowling et al (Cross section)..... 123
6.3 Model 2 of Dowling et al(Results) 124
6.4 Model 4 of Dowling et al (Results) 125
6.5 Models of Reckling (Cross-section)..... 127
6.6 Model 23 of Reckling (Results) 128
6.7 Model 31 of Reckling (Results) 129
6.8 Destroyer midship section 130
6.9 Moment-curvature curves for the destroyer 131
6.10.a Stress-strain for elements of the destroyer 132
6.10.b Stress-strain for elements of the destroyer 133
6.10.c Stress-strain for elements of the destroyer 134
6.11 Cross-section of tanker 135
6.12 Moment-curvature curves for the tanker 136

List of Tables:

Table No	Title	Page No
5.1.a	RN College tests: Geometrical and material details	83
5.1.a(Cont'd)	RN College tests: Geometrical and material details	84
5.1.a(Cont'd)	RN College tests: Geometrical and material details	85
5.1.a(Cont'd)	RN College tests: Geometrical and material details	86
5.1.b	RN College tests: Test and numerical results	87
5.1.b(Cont'd)	RN College tests: Test and numerical results	88
5.1.b(Cont'd)	RN College tests: Test and numerical results	89
5.1.b(Cont'd)	RN College tests: Test and numerical results	90
5.2.a	Manchester tests: Geometrical and material details	91
5.2.a(Cont'd)	Manchester tests: Geometrical and material details	92
5.2.b	Manchester tests: Test and numerical results	93
5.2.b(Cont'd)	Manchester tests: Test and numerical results	94
5.3.a	Imperial College tests: Geometrical and material details	95
5.3.b	Imperial College tests: Test and numerical results	96
5.4	ARE tests	97
6.1	Models 2 and 4 of Dowling et al.	122
6.2	Models 23 and 31 of Reckling	126

Summary

The aim of the research work presented in this thesis is to develop analytical equations for approximately modelling the collapse strength and post-ultimate behaviour of longitudinally stiffened plate panels under compressive loads. Using a parametric analysis, carried out with the aid of a finite element program, a simplified design approach is derived which includes the effects of geometrical and material parameters (including fabrication factors). Another purpose of the thesis is to demonstrate the close correlation that exists between the box girder strength and the maximum load capacity of its components. In order to refine this to determine the collapse moment of a ships hull girder, the load-shortening curves need to be established for panels forming parts of the cross-section so that post-buckling propagation through the whole cross-section can be allowed for. Correlation with box-girder and with tanker bending results is provided.

Chapter 1 presents a literature review and theory related to the stability of unstiffened and stiffened panels under uni-axial compression.

Chapter 2 outlines the main features of the finite element program [28] with the beam-column approach used during this work in order to allow a parametric analysis for the strength of longitudinally stiffened panels to be carried out.

In chapter 3, in order to investigate the effects of the geometrical and material parameters, a parametric study for the strength of stiffened panels subjected to axial compression is carried out. The analysis is based on the results of a numerical method. Parameters found to have a considerable effect on the strength and post-ultimate strength of the panel, were plate slenderness, column slenderness, plate residual stress and initial distortion and stiffener to plate area ratio. Of less significance were the effects of stiffener residual stress and initial distortion.

Chapter 4 contains the description of an approximate collapse model in terms of the geometrical and material parameters, developed using a parametric analysis derived with the aid of a finite element computer program.

Analytical expressions describing the collapse of stiffened plates, covering pre- and post-ultimate strength behaviour and accounting for all stiffened panel parameters, are derived using the results of the parametric analysis.

In chapter 5 the results obtained using the approximate model are compared with existing test results and with numerical results. The present approach shows good agreement with these. A mean error value of -1.7% and a standard deviation of 8.4% were found from comparisons with 75 tests.

Chapter 6 presents a simple method to derive the strength of longitudinally framed vessels using the models derived in chapter 4 for the strength and behaviour of the components used. The procedure is applied to some longitudinally stiffened box girders and good agreement is provided with tests and with numerical techniques. The results clearly show the strong correlation that exists between the hull girder strength and those of the components forming part of this girder.

Finally, chapter 7 draws some conclusions and outlines future possible developments. The results of the work can be directly used in ultimate strength design and for in-service assessments.

Abstract

A review of previous studies in stiffened and unstiffened plates is presented. A numerical method developed by Smith et al [28] for the analysis of stiffened panels under uni-axial loading is used. The analysis takes into account buckling and post-buckling behaviour of plate and stiffener elements. The thesis contains a description of this beam-column approach which uses an inelastic non-linear finite element technique.

A parametric study which includes the effects of plate slenderness, column slenderness, initial deformations, stiffener to plate area ratio and residual stresses is carried out. Using this parametric study, simplified analytical models for deriving the maximum compression strengths and post-buckling behaviour and strengths of a practical range of stiffened panels are derived.

The results are compared with existing numerical and experimental data.

This modelling derived for the strength and post-ultimate behaviour of longitudinally stiffened panels, under uni-axial compression loading, is used for estimating the ultimate longitudinal bending strength of some box girders.

Introduction:

Stiffened panels represent a major component of most marine steel structures. These elements are designed to provide watertightness and strength.

An optimum ship structural design requires a rational design procedure which is governed by safety and cost. A safe structure is related to certain failure modes cited as follows: Fracture, stability and yielding. Fracture is more concerned with strength at specified points, while stability is an overall behaviour.

Unlike the elastic response of a structure, the limit state analysis has been a more complicated task due mainly to the non-linear behaviour of the material. However, with the advent of high speed digital computers, the use of numerical techniques for the analysis of the behaviour of plates and stiffened panels under axial loading or combined axial-lateral loading has became the subject of a wide application [1] to [12] and [15] to [24].

Numerical methods, like finite element and dynamic relaxation, provided vital tools to tackle the plastic and post-ultimate strength of stiffened plates, accounting for initial imperfections and residual welding stresses.

The hull girder is an assembly of structural elements with different geometrical and material configurations. Under loading these elements may behave differently and realistic assessment of the structural response may involve various interactions of failure modes. This, however, is very complicated and the finite element method of three dimensional plate structures provides the more realistic idealisation of actual ship structures. Generally the use of such computer programs is very expensive and time-consuming, therefore frequent use of such programs is not economical. It is the purpose of the present thesis to propose a simplified analytical approach for the pre- and post-buckling of stiffened panels under axial loading, accounting for the effect of geometrical and material parameters. The design approach is based on a parametric study using a non-linear finite element program and test results. The procedure is used for the analysis and evaluation of the longitudinal strength of longitudinally framed box-girders.

CHAPTER 1:

Review and theory

1.1 Unstiffened Panels:

1.1.1 Introduction and review:

1.1.1.1 Theory:

Major marine structures consist mainly of steel plated structures which may represent more than 75% of the total steel weight. This indicates the important role that these elements play in structural behaviour. These components are connected by means of welding to provide watertightness and strength. As far as the strength of the structure is concerned, the behaviour of the plating depends upon the type of loading and is related to the possible modes of structural failure. These plate elements behave differently with different geometrical configurations and material parameters.

For unstiffened plates, various authors used numerical methods to predict the strength of plates under compressive loads. Unlike elastic analysis, plastic analysis, collapse and post-buckling behaviour require the use of the large deflection elasto-plastic theory for the strength of plates subjected to in-plane compressive loads.

Plate strength has been the interest of various researchers. Methods using energy principals [1], Ritz procedures [2], finite element analysis [3], and finite difference using dynamic relaxation [4], [5] have provided a good knowledge of the complicated behaviour of plates with initial deflected forms and residual stresses.

An extensive literature exists related to the use of incremental finite elements for the analysis of stability and strength of plates. Reference [3] cited a number of them from the early work related to the linear buckling problem to the geometric and material non-linearity adopting an incremental procedure in a modified Newton-Raphson approach. For the

analysis of large elasto-plastic deflections Crisfield [3] used a finite element method. In this work he outlined two approaches to allow for plasticity: "volume approach" using the Von-Mises criteria and the "area approach" using Illushin criteria.

Parametric studies [5], [6], [7] and [8] using these programs yielded valuable design curves (like those presented in references [28] and [30] and reproduced in Figs. 1.1 and 1.2), introducing the concept of strength beyond collapse and covering a practical range of plate slendernesses, initial distortions and residual stresses. Interpolation similar to the one in reference [9] may be used for determining the magnitude of strength parameters for different design values.

1.1.1.2 Tests:

Tests of plates have often encountered the problem of creating realistic boundary conditions at the unloaded edges. Although enormous effort has been given to this, various tests did not succeed in offering the appropriate boundary restraints, as noted by Davidson [10]. Ractliffe [12] used a " finger system" which served to test plates for simply and clamped edges and which were free to pull in, this however requires considerable care for the preparation of the plate edge. Edge preparation was avoided by Moxham's rig [13] for testing plates of uniform thickness. Bradfield [14] used Moxham's rig to test plates of varying thickness. A survey of the results of reputable test data is provided in reference [31]

1.1.2 Buckling of Plate elements:

The collapse of plates under in-plane loads is influenced by:

1. Plate slenderness (the width to thickness ratio b/t).
2. Type of loading.
3. Aspect ratio (the length to width ratio a/b).
4. Edge restraint.
5. Residual stresses.
6. Initial deformations.

For a square plate under uni-axial compression simply supported at the

loaded edges and free to pull in at the unloaded edges, the buckling mode shows three different behaviours depending on the plate slenderness:

1. Slender plates ($\beta > 2.4$ say):

The analysis of such plates reveals that the plate buckles elastically because the theoretical buckling stress is well below the yield stress of the material and also below the collapse stress. In consequence, the middle region of the plate moves away from the axial shortening imposed by the load. As a result, a greater portion of the load must be carried by the sides of the plate. This causes a non-uniformity in the distribution of the compressive stresses in the plating, but the plate is still able to carry further load and no collapse has yet occurred. The overall axial stiffness is reduced as due to the deflected shape of the buckled portion. As the load is increased further, the shirking of load in the middle region becomes significant and the maximum stress at the edges increases until it reaches the yield stress. Observations show that at this point the plate elements reach their maximum value referred to as "plate strength".

2. Moderate slenderness:

The buckling stress in this case ($1.4 \leq \beta \leq 2.4$ say) is nearly equal to the yield stress. Such plates reveal that an increase in load gives rise to a magnification of the initial distortion resulting in some reduction in stiffness and some local yielding and the stress is no longer uniform. Analyses show that collapse occurs when the average equivalent stress estimated by the Hencky-von Mises criterion reaches yield stress. The behaviour of the plating does not present noticeable preliminary buckling and the maximum strength is followed by a sharp reduction in load carrying capacity.

3. Stocky plates:

The elastic buckling stress is very high, initial distortion is smaller relative to the thickness and its magnification caused by increasing the load is less significant. Hence these plates can carry further increase of load to nearly equal to the squash load. Analysis indicates that there is no

apparent warning before the collapse. However, after the maximum load is reached, the load carrying capacity remains approximately constant up to $2\varepsilon_y$ (where ε_y is the yield strain).

1.1.2.1 Effect of material and geometrical parameters:

A fuller discussion of the subject appears recently in references [64] and [64].

1.1.2.1.1 Residual stress:

Residual stresses cause some reduction of compressive strength and stiffness over the range of strain $(\sigma_y - \sigma_r)/E$ to $2\varepsilon_y$. They accelerate yielding, cause greater shortening and generally remove the sharp drop in load beyond the peak.

1.1.2.1.2 Initial distortion:

Initial distortion generally have less effect on strength and stiffness than do residual stresses unless the initial distortions coincide with the lowest buckling mode. They reduce the strength and change the pattern of behaviour to a more gradual process with a less severe post-collapse load reduction. This effect is more pronounced for moderate plate slendernesses ($1.4 < \beta < 2.4$).

1.1.2.1.3 Boundary conditions:

The loaded edges are assumed to be simply supported in most of the analyses undertaken for plate elements in compression, because stiffeners generally offer only low torsional restraint on the plate edges.

For steel plates of low or medium b/t, concerning failure stress, it has been found [3], [7] that the difference between the condition where the unloaded edges are free to deflect in-plane and those where they remain straight is negligible. Plates with b/t of 80, had these difference no greater than 5% for example.

1.1.2.1.4 Plate aspect ratio (a/b):

The minimum critical stress occurs when the number of buckled half waves along the length of the plate is equal to (a/b). The critical aspect ratio into which practical plates buckle depends on the

magnitude of the initial deformation as well as the plate slenderness [4]. Results on the strength of plates, for aspect ratios close to unity are found to vary only within 1 or 2% [7].

1.2 Stiffened Panels:

1.2.1 Introduction and review:

A realistic assessment of stiffened panel strength can only be made if account is taken of plastic flow, initial geometric imperfections and residual stresses in addition to plate and column slendernesses.

The problem of post-buckling behaviour and ultimate loading must of course be closely related to the ultimate carrying capacity of the various plate elements between stiffeners and with the question of the effective plate width of the stiffener-plate column cross- section. The application of large deflection theories, for instance by Marguerre and Levy, were considered initially for plate element effectiveness but a more recent review has been made by Faulkner [31].

In reference [26] the authors used a finite element formulation to predict the strength of perfect and initially deflected stiffened panels under axial loading. Single span and two span beam-column analyses were introduced. Crisfield [27] presented a finite element modelling for the pre- and post-buckling strength of stiffened panels and pointed to the use of local (finite element) displacement functions rather than global functions. The method has been applied to the collapse of box-girder bridges.

1.2.2 Tests:

During test experiments some points should be considered:

1. Realistic boundary conditions.
2. Eccentricity of axial applied load.
3. Grillage of various spans.
4. Survey of initial distortions and measurement of residual stresses during the process of welding.
5. Control of applied load.

At Manchester [59], [60] tests were conducted to investigate the influence of a number of different parameters, for instance, flexural boundary constraint at the loaded edges, initial distortions, the use of intermittent welds and the eccentricity of applied loading. The panels were of single span and were free on the unloaded edges. The majority of the stiffeners were flat bars, continuous and intermittent welding were used. The tests included both fixed ends and pinned ends. The failure of these models generally occurred towards the stiffeners with little or no evidence of stiffener tripping.

At Imperial College tests (reference [34]) were carried out on stiffened panels supported laterally along all sides. The stiffeners were of an angle cross-section and were welded continuously to the plating.

At the Royal Naval College, Greenwich [65], 65 models of single bay construction were tested. The panels were simply supported on the unloaded edges and free to deflect out of plane on the loaded edges. Most of the models were stiffened by tee section girders, the rest having stiffeners of flat cross-section. All stiffeners were welded continuously to the plating.

1.2.3 Stiffened plate model:

1.2.3.1 Introduction

The early work carried out at Lehigh university by Ostapenko and Lee[25] on testing longitudinally stiffened plate panels (which were pin-ended not supported at sides and the end displacement was constant over the panel width) subjected to the combined action of uniform lateral loading and axial compression yielded the following conclusions:

(a) The panel behaved as a beam-column.

(b) The strength of the panels was governed by the strength of the plate.

(c) The axial plate strength was not materially affected by lateral loading.

The two first points are most important as far as the strength of the

panels under compressive load is concerned. Point (a) indicates the use of a beam-column modelling of the plate-stiffener combination for the analysis of stiffened panels, point (b) allows the importance of the effect of plate buckling and strength on the behaviour of the stiffened panel and the requirement for data from testing plates and from plate analyses.

1.2.3.2 Beam-column approach:

The longitudinally stiffened panels between transversals are treated as a series of beam-columns formed by the stiffener with an associated width of plates. One approach is to assume that the plate width is equal to the stiffener spacing, and allow for plate buckling effects by considering the limiting stress in the plate as those predicted by a buckling analysis of the plate panel. An alternative approach is to assume an effective plate width either derived by theoretical analyses or by using semi-empirical formulae and to limit the maximum stress to yield.

For the analysis, the stiffened plate can be modelled as a one-dimensional beam-column (Fig. 2.1). The plate is considered as one unit and the loss of stiffness can be introduced using numerical results of previous analyses [5], [6], [7]. The length of the column is divided into several elements and the stiffener is also divided into layers over the depth (Fig. 2.1).

The mode of failure treated is plate or stiffener induced failure caused by an interaction of overall column and local plate buckling. Residual stresses in the stiffener can be included as well as the initial distortion. Finite difference using Dynamic relaxation [4], [52] or finite element [26], [27], [38] are the tools used to describe the complex elasto-plastic behaviour of the beam-column. The methods include the effects of geometrical, material and fabrication parameters and extend to the unloading path. Two approaches were used: one is to use a full effective width equal to the stiffeners spacing and limit the stress to the ultimate stress of the plating estimated by other numerical analysis, the other approach is to use an effective width derived by empirical or semi-empirical formulae and

limit the maximum stress to the yield stress.

1.2.4 Effect of stiffened panel parameters

1.2.4.1 Plate slenderness:

Low column slenderness stiffened panels collapse is mainly due to yielding of stiffener material or buckling of the plate. For particular values of (λ), increasing the plate slenderness (β) results in a significant drop in load-carrying capacity. Increasing (λ) changes the dominant mode of failure from one of yielding or plate buckling to one of overall column buckling and then the effect of plate slenderness (β) is reduced.

1.2.4.2 Initial plate deformation:

Initial plate deformation reduces the strength and changes the pattern behaviour to a more gradual process with a less severe post-collapse load-reduction. This effect is more pronounced for moderate plate slenderness as defined earlier where the yield stress (σ_y) is nearly equal to the plate critical buckling stress (σ_{cr}).

1.2.4.3 Compressive residual stresses:

Residual stresses cause some reduction of compressive strength and stiffness over a range of strain from $(\sigma_y-\sigma_r)/E$ to $2\varepsilon_y$ as described in 1.1.2. This allows for more load redistribution between the plate edges and longitudinal stiffeners.

1.2.4.4 Column slenderness:

Generally speaking, increasing the column slenderness (λ) leads to a reduction in the ultimate strength. For values of intermediate column slenderness ($0.77<\lambda<1.27$) as will be discussed in chapter 3, the mode of failure will be an interaction of yielding and flexural buckling of stiffened panels and the drop in strength after peak load is most pronounced.

1.2.4.5 Initial column deflection:

The influence of initial stiffener distortions is more dominant in the range of moderate slendernesses and the effect is to reduce column load capacity and is naturally most pronounced in the region close to peak load.

1.2.4.6 Stiffener to plate area ratio:

The increase of stiffener to plate area ratio slightly improves the load carrying capacity and post peak load behaviour for most practical structures. This is because the stiffener cross-section proportions are chosen to avoid local buckling and hence they mostly fail close to the yield stress. In contrast plate elements will often buckle before ultimate failure of the whole cross-section.

1.2.5 Failure modes:

Flexural buckling induced by plate failure:

This mode involves buckling towards the stiffener and precipitated by loss of compressive strength of the plate.

Flexural buckling induced by stiffener failure:

This mode of failure involves buckling towards the plating.

The collapse is sensitive to the magnitude and direction of initial imperfections. It is then necessary to represent correctly the form of initial distortion and allow for interaction of adjacent spans.

In some cases, initial distortion may be directed towards the plating, inducing buckling towards the plating. The buckling of stiffeners away from the plating in one interframe bay may induce buckling towards the plating in adjacent spans. In other cases, when buckling is towards the plating, flexure may be coupled with side ways tripping of the stiffeners. It is often weak stiffeners which induce this mode of failure.

Tripping induced by compression:

Stiffener tripping has not been considered as a significant basis for modelling in this work as it is generally avoided in design. However, tripping correction factor is developed. The phenomenon is observed to occur in several of the tests reviewed and a further discussion can be found in Ref [61].

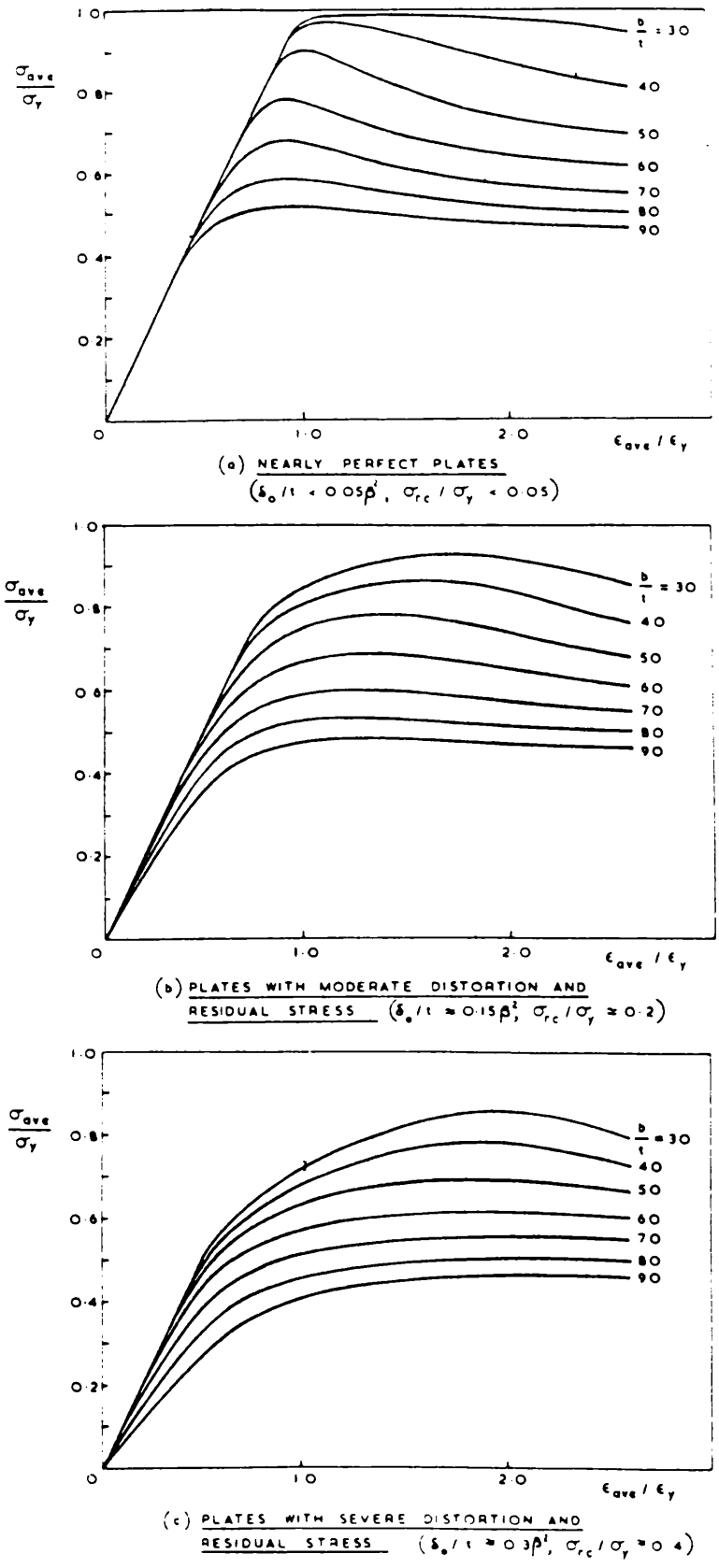

Figure 1.1 Load-shortening curves for square plates under uni-axial compression.

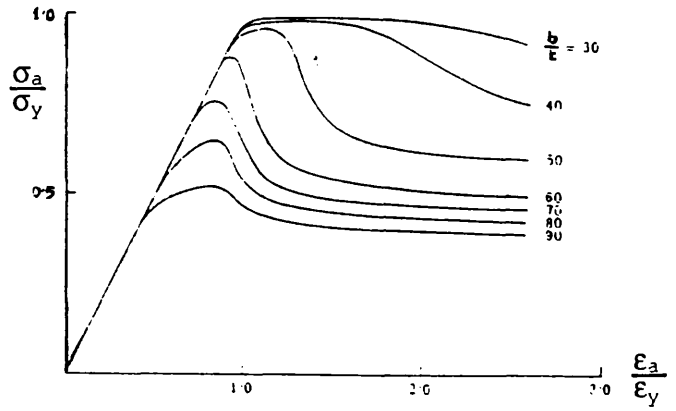

NEAR PERFECT PLATES- SMALL RESIDUAL STRESSES & INITIAL DISTORTIONS

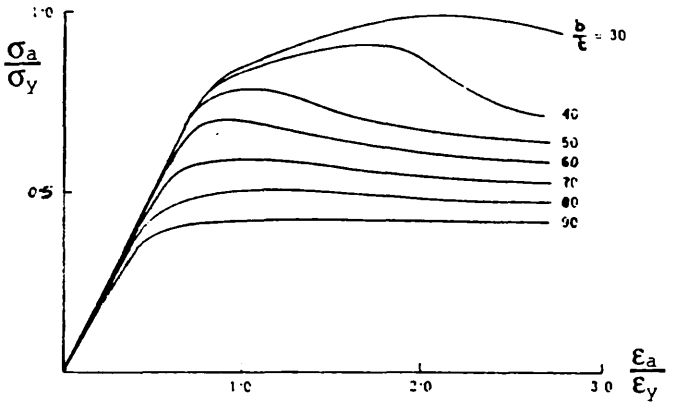

PLATES WITH MODERATE RESIDUAL STRESS & INITIAL DISTORTION

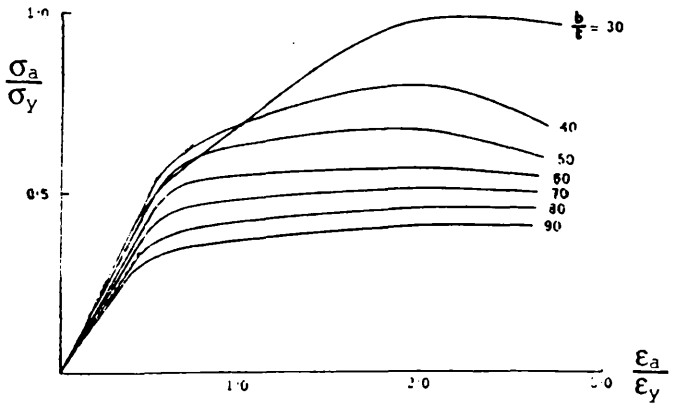

PLATES WITH SEVERE RESIDUAL STRESS & INITIAL DISTORTION

Figure 1.2 Load-shortening curves for rectangular plates under uni-axial compression.

CHAPTER 2

The Finite Element Program

The numerical program (FABSTRAN) used in this stage of the work was developed at ARE (Dunfermline) for determining compression behaviour of longitudinally stiffened plate panels.

2.1 General aspects of the program

The program is a non-linear finite element program which uses beam-column modelling with the effective width approach and limits the maximum stresses to yield.

The structural geometry is defined by specifying element length, together with element orientations and the co-ordinates of elements ends relative to nodal reference axes (global references are not used). Each nodal reference axes may be oriented in any desired way. Sectional proprieties are assumed to be constant within an element and may vary from one element to another. Each cross-section is divided into elemental areas.

Large deflections are represented by modifying the definition of structural geometry. Initial distortions are represented by including initial deformations as in the initial definition of structural geometry. For loss of plate stiffness the program uses an approximate formula or data curves introduced numerically into the program. Simplified modelling is assumed for magnitude and distribution of residual stresses in the plating and the stiffeners, as illustrated in Fig. 2.2.

The program is applicable to frames of general geometry including circular rings. The program follows an incremental analysis procedure allowing direct treatment of general frame buckling problems in which interaction between bending and extensional deformation may cause non-linear variations in the distribution of destabilising forces in frame elements. Thus local buckling of the frame cross-section is approximately allowed for.

2.2 Assumptions:

Frames of arbitrary curved geometry are represented as assemblies of straight beam elements. Distributed line loads acting on a frame are represented by equivalent concentrated loads acting at node points. Plane sections are assumed to remain plane under conditions of elastic and inelastic bending and extension. Full account is taken of the coupled flexural and extensional deformations of a frame and of the effects of shear deformation.

Element flexural deformation (w) is assumed to be cubic in form and extensional deformation (u) is assumed to be linear.

2.3 Numerical procedure:

The analysis is an incremental procedure in which loads or nodal displacements are applied incrementally, a linear solution being obtained by the matrix displacement method:

$$\{\delta\}[K+K_G] = \{R\}$$

Where:

- K : is a stiffness matrix representing the axial and flexural stiffness of frame elements.
- K_G : is a geometrical stiffness matrix representing the destabilising influence of axial forces in frame elements.
- δ : is a column matrix of incremental nodal displacements.
- R : is a column matrix representing applied loads.

In the case of hydrostatic load, secondary terms are added to the matrix K_G which allow for the change in direction of applied loads arising from buckling and pre-buckling deflections (these forces remain normal to the deformed surface).

Cumulative values of displacements at node points and stresses, strains and destabilising forces in frame elements are updated after each incremental solution. Following each incremental solution, the stresses in each fibre of each element are examined and where the total stress

exceeds yield at mid-length of the fibre either:

1. The fibre is subsequently taken to contribute no stiffness in the next incremental solution, that is an elastic-perfectly plastic material stress-strain curve is being assumed, or:
2. A tangent modulus is adopted for the fibre in accordance with a numerically defined stress-strain curve.

In either case, the effect of shear stress on yield is ignored.

Allowance is made for elastic unloading of yielded fibres. Where strain reversal is found to have occurred in a yielded fibre following any incremental solution, the fibre is assumed to recover its elastic stiffness and contribute fully to the elastic section proprieties for the next incremental solution.

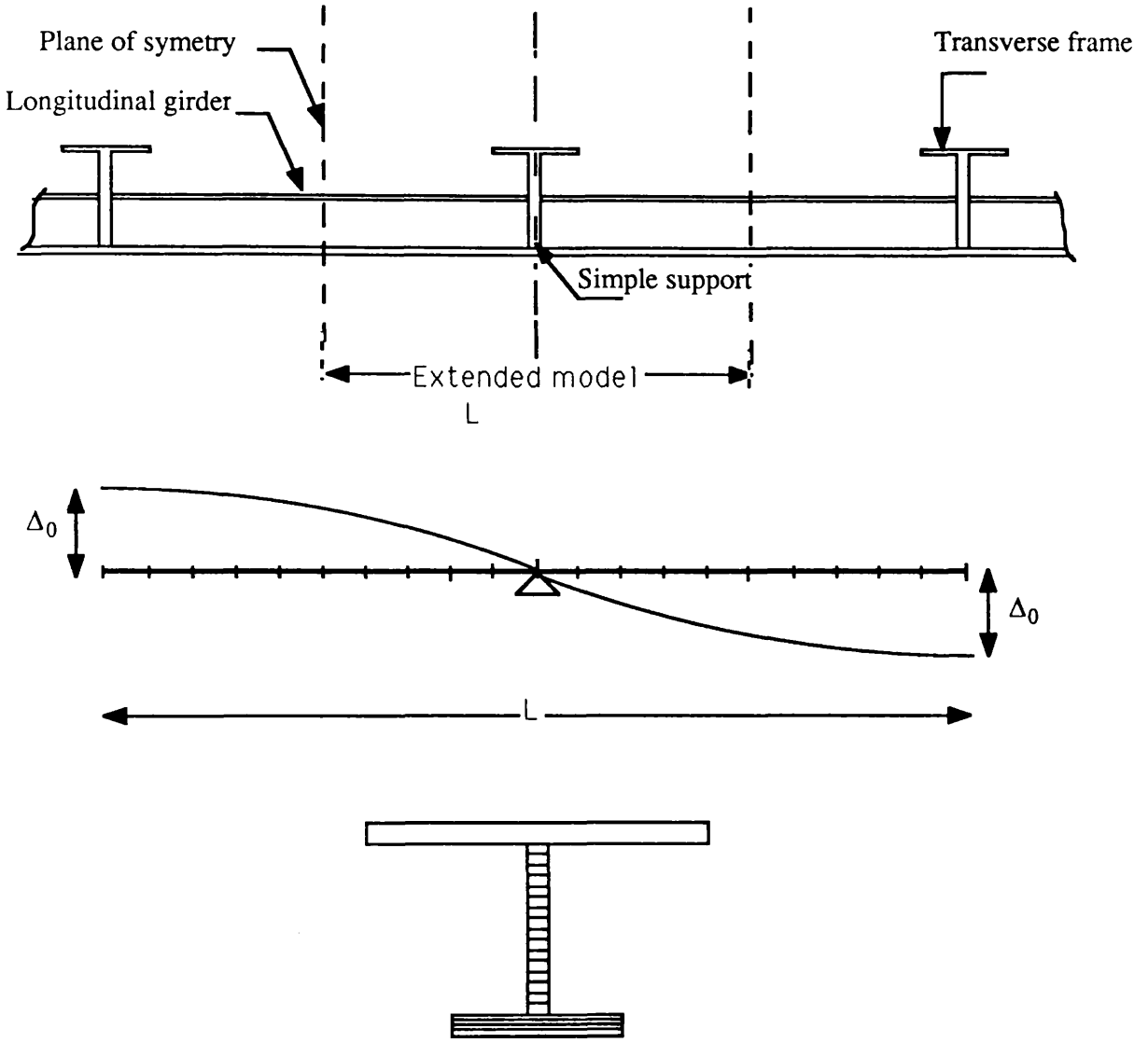

Figure 2.1 Beam-column modelling

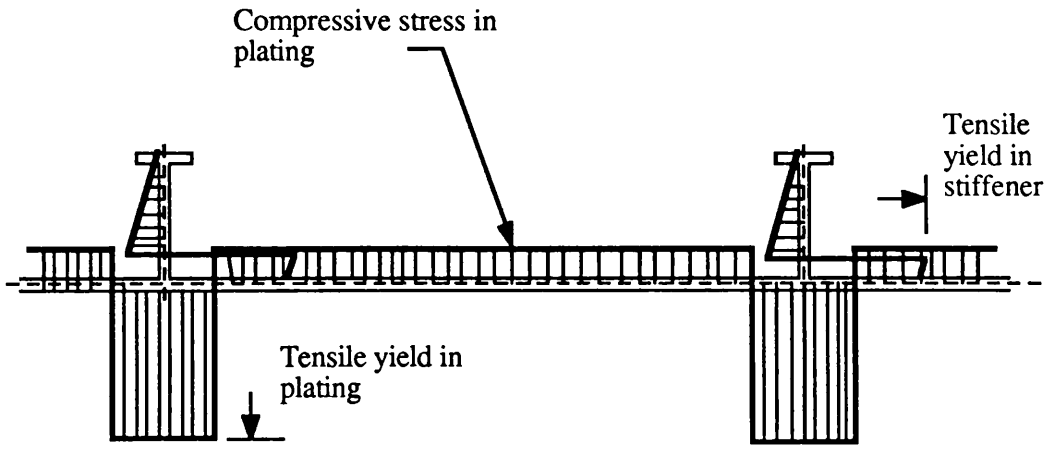

Figure 2.2 Residual stress modelling

CHAPTER 3 :
Parametric Studies

3.1 Introduction:

Using the ARE non-linear finite element program [28], a parametric analysis has been carried out to investigate the strength of stiffened panels under uni-axial compression and the behaviour of the components before and after collapse. The analysis includes the effect of initial distortions and residual stresses in addition to the effects of plate and column slenderness.

Numerical results are presented, mainly in the form of average load-end shortening curves, covering the entire loading history. Additionally, ultimate strength-slenderness curves are generated to demonstrate the predominant effect of plate and column slendernesses.

3.2 Stiffened panel parameters:

Panels are formed of plates stiffened by Tee-section longitudinal girders of a relatively low web slenderness ($h_w/t_w \approx 12$). The plating is mild steel with a yield stress of $245 N/mm^2$ and Young's modulus of $207 kN/mm^2$.

Dimension proportions are chosen regarding existing panels found in marine structures.

3.2.1 Plate slenderness:

Plate slenderness ranges are from the value $\beta = 0.7$ to 3.5 with values 0.7, 1.0, 1.37, 1.72, 2.0, 2.4, 2.75 and 3.0 which were obtained by varying the width to thickness proportions.

3.2.2 Column slenderness:

For each plate slenderness value of the above range, the range of column slenderness was obtained by varying the length of the span in some cases and cross-section geometrical proportions in other cases. For calculating λ all the plating is included in the cross-section.

3.2.3 Plate residual stress and initial distortion:

These two parameters are treated together and divided into three levels:

Level 1 -Nearly perfect plates (low residual stress and initial distortion), represented by $\mu_o = 0.05$.

Level 2 -Moderate values, represented by $\mu_o = 0.2$.

Level 3 -High values, represented by $\mu_o = 0.4$.

The term μ_o approximate to $\delta_0/t\beta^2$ and σ_r/σ_y and the reason for grouping these two influences is pragmatic, noting that high values of one seem to coincide with high values of the other. This is perhaps not too surprising as the predominant plate distortion is of course induced by the same weld contraction actions as give rise to the residual stress σ_r. This approach is also in line with ARE practice.

3.2.4 Stiffener initial distortion:

The stiffener initial imperfection (Δ_0/L) seems to lie in the range (0.005:0.0003). The mode of the imperfection adopted in the analysis is a half sinusoidal mode accounting for the interaction of the adjacent span, as shown in Fig. 2.1.

3.2.5 Summary of parameters:

The above discussion bring the analysis to four variables which are: β, λ, μ_o, Δ_o and α. For the first series of parametric analyses, the range of the factors affecting the ultimate strength has been selected as follows:

Plate slenderness (β): $0.7 \leq \beta \leq 3.5$

Column slenderness (λ): $0.1 \leq \lambda \leq 2.0$

Plate initial distortion and residual stress were amalgamated into one group and three categories: Low , moderate, and high values as explained previously.

Stiffener to plate area ratio ($\alpha=A_s/A_p$) : $0.2 \leq \alpha \leq 0.4$

Stiffener initial distortion (Δ_0/L) : $0.0005 \leq \Delta_0/L \leq 0.005$

For the above range of the plate slenderness, the column slenderness, initial plate distortion and residual stress for the following values of the

remaining two were fixed at the following values for some of the studies:

$\Delta_o/L = 0.001$

$\alpha = 0.3$

Later, other analyses were performed for different values.

3.3 Fixed load position:

Two approaches were used in order to choose the more realistic. First, the action of load is assumed not to follow the shifting of the neutral axis. Second, the applied load is assumed to follow the shifting of the neutral axis. Comparing the two suggestions the results in Figs. 3.1.a, 3.1.b, 3.1.c and 3.1.d show that for values of high column slenderness the difference is likely to be negligible. The effect, however, is more pronounced for moderate and low values of column slenderness. For values of plate slenderness ($\beta \leq 1.6$) the difference is significant for moderate values of column slenderness ($0.5 \leq \lambda \leq 1.1$). For values of plate slenderness ($1.6 < \beta \leq 2.0$) the difference in ultimate strength is less significant. For values of $\beta > 2.0$, however, the difference is significant for low and moderate column slenderness, in particular for low column slenderness. Comparing the results with the existing test data, the former approach is more realistic for panels showing an eccentricity towards the stiffener, while the second approach provides a good correlation with panels having an eccentricity towards the plating. Therefore, depending on the eccentricity of the load, the analytical expressions would be selected. It seems that the first assumption of a fixed load position provides a better agreement with most test data, although in a real structure (like a ship) the load path will be constantly changing. The second approach seems to give more realistic results for the analysis of one span beam-column.

3.4 Effect of stiffened panel parameters:

3.4.1 Effect of plate slenderness:

The finite element program is used to derive the ultimate strength for panels with a standard stiffener initial distortion of the value $\Delta_0/L = 0.001$

and a stiffener to plate area ratio $\alpha = 0.3$, with low residual stress and plate initial distortion (Level 1).

Figures 3.2.a and 3.2.b show a family of ultimate stress-column slenderness curves for a variety of plate slenderness. At low column slenderness, where failure is due to yielding or plate buckling, the effect of plate slenderness (β) is predominant. For a particular value of column slenderness (λ), increasing β results in a significant drop in strength. This effect is most pronounced at moderate plate slenderness, for instance, at value $\lambda = 0.2$, increasing the plate slenderness from the $\beta = 1.72$ to value $\beta = 2.0$, the drop in strength is 9.3%. The drop in strength is less significant at higher values of plate slenderness. Increasing β from value 2.75 to value 3.0 gives rise to a 2% drop in strength. These results seem a little surprising when compared with changes arising from plate strength alone and is almost certainly due to the different load shifting assumption.

Increasing the column slenderness, however, will change the mode of failure from one of yielding or plate buckling to inter-frame flexural buckling of columns and hence the effect of plate slenderness is reduced, as shown in Figs. 3.2.a and 3.2.b. At a value of $\lambda = 0.8$, the drop in strength is less than 5%. At high column slenderness, the effect of plate slenderness became negligible, Figs. 3.1.a, 3.1.b, 3.1.c, 3.1.d, 3.2.a and b also show the importance of the assumption made regarding load eccentricity.

3.3.2 Effect of column slenderness:

In general, increasing the column slenderness (λ) leads to a reduction in the ultimate strength, as shown in Figs. 3.2.a and 3.2.b. This effect is most pronounced at moderate values of column slenderness ($0.7 \leq \lambda \leq 1.27$), as seen in Figs. 3.1.a, 3.1.b, 3.1.c, 3.1.d, 3.2.a and 3.2.b, where the mode of failure will be an interaction of yielding and flexural buckling of stiffened panels. The post-ultimate strength of such panels gives rise to a significant drop in strength after maximum load as shown in fig. 3.2.c. At

higher values of plate slenderness the effect of column slenderness is less marked and reducing λ from value 1.0 to value 0.5, for example, causes only a little improvement in maximum strength.

3.3.3 Effect of residual stress and initial distortion:

As discussed earlier, the effects of plate initial distortion and residual stress are treated and introduced as one variable by grouping both parameters. Although residual stresses have the greater effect on plate strength and stiffness, researchers have shown a greater interest in the effect of initial distortion. This is probably due to the visibility of distortions. But it may also be due to the relative neglect of modelling of the distribution of residual stresses present in plating for incorporation in numerical analysis. This is discussed more fully in reference[64].

The presence of residual stresses and initial distortion reduces the strength; initial distortion changes the post-ultimate strength to a less severe unloading path; residual stress reduces the stiffness and strength of the panel, and shifts the collapse load which will occur after greater shortening.

Graphs representing the effect of initial distortion and residual stress are in Figs. 3.3.a and 3.3.b. The presence of these two parameters strongly affect the ultimate load of the stiffened panel. A reduction in strength of as much as 20% in heavily welded plates compared with stress free plates with intermediate slenderness values. This effect , indeed, depends on whether the failure of the panel is plate like failure or inter-frame flexural buckling. For instance, in a heavy welded grillage, the ultimate stress of the plate panel under compressive load will not normally be reached until the strain is $2\varepsilon_y$, at this stage stiffener type failure will usually occur, except perhaps in the case of stiffeners with a higher yield stress than plating.

As shown in Fig. 3.3.a, for a particular value of column slenderness (λ), increasing the plate slenderness in the moderate range leads to an increase in the effect of residual stresses and plate initial distortion. On

the other hand, for a particular value of plate slenderness $\beta = 1$ (Fig. 3.3.a), as a result of increasing the column slenderness the effect of residual stress and initial deflection reduces for moderate and high values of λ. For low values of λ, however, there is a small effect. For larger values of β, equal 2.75 in Fig. 3.3.b, the effect of μ_o is very much greater, but care is then necessary to choose the best value of μ_o for the given β, for example $\mu_o = 0.2$ would be appropriate for $\beta = 2.75$.

As seen in Figs. (3.6.a to 3.6.f), the effect of initial distortion on post-ultimate strength is more pronounced for values of β in the intermediate range.

3.3.4 Effect of stiffener initial distortion:

The assumed column initial distortion was a half sine wave, directed upward (toward the stiffener) in one span and downward (toward the plating) in the other span (Fig. 2.1) in order to simulate a realistic interaction of one span on the adjacent one. Results are presented in Fig. 3.4. In general, increasing the column initial distortion leads to a decrease in maximum strength and this is most pronounced at moderate values of column slenderness. For very low values of initial distortion, the effect on maximum strength is nearly negligible.

3.3.5 Effect of stiffener to plate area ratio:

In order to show the effect of stiffener to plate area ratio on the ultimate strength and post-buckling of stiffened panels, strength analyses of panels with values of $\alpha = 0.2$ and $\alpha = 0.4$ for the value of $L/\Delta_o = 600$ and $\mu_o = 0.2$ are produced. Plate and column slendernesses range as follows:

β: 1.0, 1.37, 2.0, 2.4, 2.75 and 3.0.

λ: 0.35, 0.55, 0.75, 0.95, 1.2 and 1.5.

Ultimate strength-slenderness curves are presented in Figs. 3.5.a, 3.5.b and 3.5.c. Load-shortening curves are illustrated in Figs. 3.7.a and b; 3.8.a, 3.8.b and 3.8.c; 3.9.a and b; 3.10.a, b, c and d; 3.11.a and b; 3.12.a and b. As seen in Fig. 3.5.a, for low values of plate slenderness the effect

of α on maximum strength is negligible at low values of column slenderness. The curves show a slight effect for moderate and high values of column slenderness being more pronounced at moderate values. At moderate values of plate slenderness (Fig. 3.5.b), the effect became more evident and it shows more or less the same effect for all ranges of column slenderness. For high values of plate slenderness (Fig. 3.5.c), the effect, however, is predominant at low values of column slenderness and decreases as the column slenderness increases. The effect of stiffener to plate area ratio on post-ultimate strength is greater, in particular, for moderate column slenderness. The effect is dramatic at moderate values of plate slenderness, as shown in Figs. 3.9.a and 3.10.b. An increase in the stiffener to plate area ratio improves the load carrying capacity which is more predominant for low and moderate values of plate slenderness. The stiffened panel behaviour path in the unloading range changes from a sudden sharp pattern to a less severe and gradual process as α increases. It is thought the dramatic drop in load and recovery exhibited with the lower stiffener areas may arise from adjacent bay effects. As these bays take more of the load they can exert stabilising moments to the collapsing bay which can arrest the growth in its deformation, see the further remarks in 6.3.2 in this respect. As a final comment it is evident that the well known trend for least weight designs to include high α values is supported.

3.3.5 Effect of stiffener residual stresses:

The failure of a stiffened panel is influenced by the residual stresses due to welding, as noted in reference [30], residual stresses vary in magnitude and distribution along the depth of the stiffener and the collapse of the panel is highly influenced by the pattern and levels of the residual stresses. Compressive residual stresses which are present in the tables of the stiffener causes a reduction on ultimate strength, while tensile stress may have a beneficial effect. Since the effect of stiffener residual stress is small compared to this of the plating, then is not included in the present modelling.

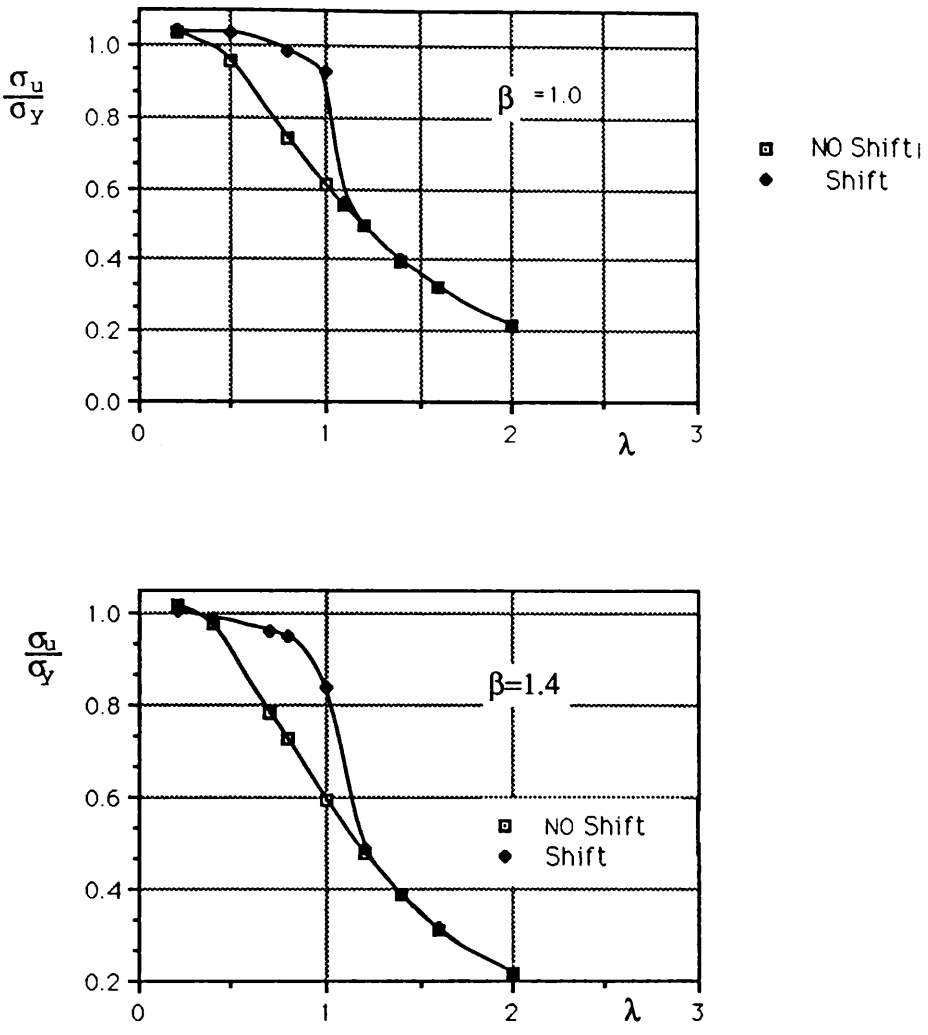

NO shift : The applied load does not follow the shifting of the neutral axis.
Shift : The applied load does follow the shifting of the neutral axis.

Figure 3.1.a Ultimate load-Slenderness curves. Shifting of the applied load

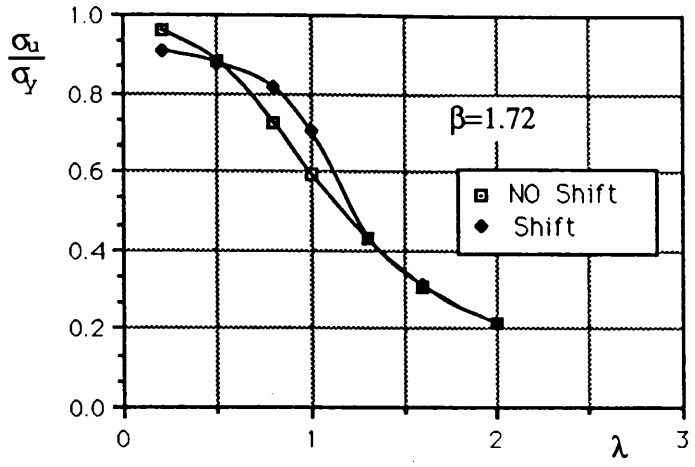

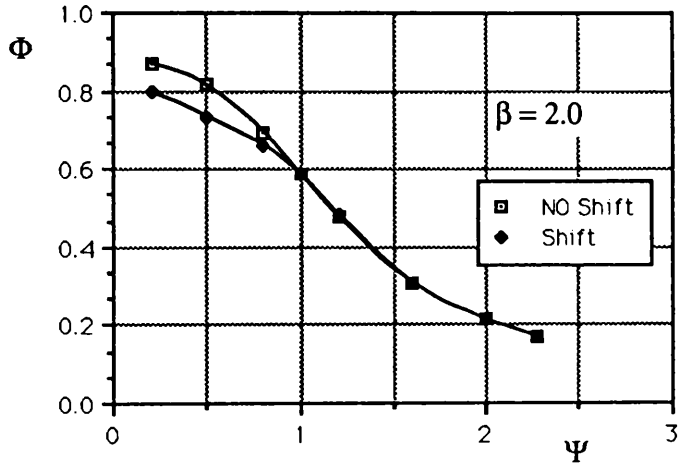

NO shift : The applied load does not follow the shifting of the neutral axis.
Shift : The applied load does follow the shifting of the neutral axis.

Figure 3.1.b Ultimate load-Slenderness curves.
Shifting of the applied load

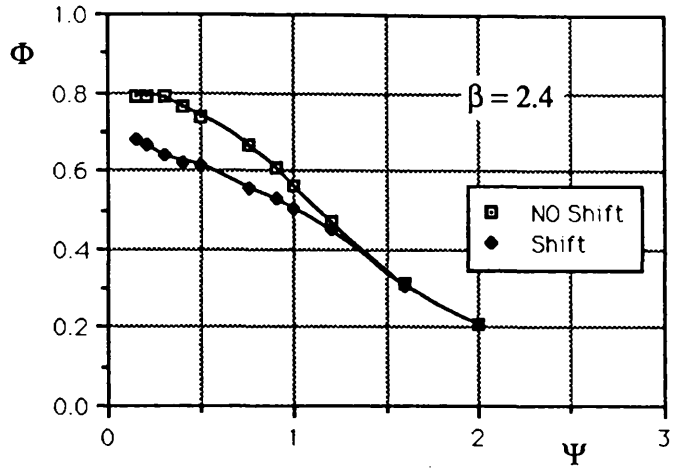

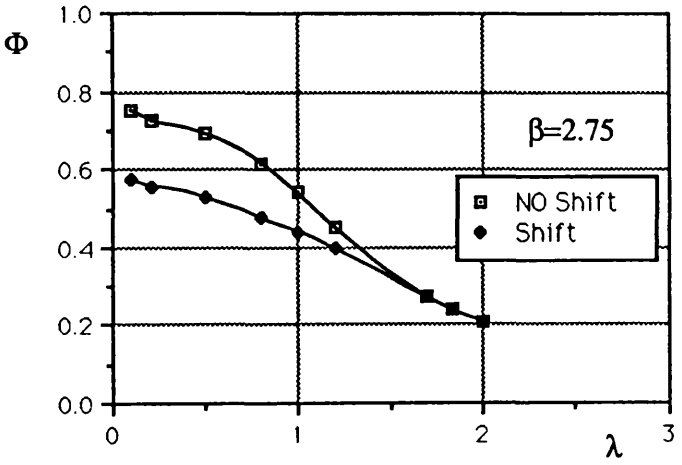

NO shift : The applied load does not follow the shifting of the neutral axis.
Shift : The applied load does follow the shifting of the neutral axis.

Figure 3.1.c Ultimate load-Slenderness curves.
Shifting of the applied load

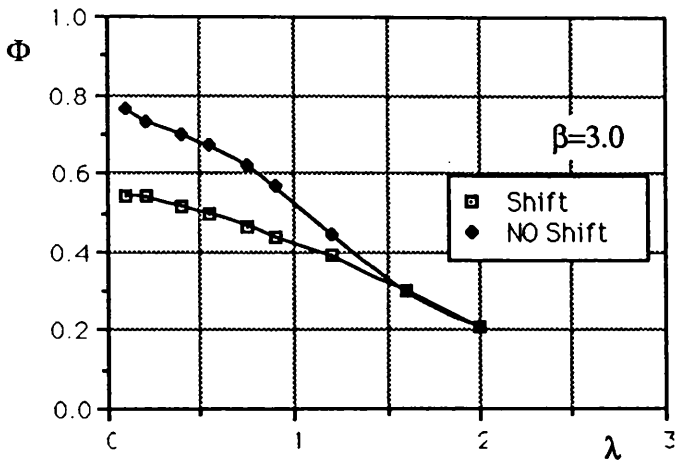

NO shift : The applied load does not follow the shifting of the neutral axis.
Shift : The applied load does follow the shifting of the neutral axis.

Figure 3.1.d Ultimate load-Slenderness curves.
Shifting of the applied load

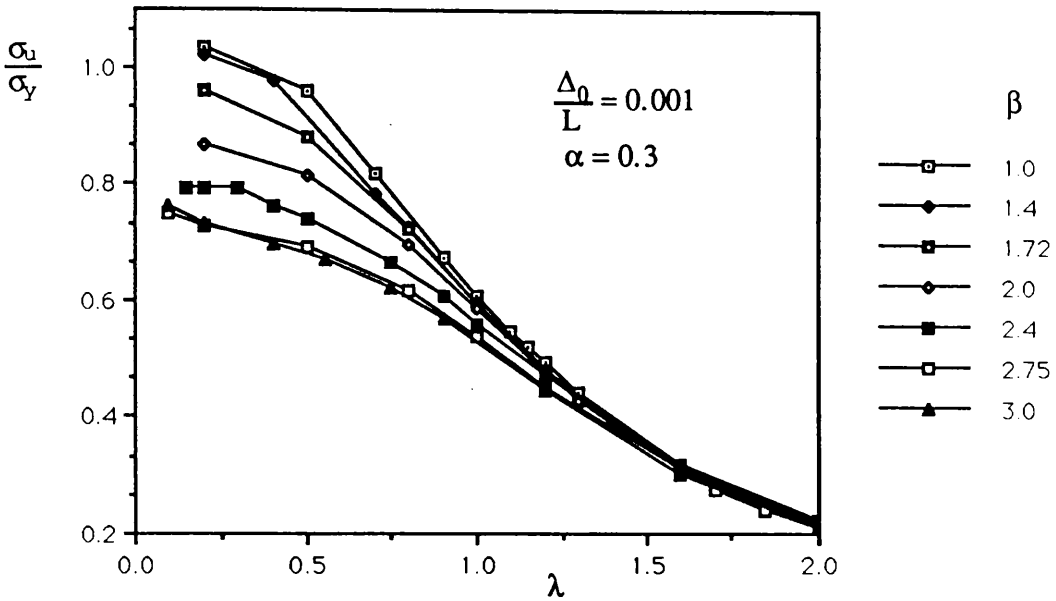

1. Load not following the shifting of the neutral axis

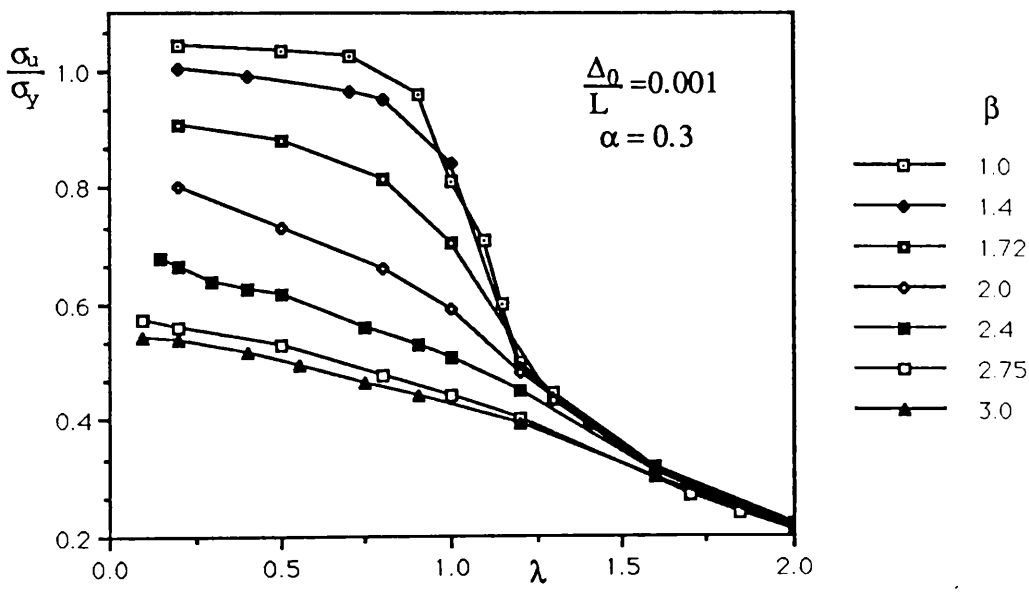

2. Load following the shifting of the neutral axis

Figure 3.2 Ultimate strength-slenderness curves

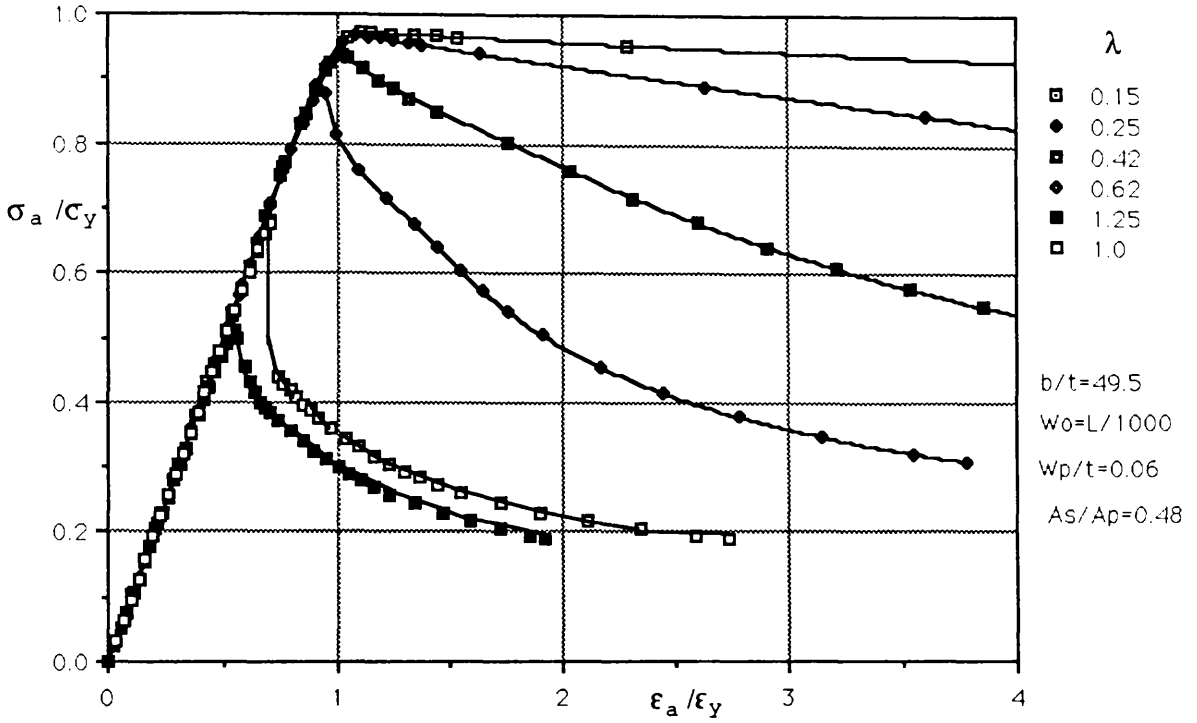

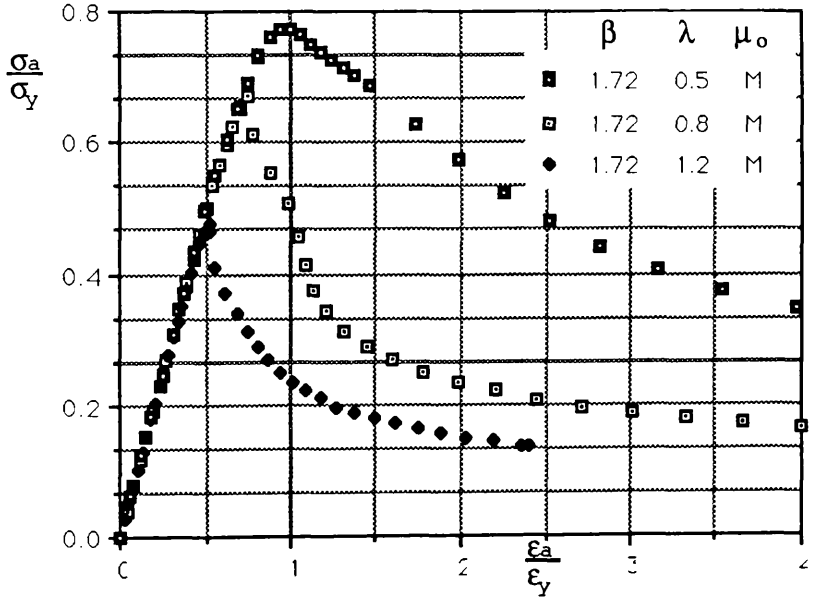

Figure 3.2.a **Average stress-strain curves**
Effect of column slenderness

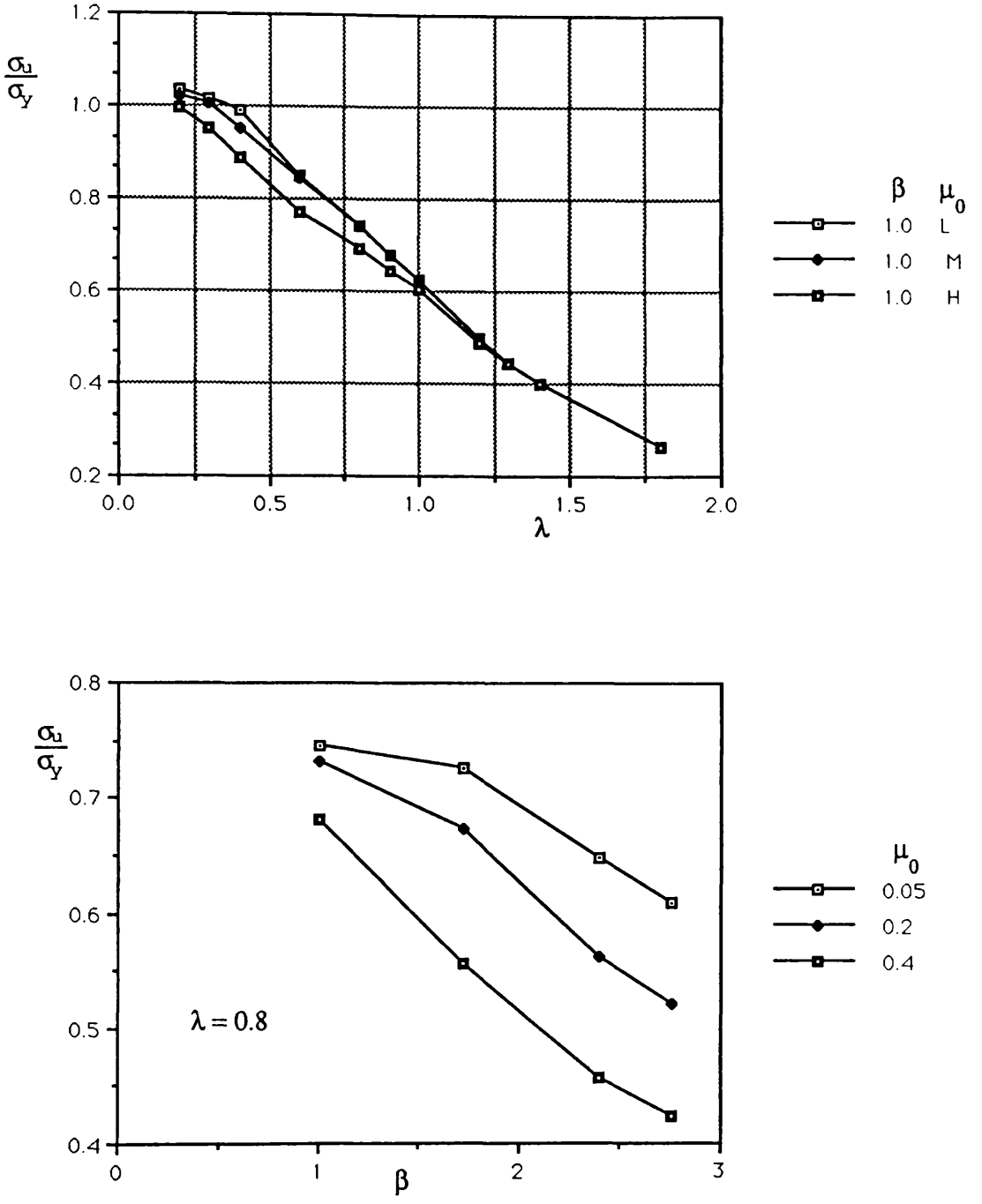

Figure 3.3.a Ultimate strength-slenderness curves
Effect of residual stress and
initial distortion

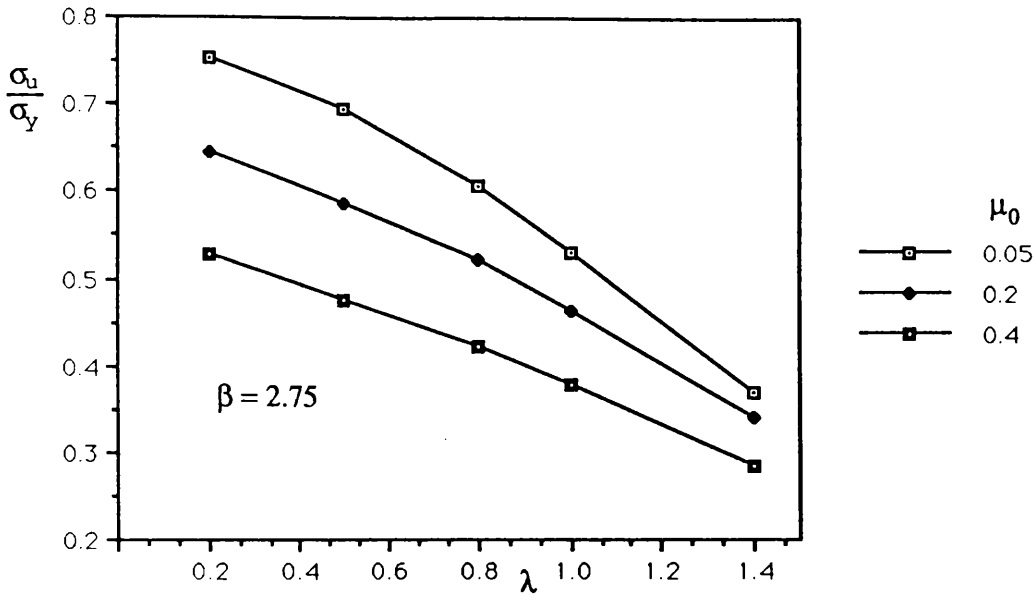

Figure 3.3.b Ultimate strength-slenderness curves
Effect of residual stress and
initial distortion

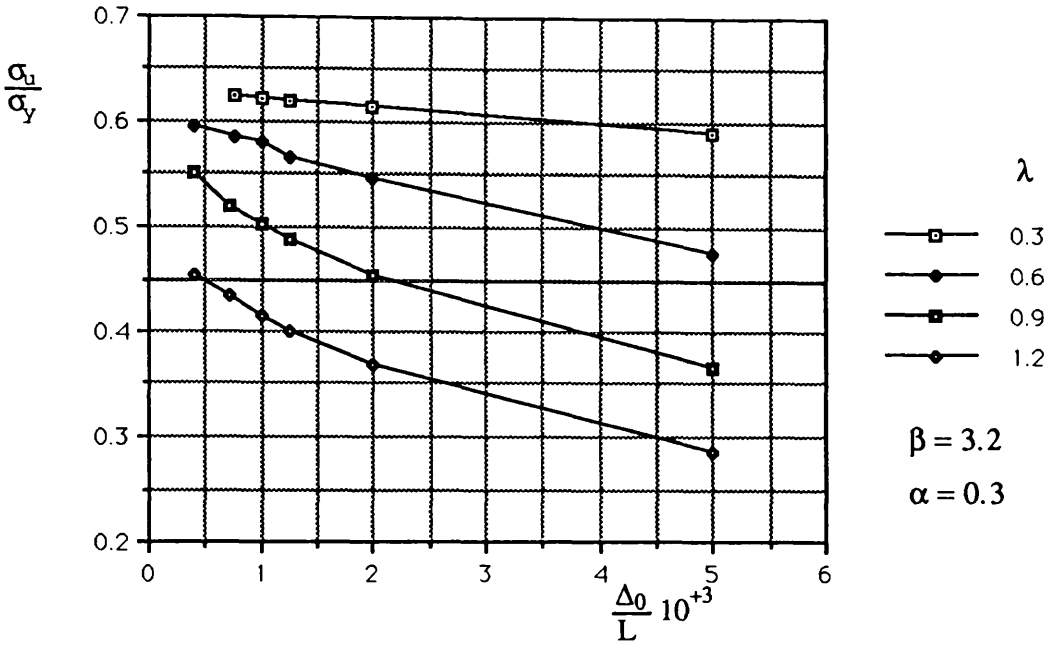

Figure 3.4 Effect of column initial distortion

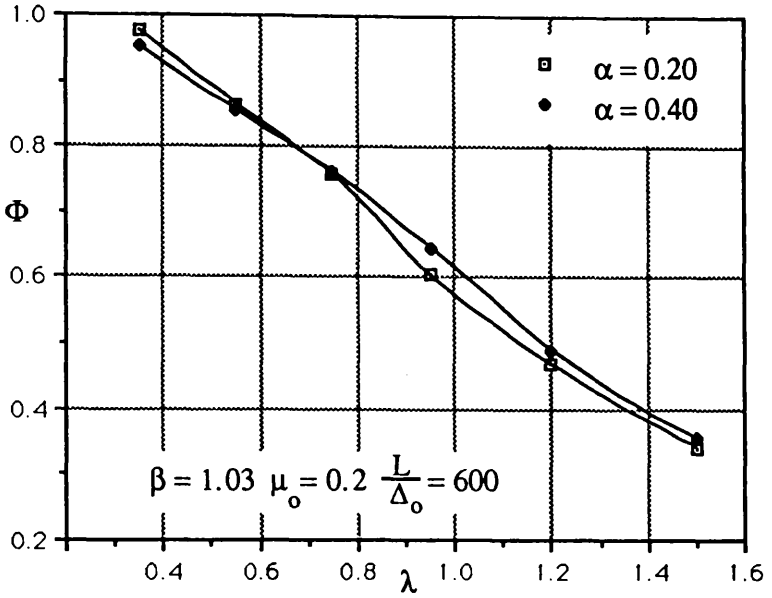

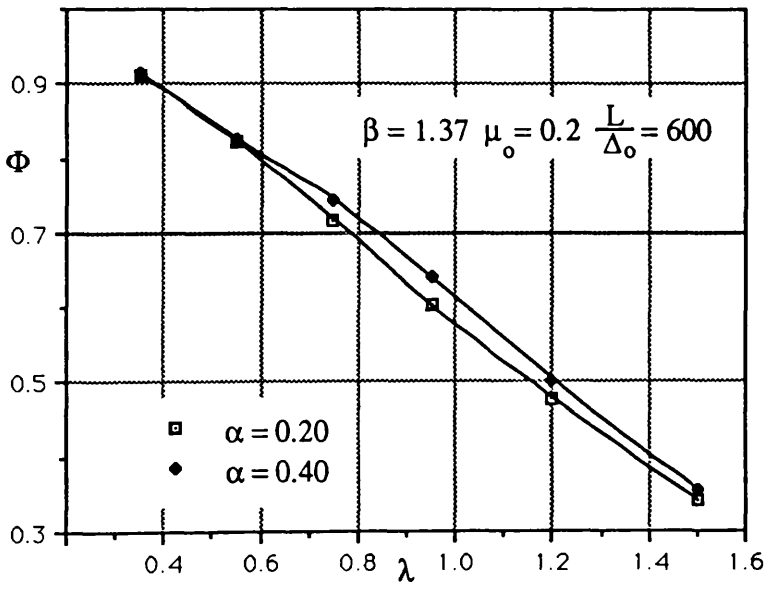

Figure 3.5.a Ultimate load-Slenderness curves
Effect of stiffener to plate area ratio

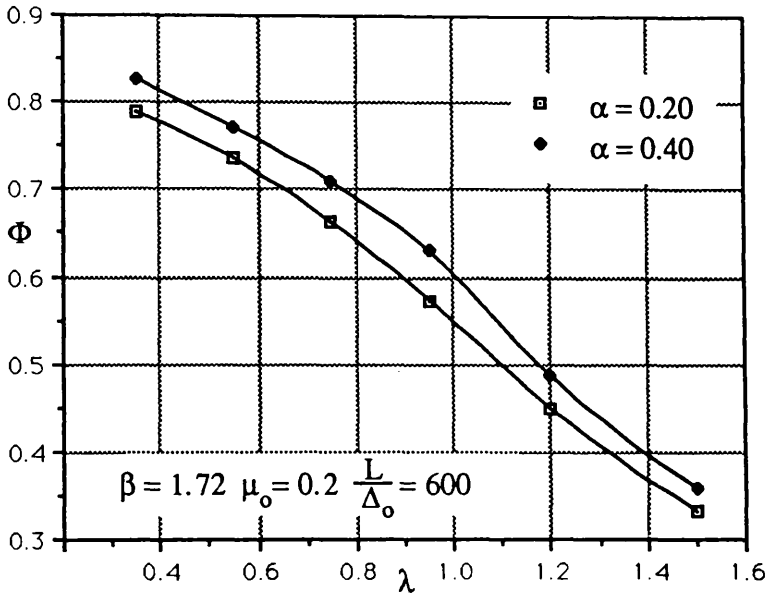

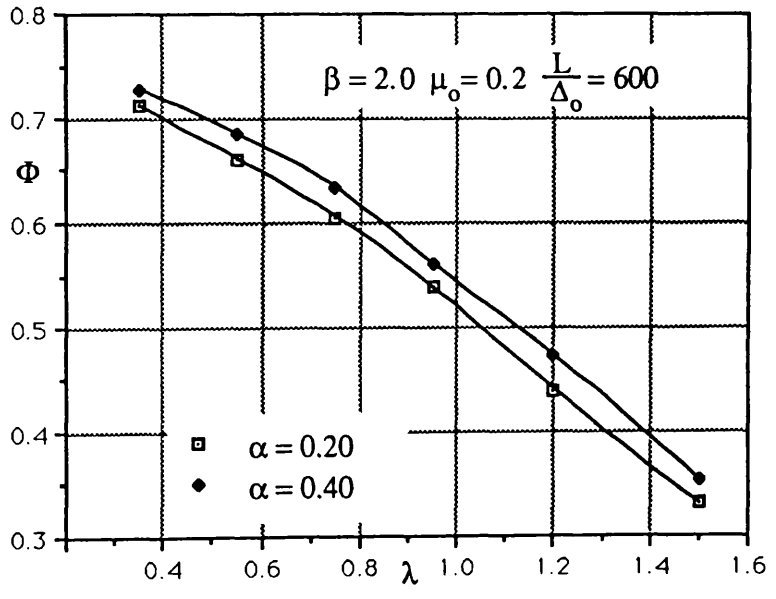

Figure 3.5.b Ultimate load-Slenderness curves
Effect of stiffener to plate area ratio

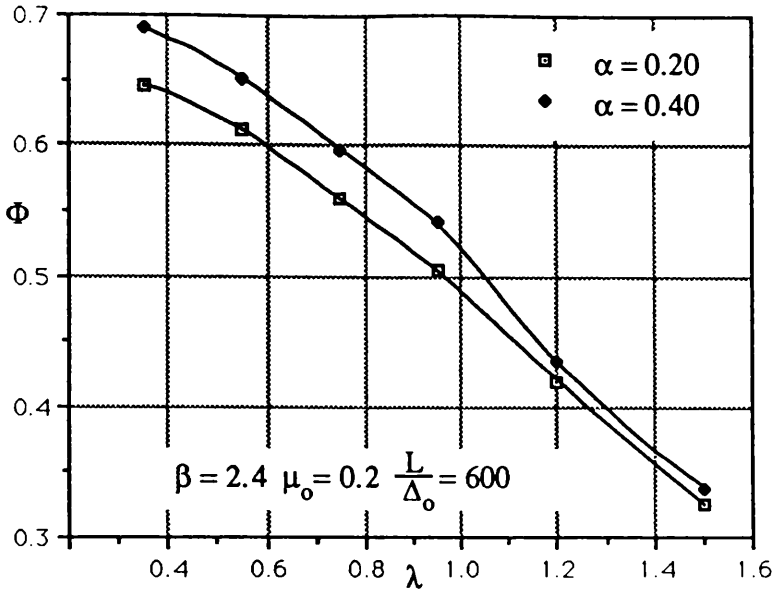

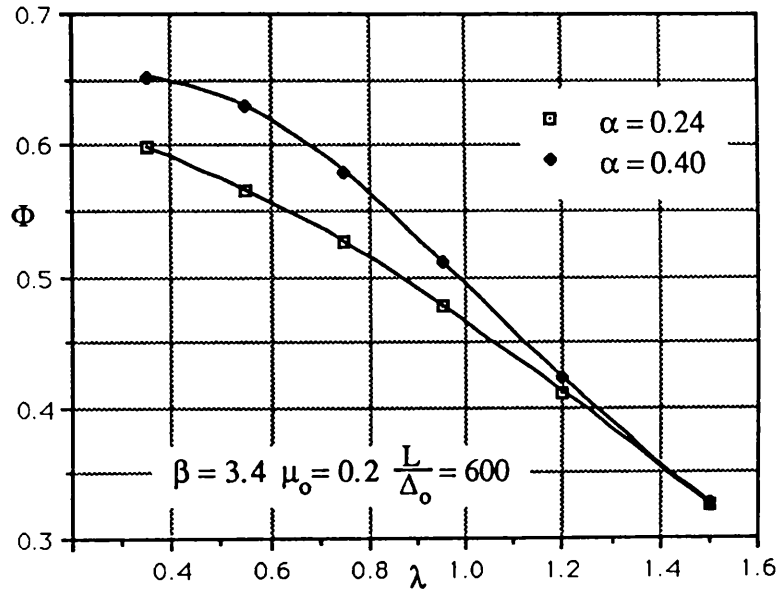

Figure 3.5.c Ultimate load-Slenderness curves
Effect of stiffener to plate area ratio

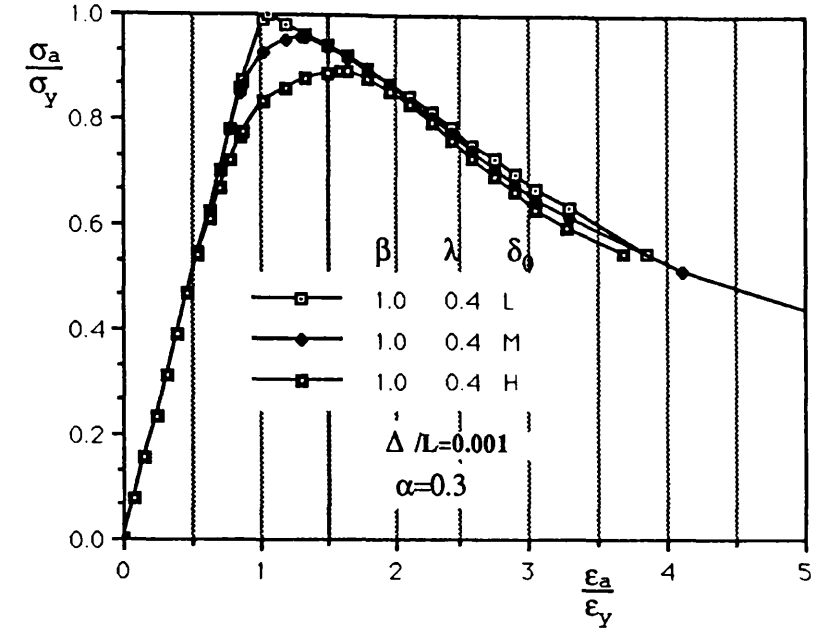

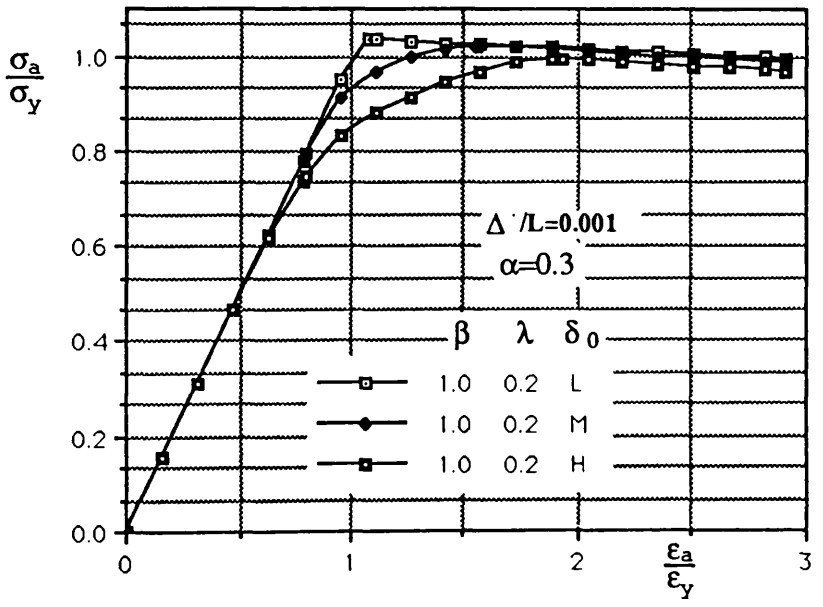

Figure 3.6.a Average stress-strain curves
Effect of residual stress and initial distortion

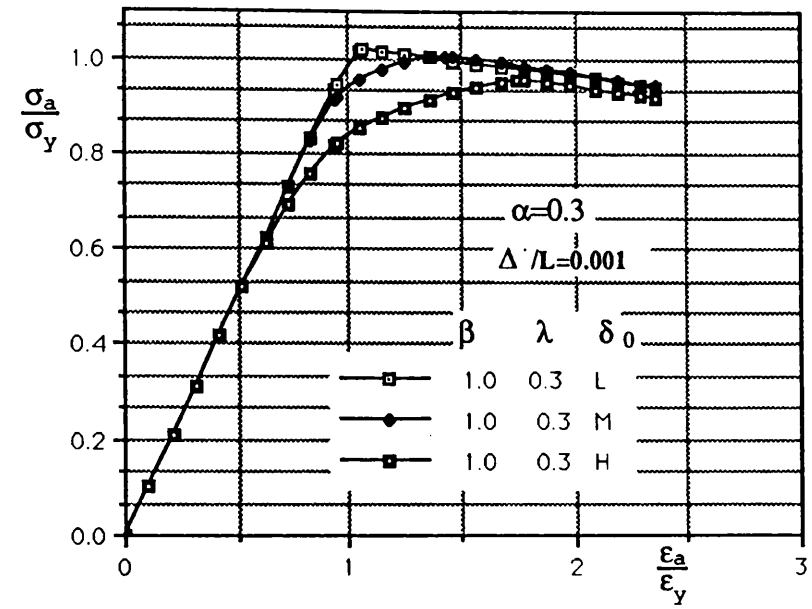

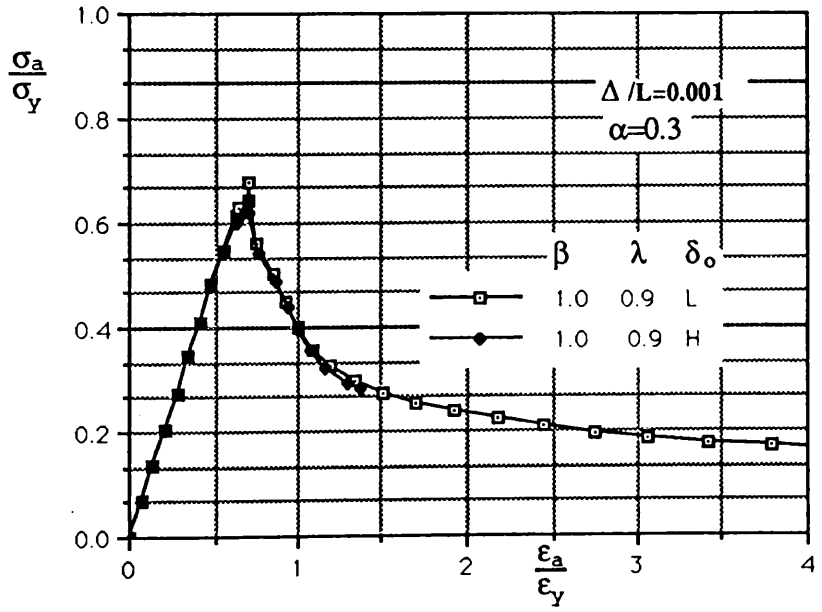

Figure 3.6.b Average stress-strain curves
Effect of residual stress and initial distortion

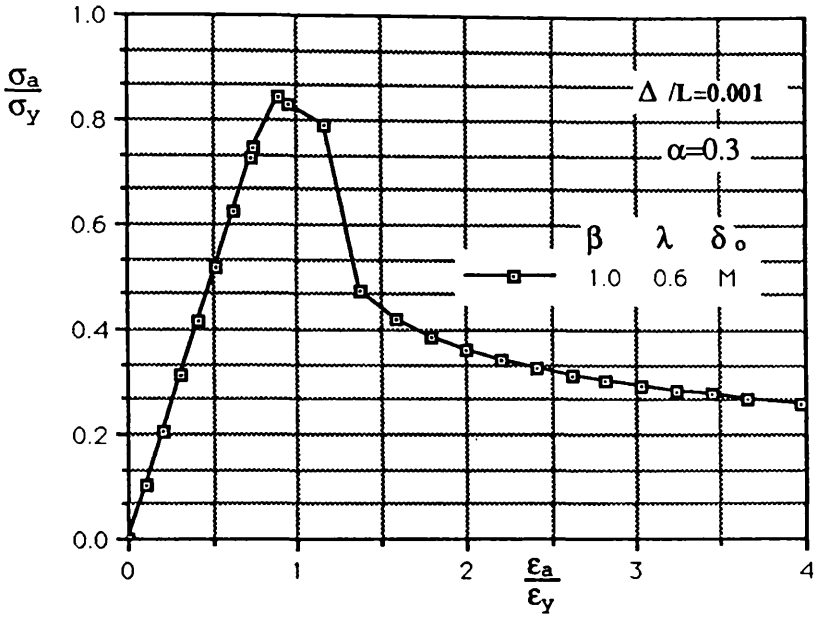

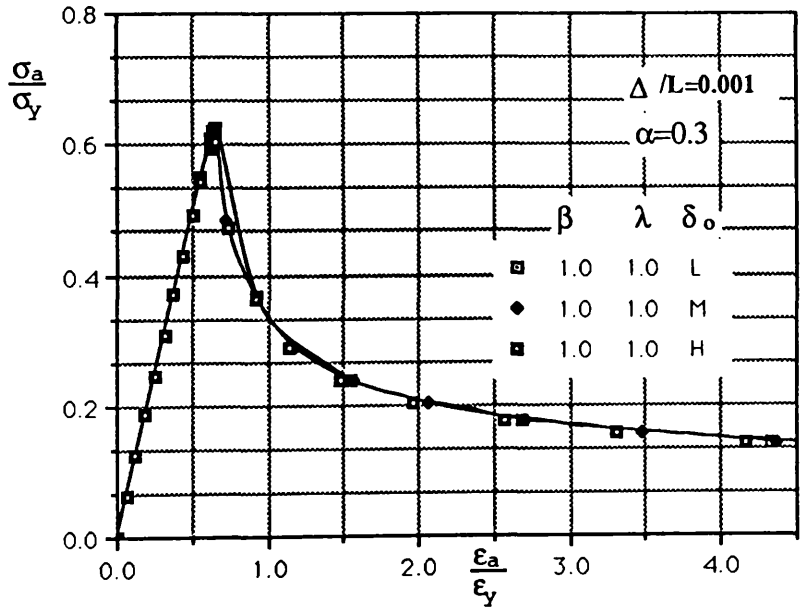

Figure 3.6.c. Average stress-strain curves
Effect of residual stress and initial distortion

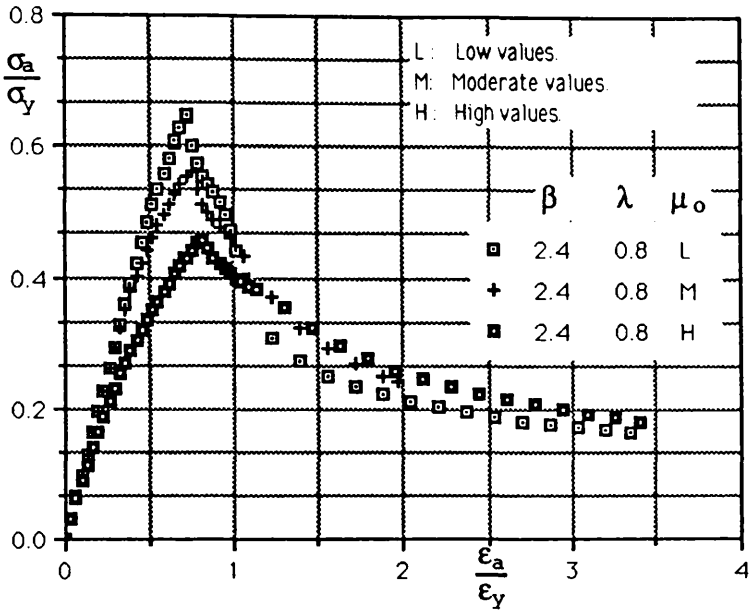

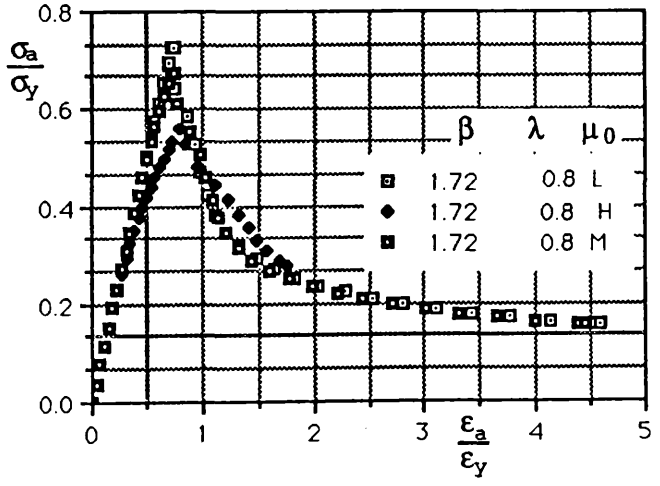

Figure 3.6.d **Load-shortening curves**
Effect of residual stress and initial distortion

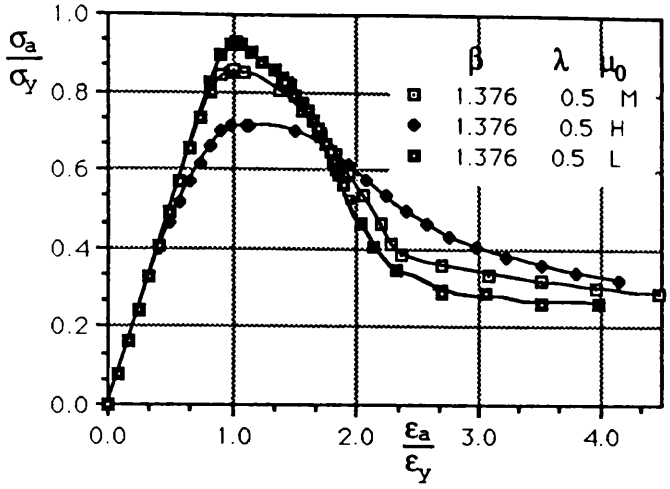

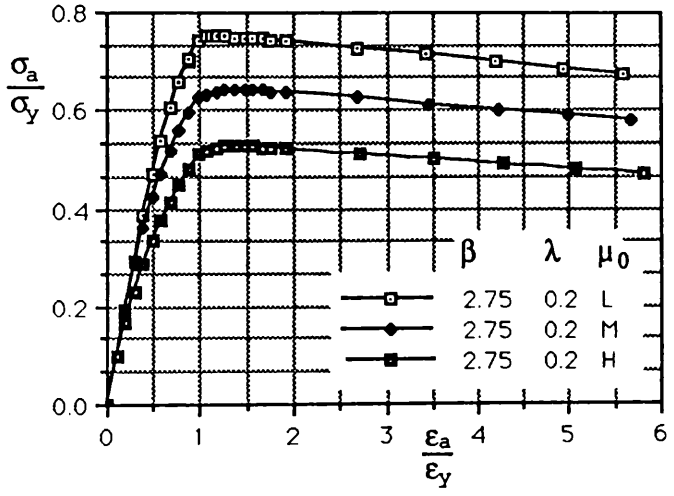

Figure 3.6.e Load-shortening curves
Effect of residual stress and initial distortion

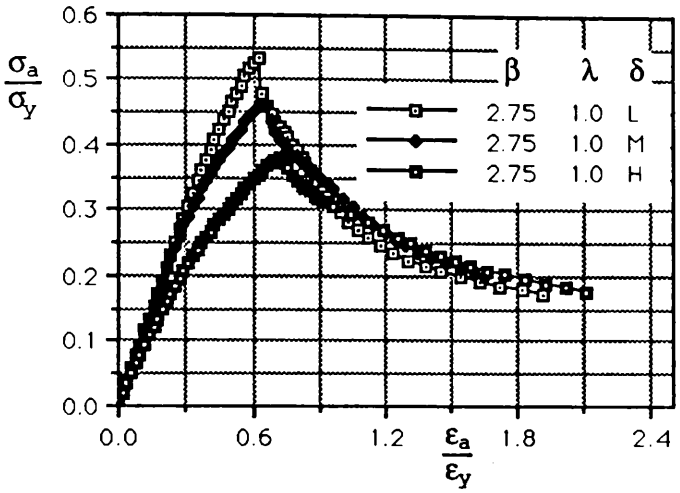

Figure 3.6.f Load-shortening curves
Effect of residual stress and initial distortion

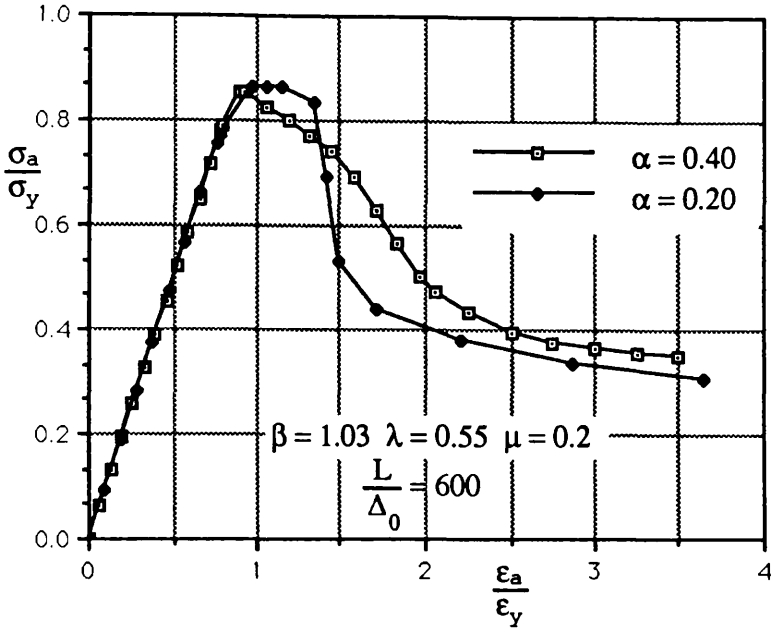

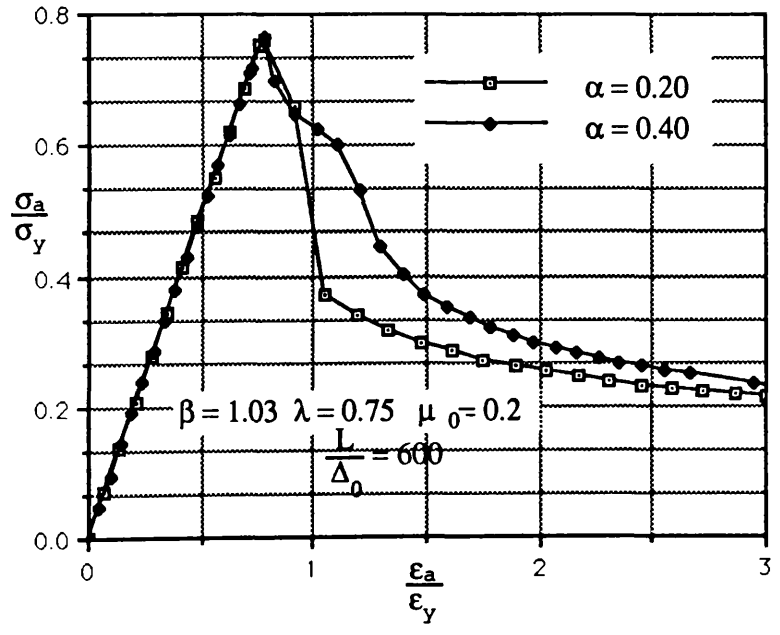

Figure 3.7.a **Stress-strain curves.**
Effect of stiffener to plate area ratio.

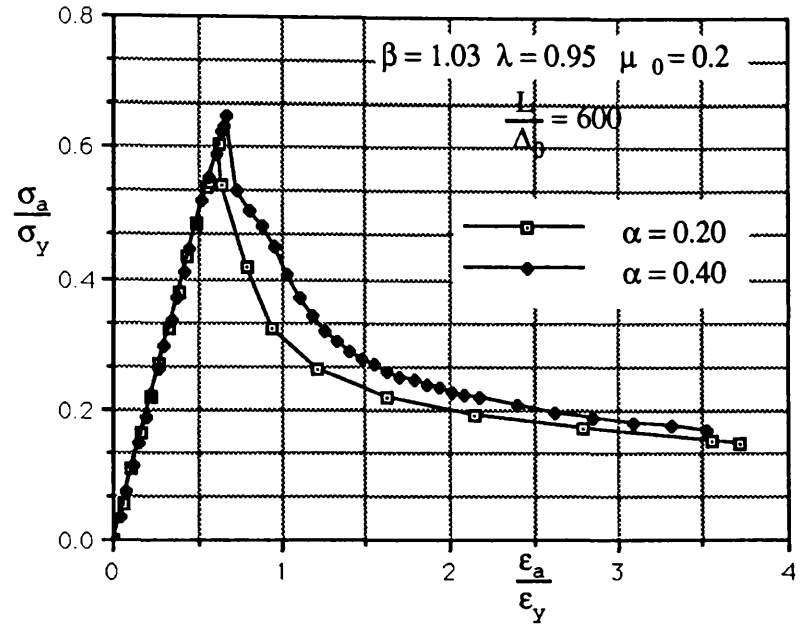

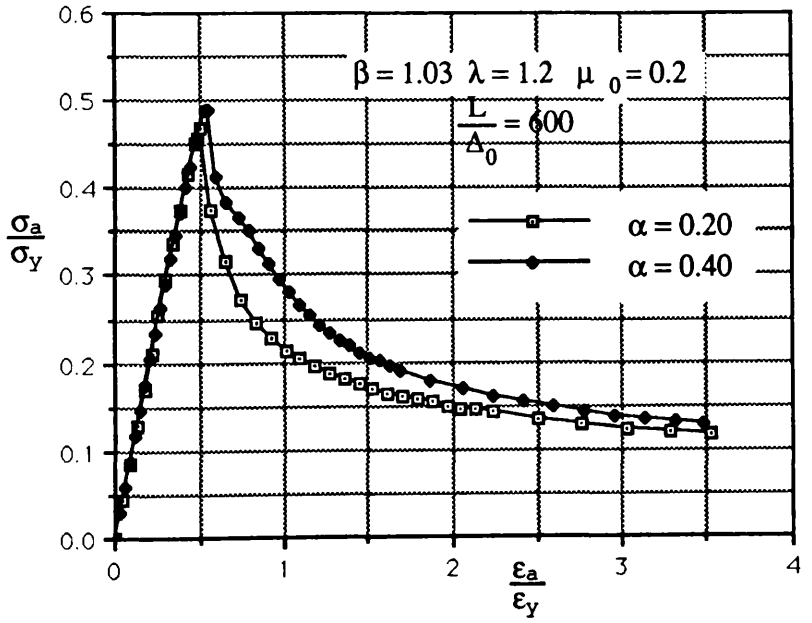

Figure 3.7.b Stress-strain curves.
Effect of stiffener to plate area ratio.

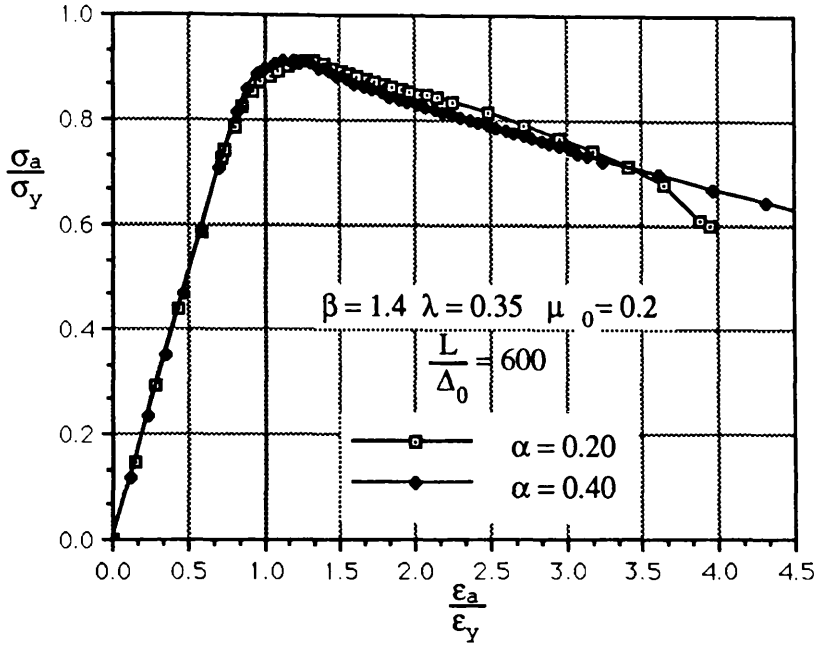

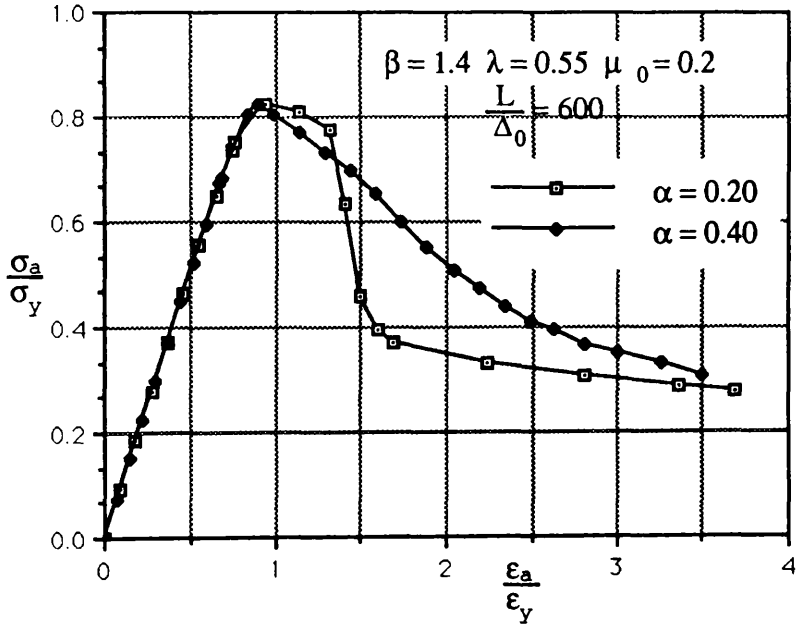

Figure 3.8.a Stress-strain curves.
Effect of stiffener to plate area ratio.

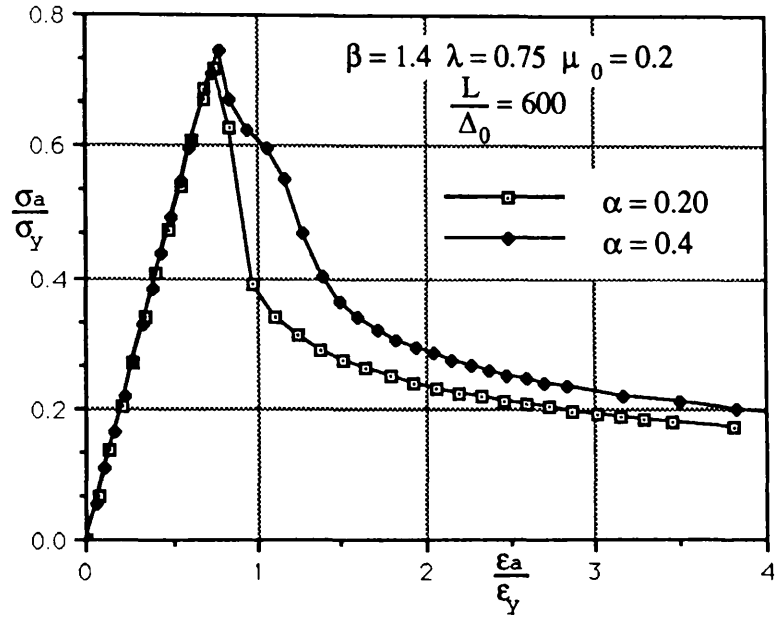

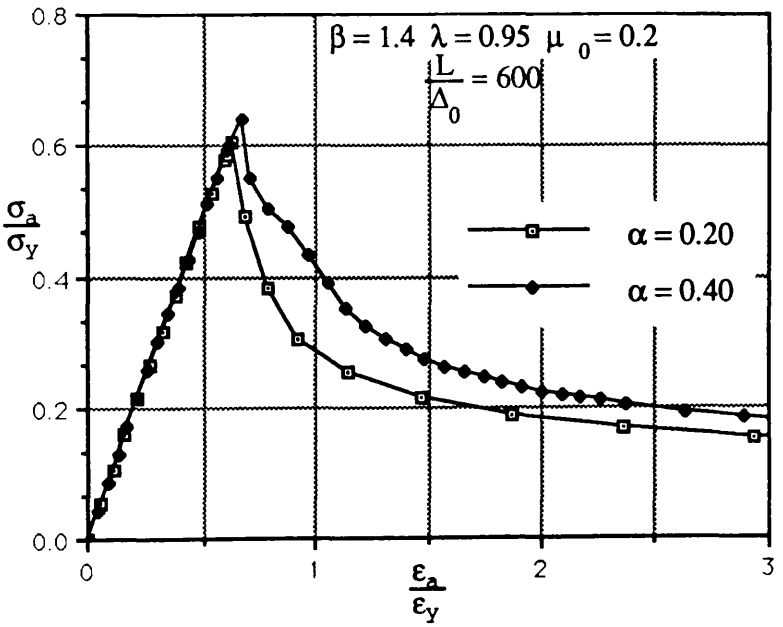

Figure 3.8.b **Stress-strain curves.**
Effect of stiffener to plate area ratio.

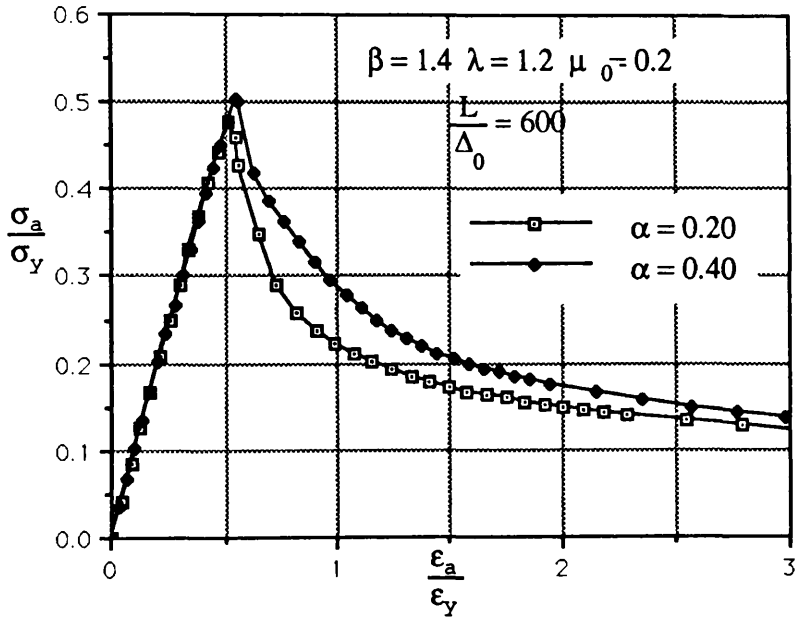

Figure 3.8.c Stress-strain curves.
Effect of stiffener to plate area ratio.

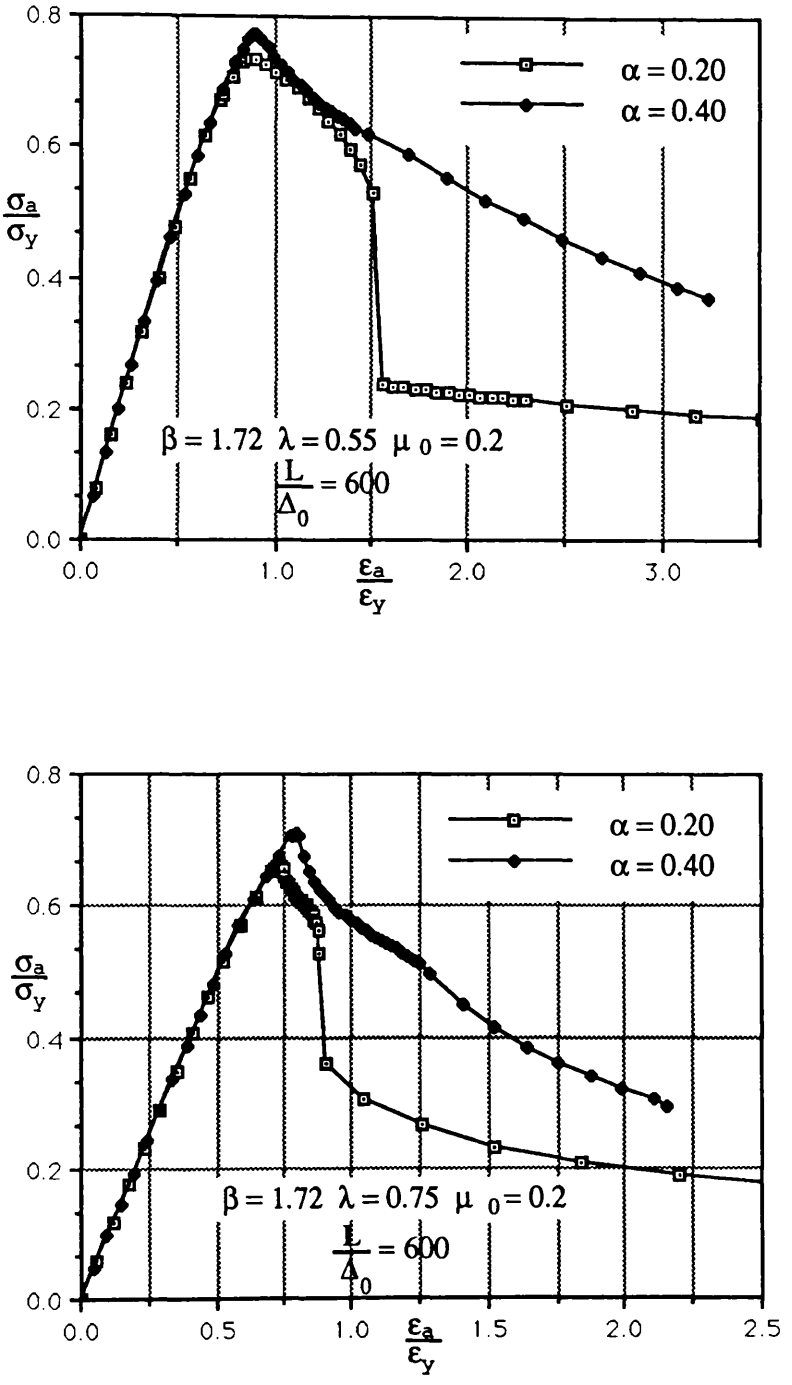

Figure 3.9.a Stress-strain curves.
Effect of stiffener to plate area ratio.

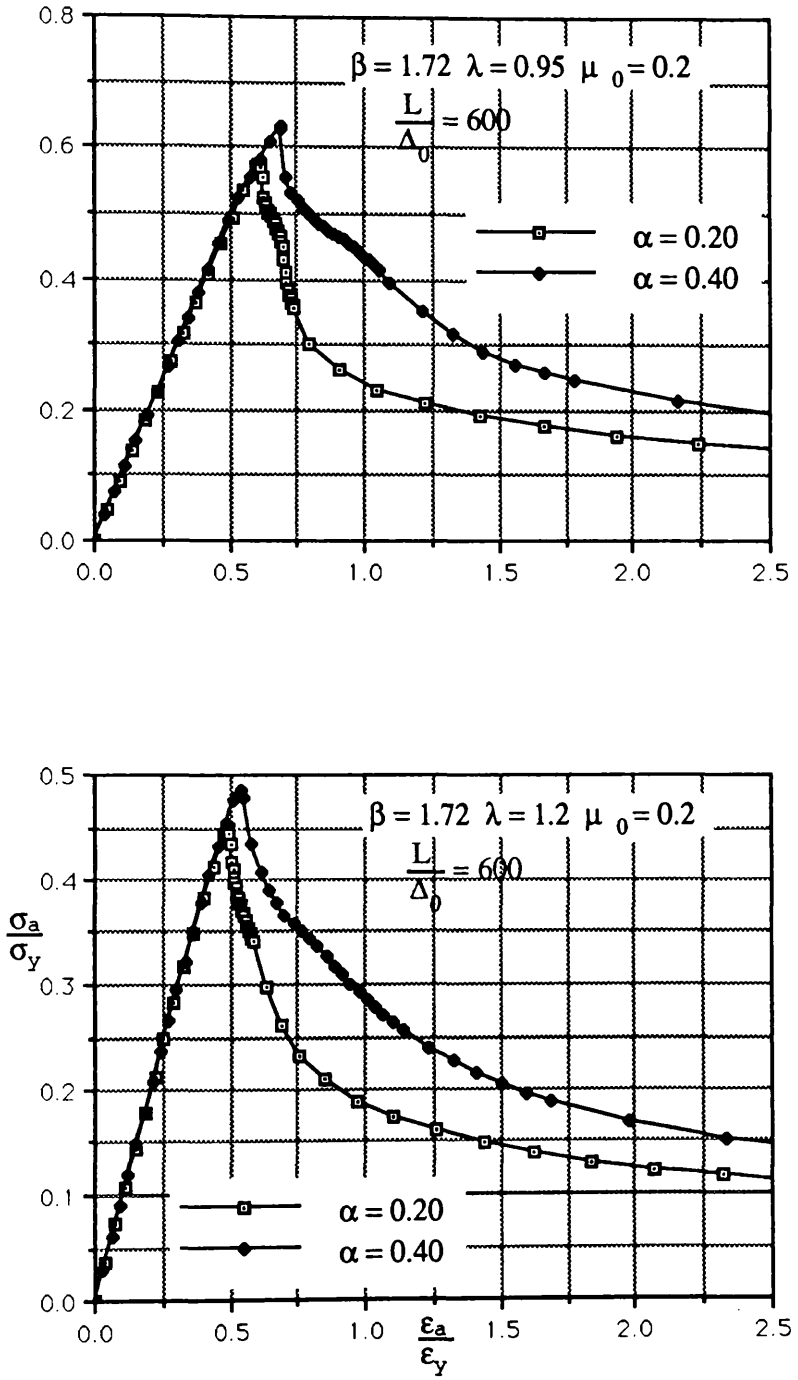

Figure 3.9.b Stress-strain curves.
Effect of stiffener to plate area ratio.

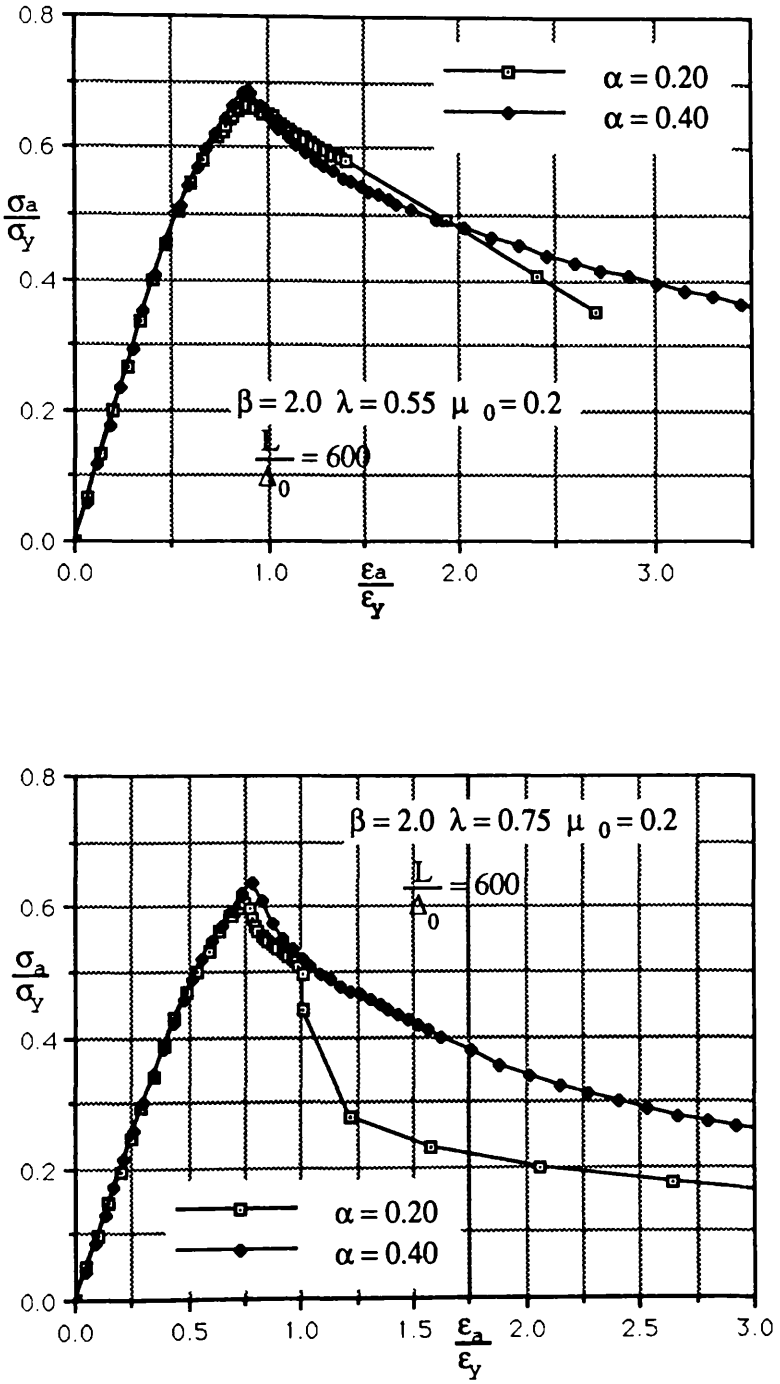

Figure 3.10.a **Stress-strain curves.**
Effect of stiffener to plate area ratio.

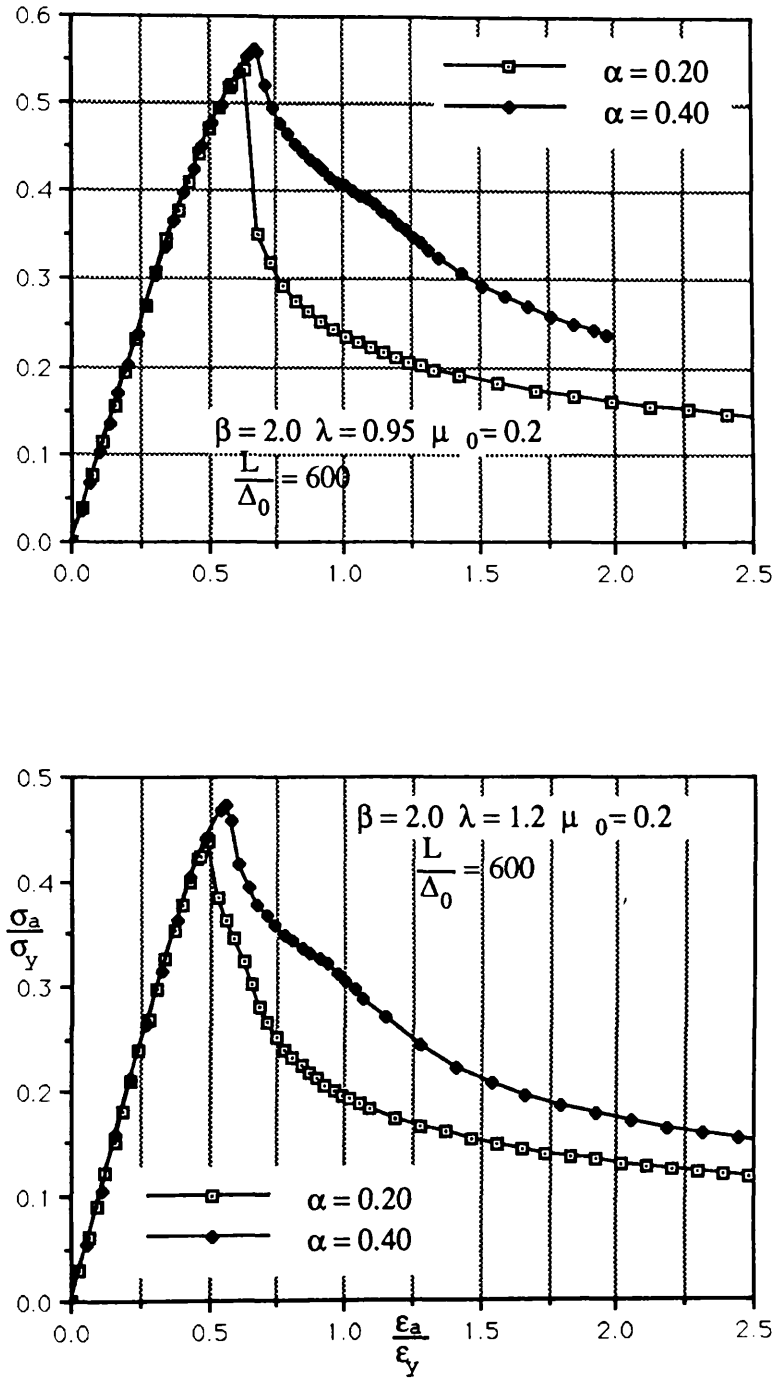

Figure 3.10.b Stress-strain curves.
Effect of stiffener to plate area ratio.

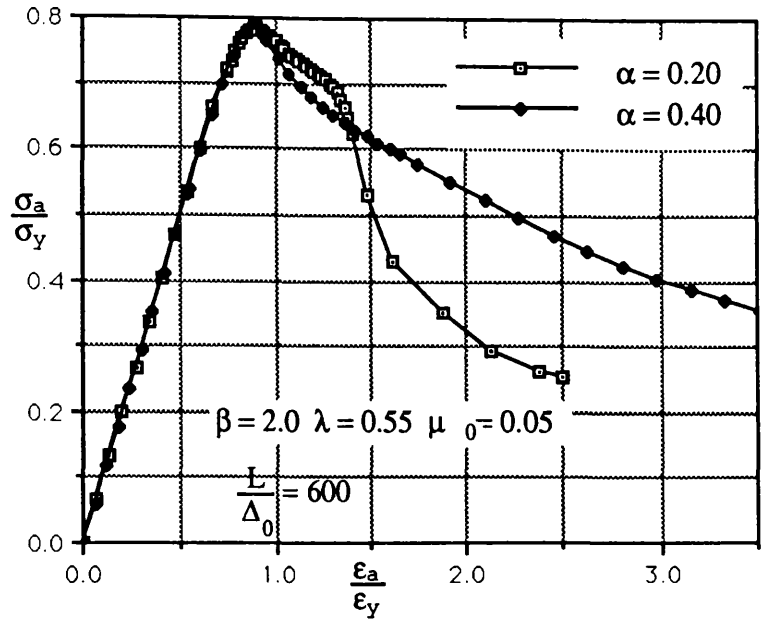

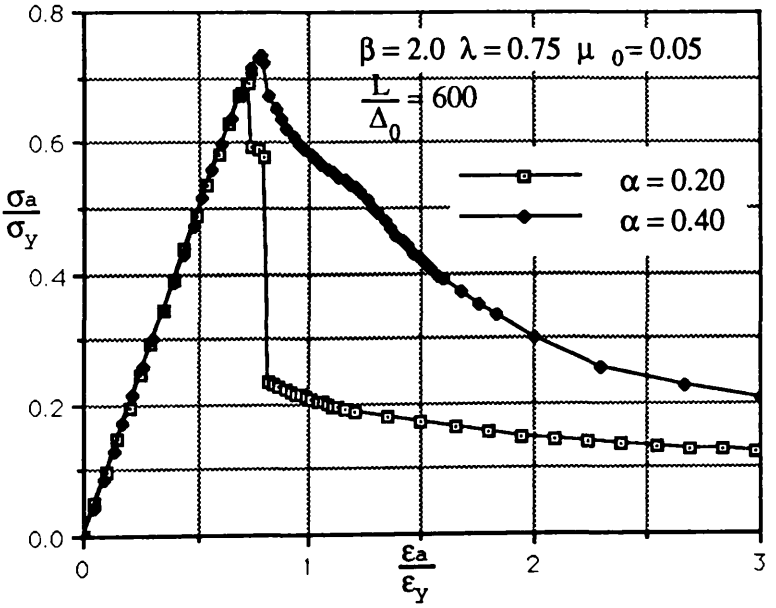

Figure 3.10.c Stress-strain curves.
Effect of stiffener to plate area ratio.

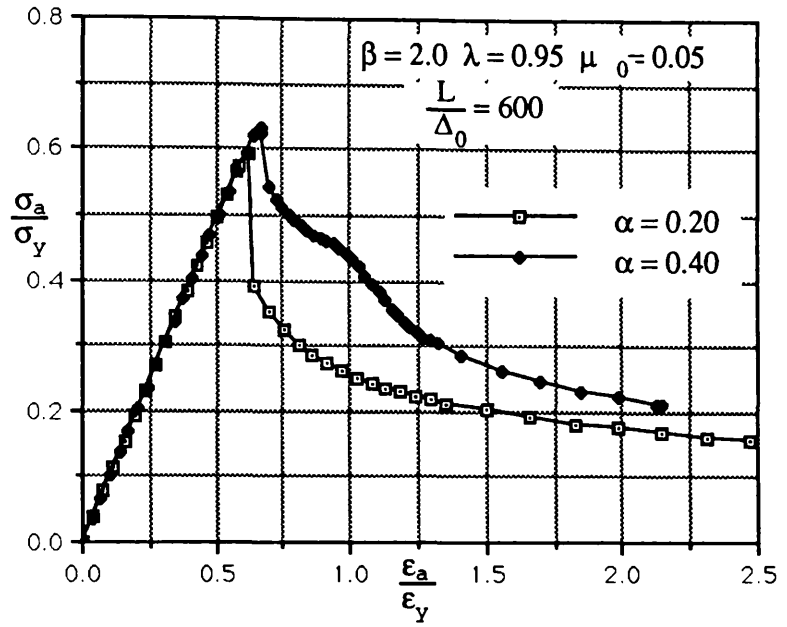

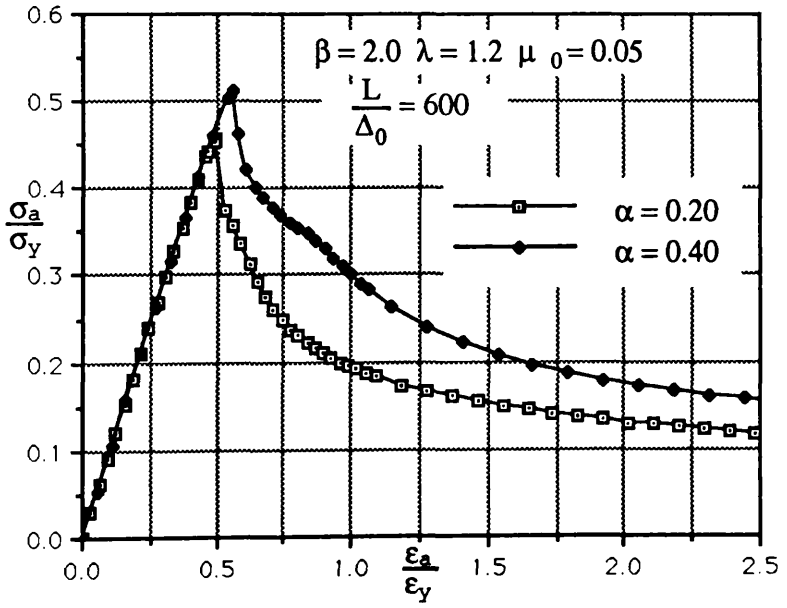

Figure 3.10.d **Stress-strain curves.**
Effect of stiffener to plate area ratio.

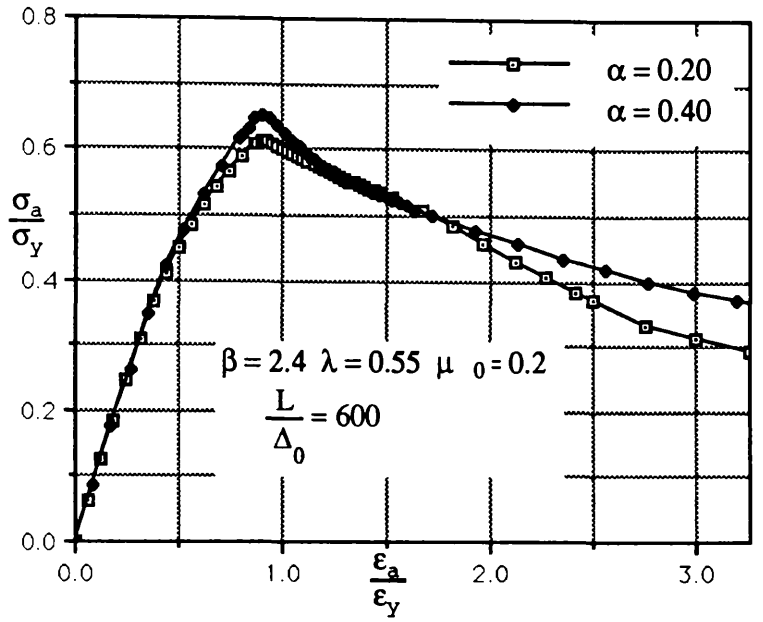

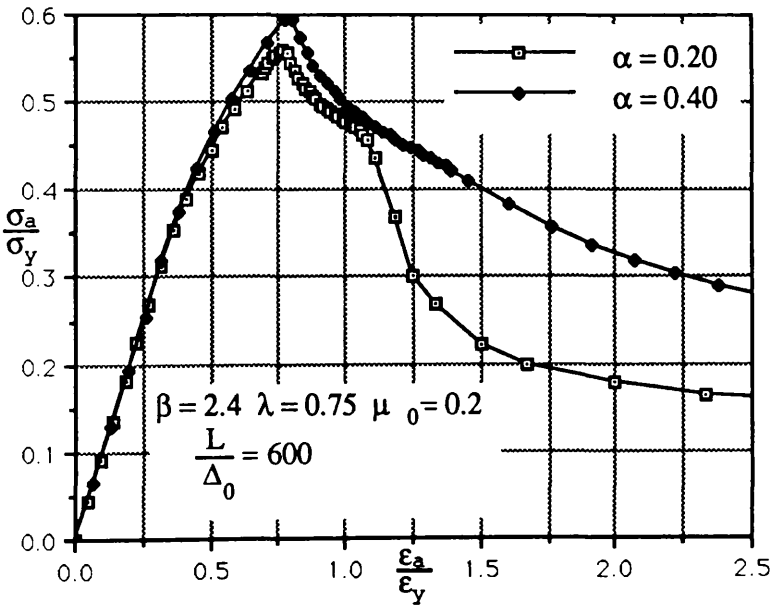

Figure 3.11.a **Stress-strain curves.**
Effect of stiffener to plate area ratio.

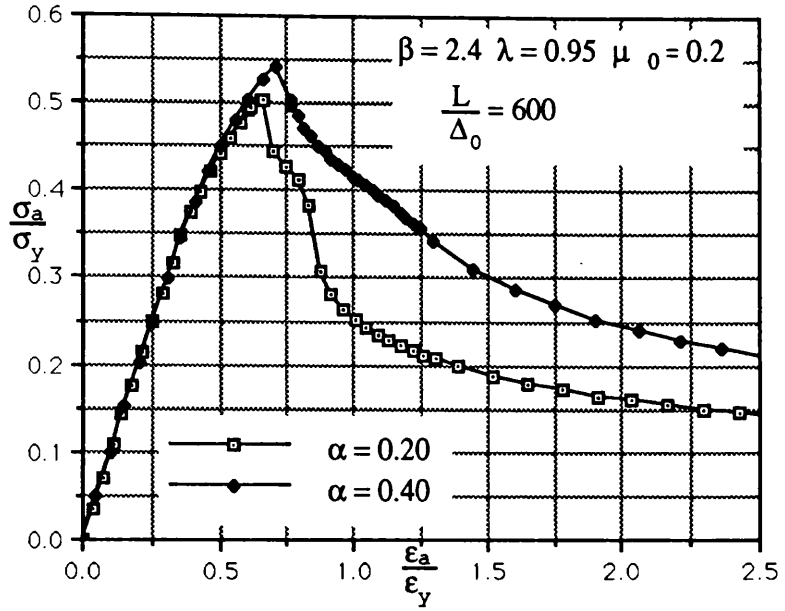

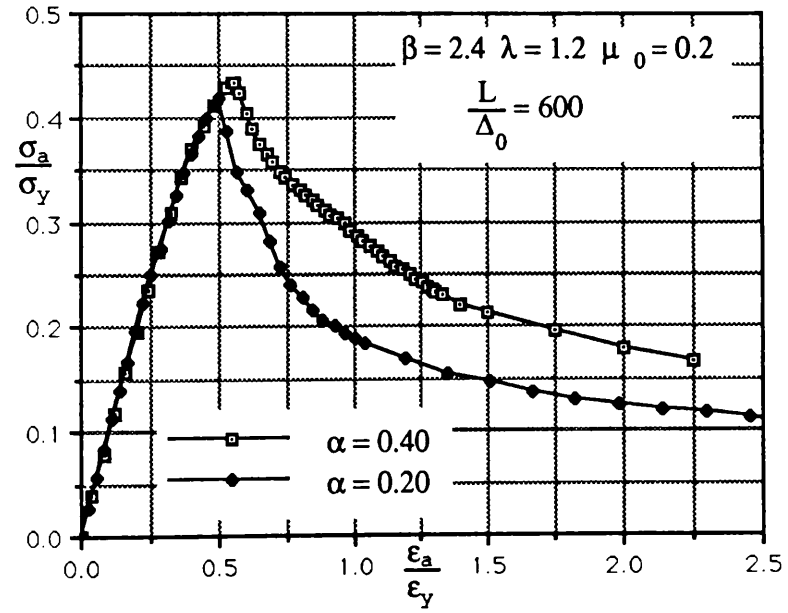

Figure 3.11.b **Stress-strain curves.**
Effect of stiffener to plate area ratio

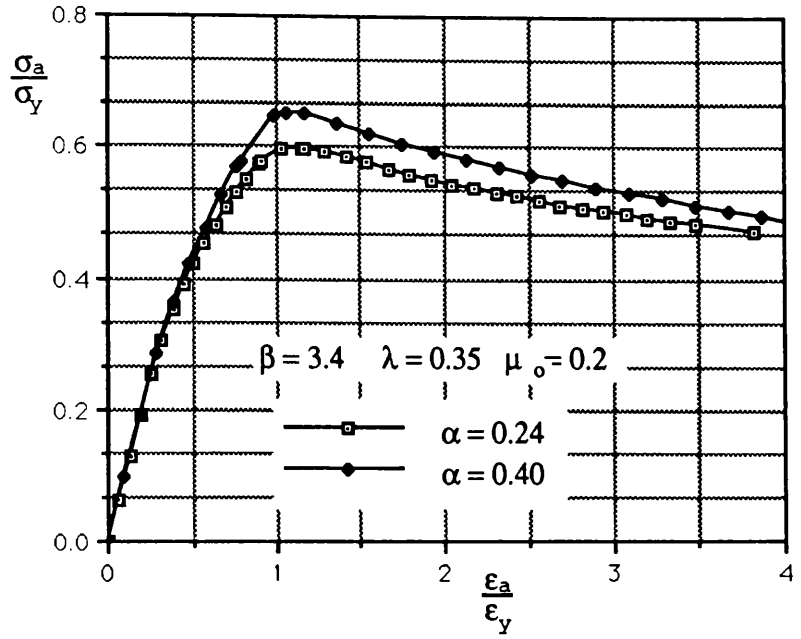

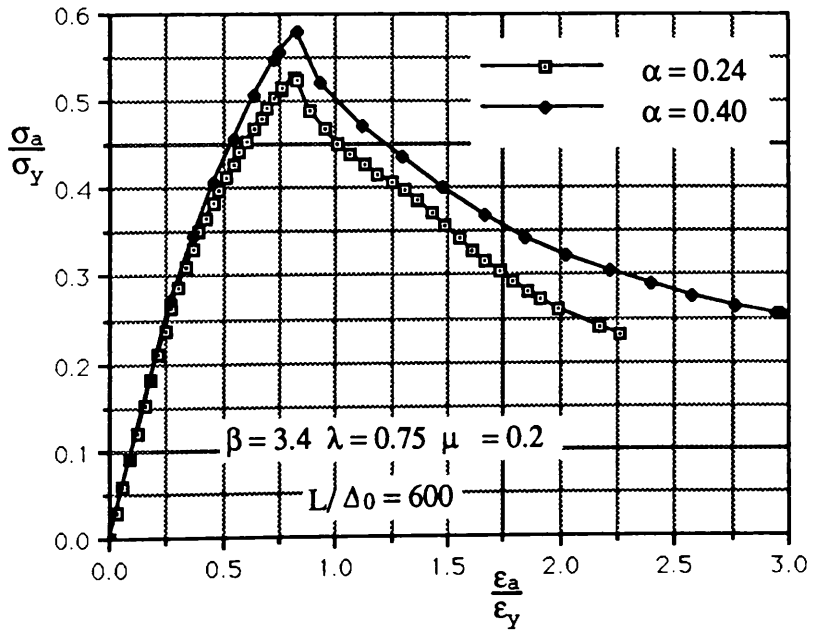

Figure 3.12.a Stress-strain curves.
Effect of stiffener to plate area ratio.

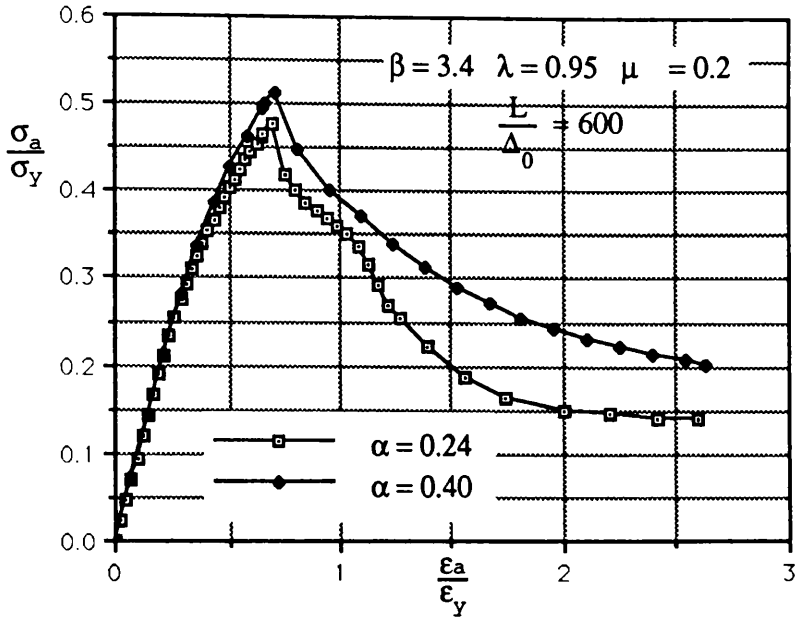

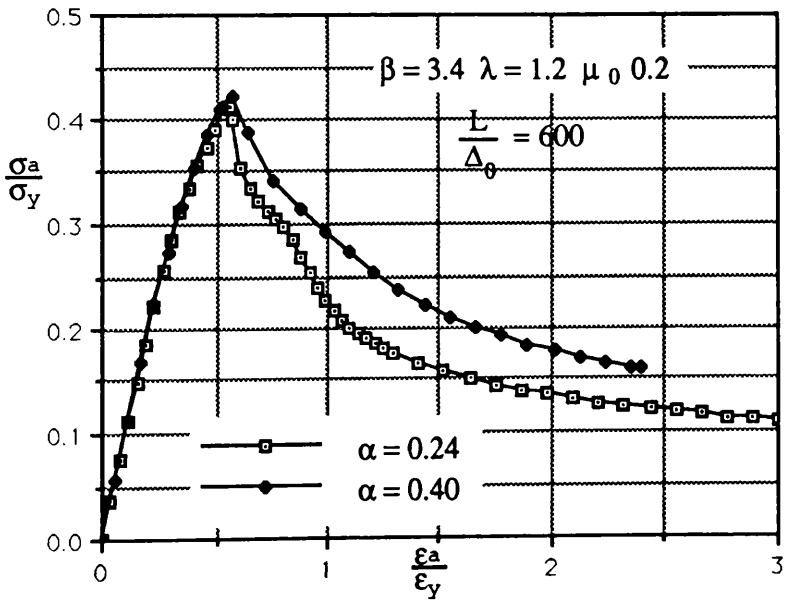

Figure 3.12.b Stress-strain curves.
Effect of stiffener to plate area ratio.

CHAPTER 4:

The Analytical Approach

4.1 Introduction:

Using the ARE program [28], a parametric analysis has been carried out to investigate the ultimate strength of stiffened panels under uni-axial stresses and the behaviour of the components before and after collapse. Using the results, simplified analytical modelling derived from a curve fit approach is suggested. Comparison with numerical and test results is presented.

Failure modes:

The failure modes considered in the present approach are :

(a) Failure by yielding.

(b) Plate instability.

(c) Interframe flexural buckling.

4.2 Least squares method:

To generate approximate equations for the ultimate strength and post-ultimate strength of stiffened panels based on a parametric study, the least squares technique is used.

The function $f(x_k, y_k, z_k)$ can be approximated to the function $g(x_k, y_k, z_k)$ in which the function g is assumed as follows:

$$g(x_k, y_k, z_k) = \sum_{j=1}^{j=MP} a_j \, p_j(x_k, y_k, z_k) \qquad (4.1)$$

where: a_j are numerical coefficients.

p_j are assumed polynomials.

The least squares method is based on the minimisation of the squares of the difference between the actual values and the assumed configuration, which leads to the following equation:

$$H = \sum_{k=1}^{k=N} \left[f(x_k, y_k, z_k) - g(x_k, y_k, z_k) \right]^2 = \text{minimum} \qquad (4.2)$$

Then :

$$\frac{\partial H}{\partial a_j} = 0 \qquad j = 1, MP \qquad (4.3)$$

which can be expressed as:

$$\sum_{k=1}^{k=N} \left[f(x_k, y_k, z_k) - g(x_k, y_k, z_k) \right] p_j(x_k, y_k, z_k) = 0 \qquad j = 1, MP \qquad (4.4)$$

$$g(x_k, y_k, z_k) = \sum_{j=1}^{j=MP} a_j \, p_j(x_k, y_k, z_k)$$

The system contains MP equations with MP unknown values $\{a_j\}$. This equation can be rearranged into the form :

$$\{a_j\}[A_{jm}] = \{C_j\} \qquad (4.5)$$

$$A_{jm} = \sum_{k=1}^{k=N} p_{mk} p_{jk} \qquad \text{where } m = 1, MP \quad j = 1, MP$$

$$C_j = \sum_{k=1}^{k=N} f_k p_{jk}$$

p_{jk} is element of the matrix containing the values of the assumed polynomials for the set of values (x_k, y_k, z_k), (j=1, MP, k=1, N).

N : Number of data of each set (f_k, x_k, y_k, z_k).

MP: Number of the assumed number of polynomial p_j.

The polynomial $p_j(x_k, y_k, z_k)$ can take any desired form in terms of the parameters x_k, y_k, z_k and also any desired number of these parameters.

4.3 The analytical approach:

4.3.1 Parametric analysis:

For the parametric analysis the range of factors affecting the ultimate

strength has been selected as follows:

Plate slenderness (β): $0.7 \leq \beta \leq 3.5$

Column slenderness (λ): $0.1 \leq \lambda \leq 2.0$

The plate initial distortion and residual stress were defined as one group into three categories: Low, moderate, and high values.

Initial distortion ($\delta_0/t\beta^2$) and residual stress (σ_r/σ_y): 0.05, 0.2, 0.4

Stiffener to plate area ratio ($\alpha=A_s/A_p$) : $0.2 \leq \alpha \leq 0.4$

Stiffener initial distortion (Δ_o/L) : $0.0005 \leq \Delta_o/L \leq 0.005$

Selecting the range of plate slenderness, column slenderness, initial plate distortion and residual stress for the following values of the other parameters:

$$\Delta_o/L = 0.001$$

$$\alpha = 0.3$$

4.3.2 The derived expressions for the ultimate strength:

Using the Finite Element Program (ARE), together with test results the maximum strength (σ_u/σ_y) of the stiffened panels was investigated over a range of plate and column slendernesses (Figs. 3.2).

Studying the graph shown in Figs. 3.2, the following analytical expressions for the maximum strength in terms of β, λ, and μ_o are derived using the least squares method and two cases are examined:

(1) Load following the shifting of the neutral axis:

For $1 < \beta \leq 1.6$ and $\lambda \leq 1.3$

$$\frac{\sigma_u}{\sigma_y} = e^{-0.7\mu_0}\left(-1.4\frac{\lambda}{\beta}+3\frac{1}{\beta}+0.9\frac{\lambda}{\beta^2}-2\frac{1}{\beta^2}\right) \tag{4.6}$$

For $1.0 < \beta \leq 1.6$ and $\lambda > 1.3$

$$\frac{\sigma_u}{\sigma_y} = e^{-0.7\mu_0}\left(0.1\frac{\beta}{\lambda}+0.06\frac{1}{\lambda}-0.2\frac{\beta}{\lambda^2}+0.7\frac{1}{\lambda^2}\right) \tag{4.7}$$

For $1.6 < \beta < 3.0$ and $\lambda \leq 1.3$

$$\frac{\sigma_u}{\sigma_y} = e^{-0.7\mu_0}\left(-0.8\frac{\lambda}{\beta}+2.0\frac{1}{\beta}+0.7\frac{\lambda}{\beta^2}-0.65\frac{1}{\beta^2}\right) \quad (4.8)$$

For $\beta > 1.6$ and $\lambda > 1.3$ ($\beta = 3.0$ When $\beta > 3.0$)

$$\frac{\sigma_u}{\sigma_y} = e^{-0.7\mu_0}\left(-0.04\frac{\beta}{\lambda}+0.25\frac{1}{\lambda}+0.05\frac{\beta}{\lambda^2}+0.42\frac{1}{\lambda^2}\right) \quad (4.9)$$

For $\beta \leq 1$, ($\beta = 1.0$ when $\beta < 1.0$

$K_{st} = 1$ and ($\mu_0 = 0.05$ when $\mu_0 \leq 0.2$) when $\lambda > 0.6$

$$\frac{\sigma_u}{\sigma_y} = K_{st}^{-0.25} e^{-0.1\mu_0}(1.17 - 0.55\lambda) \quad (4.10)$$

$K_{st} = 1$ when $\frac{h_w}{t_w} < 14$

$K_{st} = 1.1$ when $14 \leq \frac{h_w}{t_w} < 20$

$K_{st} = 2$ when $\frac{h_w}{t_w} > 20$

where K_{st} is tripping correction factor taken from test results.

Note when $\lambda > 0.6$ use $\mu_o = 0.05$ and $K_{st} = 1$ throughout.

For $\beta > 3.1$ and $\lambda < 1.3$

$$\frac{\sigma_u}{\sigma_y} = e^{-0.1\mu_0}(0.6 - 0.2\lambda) \quad (4.11)$$

(2) The load not following the shift of the neutral axis:

For $1 < \beta \leq 3.0$ and $\lambda \leq 1.3$ ($\beta = 3.$ when $\beta > 3.0$)

$$\frac{\sigma_u}{\sigma_y} = e^{-0.7\mu_0}\left(-0.5\frac{\lambda}{\beta}+2.6\frac{1}{\beta}-0.64\frac{\lambda}{\beta^2}-1.1\frac{1}{\beta^2}\right) \quad (4.12)$$

For $1.0 < \beta \leq 1.6$ and $\lambda > 1.3$

$$\frac{\sigma_u}{\sigma_y} = e^{-0.7\mu_0}\left(0.1\frac{\beta}{\lambda}+0.06\frac{1}{\lambda}-0.2\frac{\beta}{\lambda^2}+0.7\frac{1}{\lambda^2}\right) \quad (4.13)$$

For $\beta > 1.6$ and $\lambda > 1.3$ ($\beta = 3.0$ when $\beta > 3.0$)

$$\frac{\sigma_u}{\sigma_y} = e^{-0.7\mu_0}\left(-0.04\frac{\beta}{\lambda}+0.25\frac{1}{\lambda}+0.05\frac{\beta}{\lambda^2}+0.42\frac{1}{\lambda^2}\right) \quad (4.14)$$

For $\beta \leq 1$

Use equation (4.10) above.

Equations (4.10). was originally derived with no contribution to the collapse due to stiffener tripping failure. This type of failure is more likely to occur in short stiffeners with weak lateral torsional rigidity (narrow flanges), hence, a correction factor (K_{st}) in terms of web slenderness (h_w/t_w) accounting for the tripping of the stiffener has been introduced.

For low plate slenderness and a relatively moderate or high column slenderness, the effect of initial plate distortion and residual stress is likely to be negligible (Eq. 4.10).

For values of $3.0 \leq \beta \leq 3.5$, the value $\beta = 3.0$ should be used in the equations (4.9), (4.12) and (4.14) since the effect of the increase in β is in fact small. Using, for example, $\beta = 3.5$ in these equations would lead to a less accurate result..

4.3.2.1 Effect of other parameters:

The effects of column distortion and stiffener area are accounted for by equation (4.19) the other geometrical and material parameters is investigated with the assumption that these effects are independent..

Initial distortion:

Stiffener initial distortion reduces the strength, and the effect is more pronounced for moderate column slenderness. A correction factor R_w is used depending on column slenderness and Δ_o/L and λ .

$$\begin{aligned} R_w &= (W_0 - 1)(0.034 - 0.095\lambda) && \lambda \leq 0.9 \\ R_w &= (W_0 - 1)(0.034 - 0.095(1.8 - \lambda) && \lambda > 0.9 \end{aligned} \qquad (4.16)$$

$$\text{where } W_0 = \frac{\Delta_0}{L} 10^{+3}$$

Stiffener to plate area ratio:

As explained in section 3.3.5 of chapter 3, the stiffener to plate area ratio generally increases the maximum strength and the effect of this parameter

reveals a relatively different effect for different values of plate and column slendernesses. Taking this into account, a correction factor R_α to predict the strength for values of stiffener to plate area ratio different from $\alpha = 0.3$, is suggested:

The correction factor is expressed as follows:

1. For values of $\beta \geq 1.0$ and $\lambda \leq 1.0$

$$K_\alpha = 0.996\, e^{0.005\lambda}\, \beta^{0.04}$$

2. For values of $\beta < 2.0$ and $\lambda > 1.0$

$$K_\alpha = 1.0\, e^{0.005\lambda}\, \beta^{0.04}$$

3. For values of $\beta \geq 2.0$ and $\lambda > 1.0$

$$K_\alpha = 1.05 e^{0.005\lambda}\, \beta^{-004}$$

The correction factor R_α is expressed as follows:

(a) For values of $\alpha < 0.3$

$$R_\alpha = \frac{(-10\alpha+3)}{K_\alpha} - (10\alpha - 2) \qquad \text{where } \alpha = \frac{A_s}{A_p} \qquad (4.18)$$

(b) For values of $\alpha > 0.3$

$$R_\alpha = (10\alpha - 3)\, K_\alpha - (10\alpha - 4)$$

Finally, the ultimate strength will be expressed as:

$$\Phi = \frac{\sigma_u}{\sigma_y} R_\alpha + R_W \qquad (4.19)$$

4.3.2.2 Ultimate strain corresponding to maximum strength:

Using the previous parametric analysis with various ranges of plate slenderness (β), column slenderness (λ), residual stress and plate initial distortion with the other parameters taken at fixed values as follows:

Stiffener to plate area ratio α=0.3

Initial column distortion Δ_o/L=0.001

The strain at which the panel reaches its maximum strength is derived using a simple numerical approach in terms of the plate slenderness, column slenderness, residual stress and initial distortion. The results were fitted numerically using the least squares method.

$$\frac{\varepsilon_u}{\varepsilon_y} = 1.38\, e^{-0.8\lambda} \qquad (4.20)$$

Effect of other parameters:

Initial column deflection reduces the strength but on the other hand the effect on ultimate strain is more likely to be negligible. Residual stress in plating reduces the maximum strength which occurs at a greater strain. For various ranges of plate slenderness and column slenderness, the results show a different effect of residual stress and initial distortion on the ultimate strain, which are expressed as follows:

$$\Psi = \frac{\varepsilon_u}{\varepsilon_y} + 0.2(\mu_0 - 0.05) \qquad \beta > 1.0 \qquad (4.21)$$

$$\Psi = \frac{\varepsilon_u}{\varepsilon_y}\left(\frac{\mu_0}{0.05}\right)^{0.25} \qquad \beta \le 1 \quad \text{and} \quad \lambda \le 0.4 \qquad (4.22)$$

$$\Psi = \frac{\varepsilon_u}{\varepsilon_y} \qquad \beta \le 1 \quad \text{and} \quad \lambda > 0.4 \qquad (4.23)$$

where Ψ is the non-dimensional strain corresponding to the ultimate stress.

The analysis conducted using the Finite Element Program was performed for three levels of initial distortion and residual stress as discussed earlier.

The stiffener to plate area ratio shows a relatively small effect on ultimate strain and can be expressed as follows:

$$\Psi = \frac{\varepsilon_u}{\varepsilon_y} + 0.8\,\alpha^2 - 0.5\,\alpha - 0.2 \qquad \alpha = \frac{A_s}{A_p} \tag{4.24}$$

4.3.3 Post-buckling modelling:

4.3.3.1 Introduction:

Recent numerical methods using finite element or finite difference using dynamic relaxation techniques [30], [35], [36], [37], [38], [39] were used to investigate the non-linear behaviour of stiffened panels under uni-axial loads or combined loading to examine the effect of a number of geometrical and material parameters. These techniques are vital tools to analyse the behaviour before and after collapse. All methods use the beam-column modelling, generally with two approaches: one is to use an effective plating width and to limit the maximum stress to the yield stress, the other is to use a full effective plating and limit the stress to the maximum plate buckling stress.

The unloading path has been of interest to various researchers. The importance is clearly identified for system strength analyses and for associated reliability analyses. Due to the complexity of the non-linear problem, reliability studies are more complicated.

The present report proposes a simplified modelling for the analysis of the ultimate strength of stiffened panels and the behaviour before and after collapse is introduced.

4.3.3.2 Unloading strength path:

The unloading pattern is simplified to a piece-wise linear formulation as shown in Fig. 4.1. The tangentional stiffness is estimated from simplified modelling which incorporates as necessary the effects of column slenderness, plate slenderness, stiffener to plate area ratio, residual stress and plate initial distortion. The following expressions for the parameters describing the straight lines pattern shown in Fig. 4.1 are suggested as a result of extensive numerical studies:

$$\bar{E} = -0.525\,\beta^{-0.5}\lambda^{2}\alpha^{-0.6}e^{-0.2\mu_o} \qquad \text{For } \beta \le 1.6 \text{ and } \lambda \le 0.8 \qquad (4.25)$$

$$\frac{\Phi_r}{\Phi} = 0.24\,\frac{1}{\lambda}\,\beta^{-0.3}\alpha^{0.08}e^{-0.2\mu_o}$$

$$\bar{E} = -(1.29-1.27\alpha)(\lambda+0.2)^{-1.9}e^{-1.2\mu_o} \qquad \text{For } \beta \le 1.6 \text{ and } 0.8 \le \lambda \le 2.0 \qquad (4.26)$$

$$\frac{\Phi_r}{\Phi} = 0.27\,\lambda^{0.34}\beta^{0.4}\mu_o^{0.025}\alpha^{0.08}$$

$$\bar{E} = -1.220\,\beta^{-1.5}\lambda^{1.8}\alpha^{-0.7}e^{-2.6\mu_o} \qquad \text{For } 1.6 \le \beta \le 3.5 \text{ and } \lambda \le 1 \qquad (4.27)$$

$$\frac{\Phi_r}{\Phi} = 0.24\,\frac{1}{\lambda}\,\beta^{-0.3}\alpha^{0.08}e^{-0.2\mu_o}$$

$$\bar{E} = -(1.22-1.47\alpha)(\lambda)^{-1.9}\beta^{-0.4}e^{-1.2\mu_o} \qquad \text{For } 1.6 \le \beta \le 3.5 \text{ and } 1 \le \lambda \le 2 \qquad (4.28)$$

$$\frac{\Phi_r}{\Phi} = 0.27\,\lambda^{0.34\ 0.4}\mu_o^{0.025}\alpha^{0.08}$$

The non-dimensional strain at which the panel reaches its "residual" strength (Φ_r) can be estimated from the linear relation:

$$\frac{\Phi_r - \Phi}{\Psi_r - \Psi} = \bar{E} \qquad \text{or} \qquad \Psi_r = \frac{\Phi_r - \Phi}{\bar{E}} + \Psi \qquad (4.29)$$

4.3.3.3 Loss of plate stiffness before collapse:

The panel shows an overall loss of stiffness due to local plate loss of stiffness, which is more pronounced in stocky plating in the presence of residual stresses and in slender plating caused by buckling.

It has been seen from a series of finite element numerical results that the panel commences the loss of stiffness at a non-dimensional strain (Ψ_s) approximately equal to $k\Psi$ with a non-dimensional load ($\Phi_s \cong \Psi_s$) . In this present approach, it is assumed that when the non-dimensional strain reaches this point, the overall stiffness reduces linearly until peak load. The factor k is defined as follows:

(a) For low values of initial distortion and residual stress:

$\beta \le 2.6$ $\qquad$ $k = 0.9$

$$2.6 < \beta \leq 3.5 \qquad k = 0.6 \qquad (4.30)$$

(b) For moderate values of initial distortion and residual stress:

$$\left.\begin{array}{ll} \lambda < 0.5 & k = 0.65 \\ 0.5 \leq \lambda \leq 0.8 & k = 0.85 \\ \lambda > 0.8 & k = 0.95 \end{array}\right\} \quad \beta \leq 2.6 \qquad (4.31)$$

$$2.6 \leq \beta \leq 3.5 \quad \lambda < 0.5 \qquad k = 0.4$$

(c) For severe values of initial distortion and residual stress:

$$\left.\begin{array}{ll} \lambda < 0.9 & k = 0.45 \\ \lambda \geq 0.9 & k = 0.95 \end{array}\right\} \quad \beta \leq 2.6 \qquad (4.32)$$

$$\beta > 2.6 \qquad k = 0.25$$

In cases (a), (b) and (c) the relation must be satisfied:

$$\text{When } k \leq \frac{\Phi}{\Psi}, \quad k \text{ should take the value } k = \frac{\Phi}{\Psi}$$

The non-dimensional tangent stiffness (E^+) will be defined by the expression:

$$E^+ = \frac{\Phi - k\Psi}{\Psi(1-k)} \qquad (4.33)$$

Finally, the non-dimensional load (σ_a/σ_y) can be expressed by the linear relation:

$$\frac{\sigma_a}{\sigma_y} = A + B\frac{\varepsilon_a}{\varepsilon_y} \qquad (4.34)$$

where A and B are defined as follow:

$$\left.\begin{array}{l} A = 0 \\ B = E^* \end{array}\right\} \quad 0 \leq \frac{\varepsilon_a}{\varepsilon_y} \leq \Psi_s$$

$$\left.\begin{array}{l} A = k\Psi(1-E^+) \\ B = E^+ \end{array}\right\} \quad \Psi_s \leq \frac{\varepsilon_a}{\varepsilon_y} \leq \Psi$$

$$\left.\begin{array}{l} A = \Phi - E^-\Psi \\ B = E^- \end{array}\right\} \quad \Psi \leq \frac{\varepsilon_a}{\varepsilon_y} \leq \Psi_r$$

$$\left.\begin{array}{l} A = \Phi_r \\ B = 0 \end{array}\right\} \quad \frac{\varepsilon_a}{\varepsilon_y} \geq \Psi_r$$

The variables E+, E-, Φ, Ψ, Φ_r, Ψ_r, and k are previously defined by equations : (4.33); (4.25, 4.26 and 4.27); (4.19); (4.24); (4.25, 4.26 and 4.27); (4.29); (4.30, 4.31 and 4.32), respectively.

4.4 Variables governing the modelling:

4.4.1 Plate slenderness (β):

Plate slenderness is defined by the expression:

$$\beta = \frac{b}{t}\sqrt{\frac{\sigma_{yp}}{E}}$$

The expression includes the width to thickness ratio and material parameters: Yield stress and Young's modulus of the plating. Guedes Soares [33] presented a statistical description of plate dimensions for the cases of tankers and frigates, which is reproduced in Fig. 4.4. The author noted that the distributions are different for each ship type. In the case of tankers b/t ranges from 20 to 90 with a mean value of 60, for frigates b/t ranges from 20 to 110 with values up to 180, the mean value is 46. The mean values correspond to slenderness (β) of 2.0 and 1.5 respectively for tankers and frigates. For warships, Smith [30] stated that in existing British warships, the plate slenderness (β) ranges from 1.0 to 4.5. A preliminary survey [62] of flight decks in existing British warships and ships of the Royal Fleet Auxiliary was conducted to establish the approximate ranges of the variables involved. β was found to lie between 1.0 and 4.0 with most values below 3.5, a/b covered the range 1.0 to 8.0. Values of $\beta > 4.0$ may occasionally be found in practice (corresponding to b/t =120 in mild steel) but continuation of the parametric analysis beyond plate slenderness corresponding to the value 3.5 was not considered because of the limitation of the program to values of b/t = 90. In this analysis the range (0.7 to 3.5) has been adopted for the slenderness (β).

4.4.2 Column slenderness (λ):

Column slenderness is defined as:

$$\lambda = \frac{L}{\pi r}\sqrt{\frac{\sigma_e}{E}}$$

L -the length of the span between transverses.

r -radius of gyration of longitudinals with fully effective breadth of

plating.

E -Young's modulus.

σ_e -the equivalent yield stress for the combined cross-section.

It should be noted that the results derived using the ARE Program [28], [29] to obtain the present approach account for the effective breadth, and the radius of gyration for the use in the simplified method should be estimated using a fully effective breadth.

An approximate expression accounting for the yield stress of the stiffener and the plating is suggested and takes the following form:

$$\sigma_e = \frac{\sigma_{yp} A_p + \sigma_{ys} A_s}{A}$$

Smith [30] outlined that the column slenderness for existing British warships falls in the range interval (0.15 to 0.9). During the present method the range (0.1 to 2.0) has been adopted for the column slenderness (λ).

4.4.3 Plate residual stress and initial distortion:

It has been postulated during the discussion on the effect of these two parameters, that the ARE programs use numerical data for accounting for local plate instability. These numerical data depend upon the plate slenderness and the magnitude of residual stress and initial distortion. However, only three levels of residual stress and initial deformation have been considered, cited as follows:

Level 1. Low values, $\delta_o/t\beta^2 \leq 0.05$ and $\sigma_r/\sigma_y \approx 0.05$ $\mu_0 = 0.05$

Level 2. Moderate values, $\delta_o/t\beta^2 \approx 0.15$ and $\sigma_r/\sigma_y \approx 0.2$ $\mu_0 = 0.2$

Level 3. High values, $\delta_o/t\beta^2 \approx 0.3$ and $\sigma_r/\sigma_y > 0.4$ $\mu_0 = 0.4$

This effect is incorporated using a parameter (μ_o) which accounts for both effects.

Faulkner [31], from the theory of welding contractions and confirmed by a series of measurements of initial distortions in warships, indicated that initial distortion takes the form:

$$\frac{\delta_0}{t} = K\beta^2 \qquad K = 0.12 \text{ when } \beta < 3 \quad \text{and} \quad K = 0.15 \text{ when } \beta > 3$$

Other researchers [32] conducted measurements of initial distortions in merchant ships and suggested the following expression which is linear with b/t:

$$\frac{\delta_0}{t} = 0.0094\,(\frac{b}{t}) - 0.205$$

Other surveys of plate initial distortions in ships can be found in references [30], [44] and [45].

In this modelling, the form $\delta_0/t = K\beta^2$ is used depending on the level of residual stress and initial distortion, and any magnitude of residual stress and initial distortion should be identified to one of the three levels previously defined.

4.4.4 Stiffener initial distortion:

Design values of stiffener initial distortion can be used like those in the Merrison rules [40] which proposed tolerances $L/\Delta = -1200$ and $+900$. A Suggested design values of $L/\Delta_o = 750$ is is used in the new UK Bridge Codes [41] and by the European recommendations for Steel Construction [42], [43]. Reference [44] presented tolerances of initial distortions based upon surveys of frigate structures with a mean value (Δ_o) equal to 0.0025 L.

Stiffener initial imperfection (Δ_o/L) seems to lie in the range (0.005:0.0003). The mode of the imperfection adopted in the analysis is a half sinusoidal mode accounting for the interaction of the adjacent span, as shown in Fig. 2.1.

4.4.5 Eccentricity of the applied load:

Load eccentricity represents an unknown quantity in most test data. An error in the position of the applied load can influence the direction of buckling. In the present approach the term eccentricity (E_C) refers to whether the load is considered to follow, or not follow, the shifting of the neutral axis. When the term E_C is positive (Eccentricity toward the

plating) the assumption that the load follows the shift of the neutral axis, while for fixed load which does not follow the shift of the neutral axis the term E_c is negative or equal to zero (eccentricity zero or toward the stiffener).

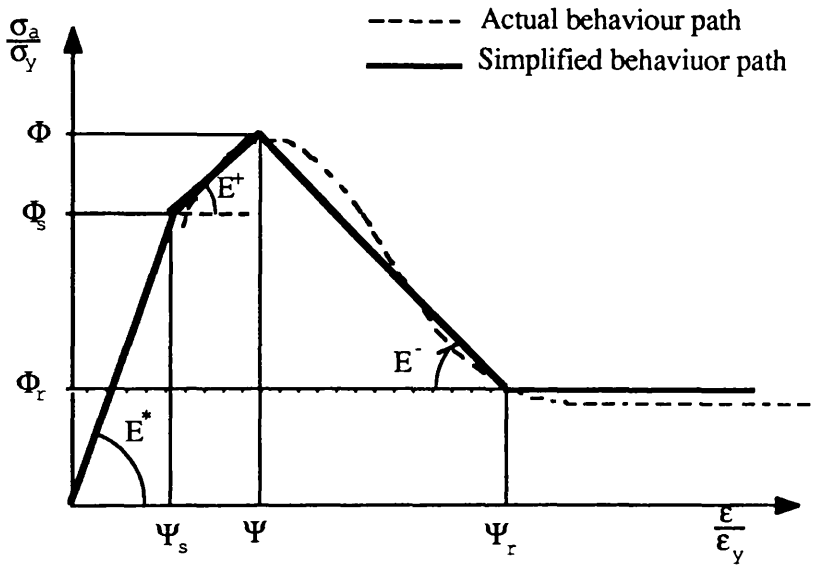

Figure 4.1 Linear modelling of the stress-strain curves

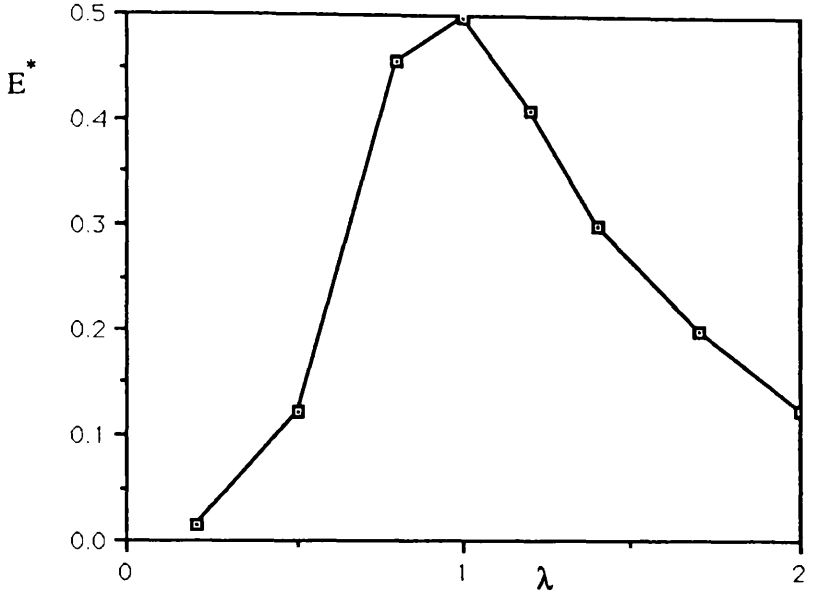

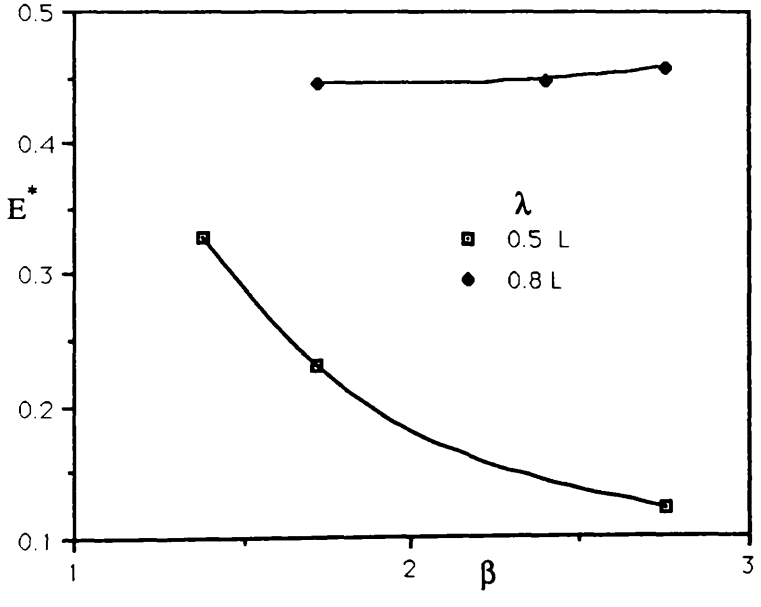

Figure 4.2.a Stiffness of the combined plate-stiffener During post-buckling

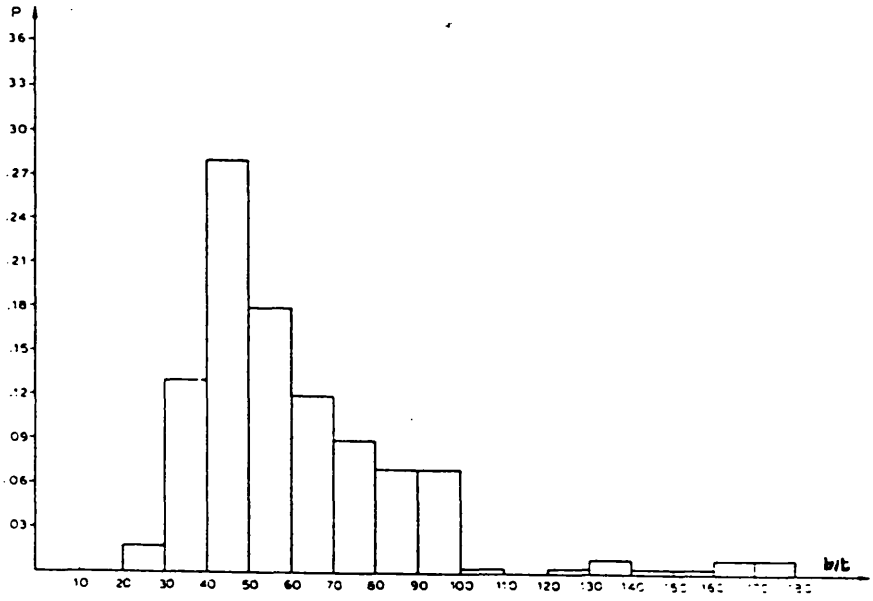

Frigates

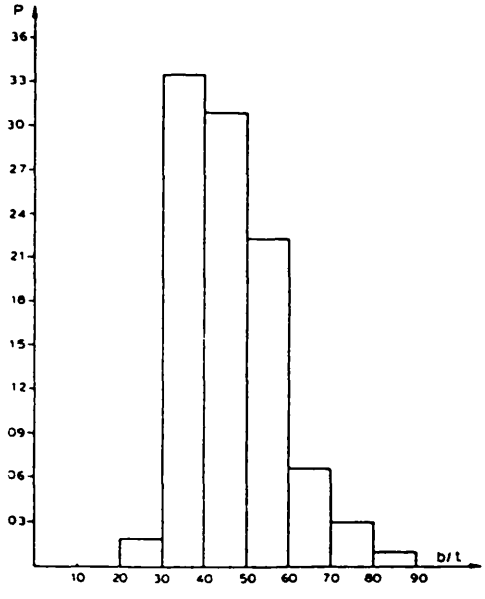

Tankers

Figure 4.4 **Probability density distribution of plate slenderness in frigates and tankers.**

CHAPTER 5

Correlation with test and numerical results

5.1 Maximum-load capacity:

5.1.1 Correlation with test results :

Lloyd's Register of Shipping commissioned a study and a Technical Report [34] in which the authors provided a discussion and comparison of four approaches: Cambridge, Manchester, Monash and Imperial College methods for obtaining the ultimate strength of stiffened panels under uni-axial loading. Comparing the methods with the existing test results and after accounting for modification to the methods, the authors concluded that the Imperial College approach was the most satisfactory and has therefore been used as the basis for deriving the method for use by Lloyd's Register. A later review [66] included the RN College test data [65] and concluded that the formulation of Faulkner [31] in fact give the best statistical fit of any to the worlds reputable test data. Nevertheless, an attempt is made to compare the present suggestion with test results and with the four approaches and the test results. For the purpose of comparison an absolute error band of 15% is suggested.

5.1.1.1 Manchester Tests:

The Manchester tests were conducted to investigate the influence of a number of different parameters. The panels were of single span and were allowed to pull in on the unloaded edges. Since the present method is derived for only pinned loaded edges the comparison was limited to this boundary constraint.

Geometrical and material parameters, together with analytical and test results, are presented in Tables 5.2.a and 5.2.b respectively. The results show a good agreement with the test results and only two models fall outside the suggested error band: Panels D12(-17.5%) and D11(-18.9%). This may be due to residual stresses in the plating since intermittent

welding is less severe than continuous welding. For low residual stresses, the errors for panels D12 and D11 are -6.2 and -12.1% respectively.

5.1.1.2 RN College tests:

These 65 models [65] were of single span construction, simply supported on the loaded edges and free to deflect out-of-plane on the unloaded edges. All stiffeners were welded continuously to the plating and the load was aligned with the initial neutral axis. Details of these models and the comparisons are shown in Tables 5.1.a and 5.1.b respectively.

Four results fall outside the suggested error band; panels P21(-32.3%), F2(-21.0%) and P9(-17.5%), panel P21 shows a poor correlation for all five methods but ref.[65] suggest this test result should be discarded as the model had a high but unknown yield stress. For panels P9, F2 and F3, the results underestimate the measured strength. This is may be due to the high measured stiffener initial deformations, Δ_o/L= 0.004, Δ_o/L= 0.005 and Δ_o/L= 0.004 respectively. Using the Imperial College design values Δ_o/L = 0.001 and Δ_o/L = 0.001 will improve the results to errors of 8.1, -11.5 and 7.8%. However, this is not the case for panel F4 which has similar geometrical configurations. Using the Imperial College design value Δ/L= 0.001 will give an error of 20.9%. Panel T2 has a measured initial distortion of Δ/L= 0.0004 which is a low value . Here again using a design value of Δ/L = 0.001 improves the result to an error of 10.4%. It must be restated, however, that agreement of these test data with a structural tangent modulus and effective width approach [31] is very much better [66].

5.1.1.3 The Imperial College Tests:

These models were laterally restrained on the unloaded edges. Details of the models and collapse load results can be found in Tables 5.3.a and 5.3.b. All the methods show satisfactory results. In addition, the results show that for these models the lateral restraint boundary condition has a negligible effect on the collapse load.

5.1.1.4 ARE tests:

Smith [30] presented a series of tests on full scale welded grillages. The author outlined a clear discussion of the collapse of the models describing the modes of failure. The grillages represented typical warship deck and single bottom structures under compressive load combined in some cases with lateral pressure.

Grillages 1a, 2b, 3b, 4a, 5, 6, and 7 were chosen for the correlation because they were tested with no contribution from lateral pressure.

The first four grillages represent possible ship bottom structures, panels (5 and 7) represent frigate strength decks, and grillage number 6 corresponds to a light superstructure deck. Details of the panels are shown in Table 5.4.

In general, the results obtained using the present method show a good agreement with the test results within an error of 15%. However, the mode of failure is different since the present method does not account for overall grillage instability and tripping of the stiffener, and this latter failure mode is restricted to panels with low values of plate and column slenderness and high values of stiffener slenderness (h_w/t_w).

Failure of grillage 1a was preceded by buckling of the plate panel accompanied by a significant loss of plating stiffness which is well predicted by the present method. However, collapse of grillage 1a finally occurred by interframe tripping of longitudinal stiffeners. This test has been reanalysed recently [61] and the reference is recommended to those seeking a better understanding of interactive plate buckling and stiffener tripping.

Collapse of grillage 2b occurred by interframe buckling of longitudinals associated with inelastic buckling of plate panels. The mode of collapse of this panel was well predicted by the present approach.

Failure of grillage 3b occurred by upward flexural buckling of longitudinals, accompanied by downward buckling in the adjacent span. This type of failure is the basic modelling considered in the Finite

Element Program [28] used to generate this simplified modelling.

Failure of grillage 4a occurred by flexural buckling of the longitudinals and sideways tripping of deep fabricated girders, accompanied by local inelastic buckling of the plating and of the webs of deep girders. The present approach is restricted to the failure type occurring by flexural buckling of longitudinal stiffeners, accompanied by local inelastic buckling of plating. Again, ref [61] offers a fuller discussion of this grillage.

Failure of grillage 5 was preceded by buckling of the plate panel, and occurred by interframe buckling of longitudinals.

Failure of grillage 6 occurred by overall instability involving upward and downward bending of transverse frames as well as longitudinal girders. The failure was preceded by buckling of plate panels.

The type of failure of grillage 7 was similar to the one of grillage 5.

Finally, a histogram configuration showing a distribution of the results for 75 tests is presented (Figs. 5.1.a and 5.1.b).

5.2 Post-buckling strength:

5.2.1 Test results:

A comparison is made with test results presented in the technical report [6], as shown in Figs. 5.2.a, 5.2.b and 5.2.c and the results indicate a good correlation with those of the tests for models 11 and 15. However, this is not the case for models 19 and 29, shown in Fig. 5.2.b in which the test results present a more severe unloading pattern. This may be due to the tripping of stiffeners which influences the mode of collapse of the panel. It should be noted that tripping is not included in the finite element analysis.

5.2.2 Numerical results:

5.2.2.1 Correlation with the finite element method:

Present modelling is compared with the results derived using the ARE non-linear finite element program [28] and the results are shown in Figs. 5.3.a, 5.3.b, 5.3.c and 5.3.d. In general the present modelling reveals a

good correlation with the finite element results.

5.2.2.2 Correlation with the dynamic relaxation technique:

Results derived using finite differences with the dynamic relaxation technique [52] are compared with the present simplified approach. Panels of b/t = 30, α= 0.2 and b/t = 60, α = 0.4 are selected for comparison. Results are presented in Figs. 5.4.a and 5.4.b. Correlation shows a reasonable agreement with a mean value of error -1.8% and a standard deviation of 8.0%.

Model Number	b mm	t mm	h_w mm	t_w mm	b_f mm	t_f mm	L mm	MEASURED Δ_0 (mm)	δ_0
P1	88.4	3.07	17.4	4.88	12.7	6.17	244.0	0.05	----
P2	147.0	2.62	30.4	4.83	12.7	6.22	384.0	0.04	----
P3	221.0	2.54	54.1	4.90	12.7	6.10	638.0	0.21	----
P4	236.0	2.01	43.6	4.80	12.7	6.25	523.0	0.16	----
P5	88.4	3.07	17.4	4.88	12.7	6.17	488.0	1.20	0.08
P6	147.0	2.62	30.4	4.83	12.7	6.22	767.0	0.78	0.76
P7	221.0	2.54	54.1	4.90	12.7	6.10	1275.0	1.08	1.47
P8	236.0	2.01	43.6	4.80	12.7	6.25	1046.0	0.49	2.73
P9	88.4	3.07	17.4	4.88	12.7	6.17	732.0	1.78	----
P10	147.0	2.62	30.4	4.83	12.7	6.22	1151.0	1.53	----
P11	221.0	2.54	54.1	4.90	12.7	6.10	1913.0	3.37	----
P12	236.0	2.01	43.6	4.80	12.7	6.25	1570.0	1.13	----
P13	88.4	3.10	26.4	3.10	0.0	0.0	262.0	0.04	----
P14	177.0	3.05	17.5	4.85	12.7	6.15	244.0	0.07	----
P15	265.0	3.07	34.0	4.95	12.7	6.20	422.0	0.15	----
P16	295.0	2.57	30.5	4.90	12.7	6.12	384.0	0.07	----
P17	88.4	3.10	26.4	3.10	0.0	0.0	523.0	0.37	0.10
P18	177.0	3.05	17.5	4.85	12.7	6.15	488.0	0.19	0.62
P19	265.0	3.07	34.0	4.95	12.7	6.20	843.0	0.35	2.00
P20	295.0	2.57	30.5	4.90	12.7	6.12	767.0	0.24	2.14
P21	88.4	3.10	26.4	3.10	0.0	0.0	785.0	0.88	----
P22	177.0	3.05	17.5	4.85	12.7	6.15	732.0	0.40	----
P23	265.0	3.07	34.0	4.95	12.7	6.20	1265.0	0.81	----
P24	295.0	2.57	30.5	4.90	12.7	6.12	1151.0	0.52	----

TABLE 5.1a RN College Tests
Geometrical and material details

Model Number	σ_{yp} N/mm^2	σ_{ys} N/mm^2	E N/mm^2	E_c mm	MANCH &MONASH			L.R.		
					δ_o	Δ_{o+}	Δ_{o-}	δ_o	Δ_{o+}	Δ_{o-}
P1	250.0	283.0	190000	1.9	2.69	+2.0	-2.0	0.45	0.27	-0.20
P2	250.0	262.0	190000	-0.9	5.03	+2.0	-2.0	0.74	0.43	-0.32
P3	256.0	247.0	190000	-2.6	8.74	+2.0	-2.0	1.13	0.71	-0.53
P4	221.0	250.0	190000	-2.7	9.08	+2.0	-2.0	1.12	0.58	-0.46
P5	225.0	259.0	190000	1.9	1.95	+2.0	-2.0	0.42	0.54	-0.41
P6	239.0	259.0	190000	-0.9	3.85	+2.0	-2.0	0.73	0.85	-0.64
P7	270.0	246.0	190000	-2.6	6.06	+2.0	-2.0	1.16	1.41	-1.07
P8	247.0	259.0	190000	-2.7	8.20	+2.0	-2.0	1.18	1.16	-0.87
P9	230.0	283.0	190000	1.9	1.95	+2.0	-2.0	0.42	0.81	-0.61
P10	239.0	258.0	190000	-0.9	3.85	+2.0	-2.0	0.73	1.28	-0.96
P11	239.0	252.0	190000	-2.6	6.06	+2.0	-2.0	1.09	2.13	-1.59
P12	249.0	266.0	190000	-2.7	8.20	+2.0	-2.0	1.19	1.74	-1.31
P13	253.0	261.0	190000	0.11	2.87	+2.0	-2.0	0.45	0.29	-0.21
P14	242.0	269.0	190000	-0.4	2.76	+2.0	-2.0	0.88	0.27	-0.20
P15	227.0	267.0	190000	-1.5	4.83	+2.0	-2.0	1.27	0.47	-0.35
P16	244.0	273.0	190000	-2.1	5.27	+2.0	-2.0	1.47	0.43	-0.32
P17	229.0	256.0	190000	0.11	1.94	+2.0	-2.0	0.43	0.53	-0.44
P18	229.0	246.0	190000	-0.4	5.52	+2.0	-2.0	0.86	0.54	-0.41
P19	253.0	266.0	190000	-1.5	6.06	+2.0	-2.0	1.35	0.94	-0.70
P20	261.0	247.0	190000	-2.1	6.08	+2.0	-2.0	1.52	0.85	-0.64
P21	258.0	262.0	190000	0.11	1.94	+2.0	-2.0	0.45	0.87	-0.65
P22	242.0	262.0	190000	-0.4	4.00	+2.0	-2.0	0.88	0.81	-0.61
P23	244.0	262.0	190000	-1.5	6.06	+2.0	-2.0	1.32	1.41	-1.05
P24	239.0	267.0	190000	-2.1	8.10	+2.0	-2.0	1.46	1.28	-0.96

TABLE 5.1.a(Cont'd) RN College Tests
Geometrical and material details

Model Number	b mm	t mm	h_w mm	t_w mm	b_f mm	t_f mm	L mm	MEASURED Δ_0 mm	δ_0
F1	229.0	2.54	38.1	9.53	0.0	0.0	348.0	----	----
F2	229.0	2.54	38.1	9.53	0.0	0.0	653.0	3.45	----
F3	229.0	2.54	38.1	9.53	0.0	0.0	958.0	3.43	----
F4	229.0	2.54	38.1	9.53	0.0	0.0	1262.0	----	----
FL1	136.0	4.93	63.5	3.02	0.0	0.0	577.0	0.25	0.33
FL1S	136.0	4.93	63.5	3.02	0.0	0.0	577.0	----	----
FL2	136.0	4.93	63.5	3.02	0.0	0.0	577.0	0.20	----
FL2S	136.0	4.93	63.5	3.02	0.0	0.0	577.0	----	----
T1	203.0	1.98	28.65	4.95	13.0	6.35	1224.0	0.56	1.17
T2	169.0	1.98	19.05	4.95	13.3	6.35	874.0	0.08	0.53
T3	202.0	1.91	28.45	4.95	13.3	6.35	986.0	0.33	0.74
T4	166.0	2.08	19.05	4.95	13.2	6.35	704.0	0.97	0.53
T5	159.0	2.41	29.30	5.08	13.3	6.35	1019.0	1.42	0.03
T7	157.0	2.41	29.35	4.95	13.3	6.25	775.0	0.61	0.05
T8	116.0	3.09	19.15	4.95	13.2	6.25	546.0	----	----
T9	173.0	3.07	38.25	4.90	12.7	6.25	673.0	1.3	0.18
T10	115.0	3.10	19.15	4.95	12.7	6.25	376.0	----	----
T11	82.0	4.32	19.15	4.95	12.7	6.25	409.0	----	----

TABLE 5.1.a(Cont'd) RN College Tests
Geometrical and material details

Model Number	σ_{yp} N/mm^2	σ_{ys} N/mm^2	E N/mm^2	E_c mm	MANCH & MONASH			L.R		
					δ_0	Δ_{0+}	Δ_{0-}	δ_0	Δ_{0+}	Δ_{0-}
F1	222.0	238.0	190000.0	2.3	4.77	2.0	-2.0	1.09	0.39	-0.29
F2	227.0	262.0	190000.0	2.3	8.96	2.0	-2.0	1.10	0.73	-0.54
F3	195.0	250.0	190000.0	2.3	6.28	2.0	-2.0	1.02	1.06	-0.79
F4	188.0	208.0	190000.0	0.2	6.28	2.0	-2.0	1.00	1.40	-1.05
FL1	321.0	321.0	190000.0	0.0	1.89	2.0	-2.0	0.78	0.64	-0.48
FL1S	321.0	321.0	190000.0	0.0	1.89	2.0	-2.0	0.78	0.64	-0.48
FL2	247.0	219.0	190000.0	0.0	1.89	2.0	-2.0	0.68	0.64	-0.48
FL2S	247.0	219.0	190000.0	0.0	1.89	2.0	-2.0	0.68	0.64	-0.48
T1	190.0	208.0	190000.0	0.0	7.11	2.0	-2.0	0.89	1.36	-1.02
T2	188.0	278.0	190000.0	1.6	5.88	2.0	-2.0	0.74	0.97	-0.72
T3	184.0	184.0	190000.0	2.6	7.33	2.0	-2.0	0.88	1.09	-0.82
T4	196.0	287.0	190000.0	1.6	5.49	2.0	-2.0	0.74	0.78	-0.59
T5	201.0	267.0	190000.0	0.0	4.54	2.0	-2.0	0.72	1.13	-0.85
T7	247.0	262.0	190000.0	2.6	4.48	2.0	-2.0	0.79	0.86	-0.65
T8	250.0	267.0	190000.0	2.3	2.56	2.0	-2.0	0.59	0.61	-0.46
T9	259.0	293.0	190000.0	3.0	3.88	2.0	-2.0	0.89	0.74	-0.56
T10	292.0	279.0	190000.0	0.0	2.53	2.0	-2.0	0.63	0.41	-0.31
T11	281.0	286.0	190000.0	0.0	1.28	2.0	-2.0	0.44	0.45	-0.34

TABLE 5.1.a(Cont'd) RN College Tests
Geometrical and material details

MODEL NUMBER	TEST	CAMBRIDGE		MANCHESTER		MONASH		L.R.		PRESENT METHOD	
	Φ	Φ	% ERROR	Φ	% ERROR	Φ	% ERROR	Φ	% ERROR	Φ	% ERROR
P1	0.976	0.919	-5.8	0.604	-38.0	0.702	-28.0	0.857	-12.2	1.000	2.5
P2	0.733	0.677	-7.6	0.591	-19.4	0.737	0.6	0.736	0.4	0.824	12.4
P3	0.713	0.638	-10.5	0.627	-12.1	0.602	-15.5	0.645	-9.5	0.689	-3.4
P4	0.567	0.663	14.5	0.599	5.6	0.506	-10.8	0.577	1.7	0.579	2.1
P5	0.824	0.808	-1.9	0.547	-33.6	0.715	-13.2	0.769	-6.7	0.808	-1.9
P6	0.750	0.587	-21.7	0.513	-31.6	0.726	-3.2	0.703	-6.3	0.780	4.0
P7	0.621	0.551	-11.3	0.500	-19.5	0.576	-7.3	0.604	-2.7	0.594	-4.3
P8	0.515	0.574	11.4	0.518	0.6	0.476	-7.6	0.545	5.8	0.528	2.5
P9	0.716	0.623	-13.0	0.445	-37.9	0.590	-17.6	0.626	-12.6	0.591	-17.5
P10	0.660	0.495	-25.0	0.432	-34.6	0.551	-16.5	0.622	-5.8	0.634	-3.9
P11	0.494	0.442	-10.5	0.449	-9.1	0.518	4.8	0.507	2.6	0.453	-8.3
P12	0.448	0.457	2.0	0.435	-2.9	0.413	-7.8	0.464	3.6	0.410	-8.5

Φ : Collapse Load L.R : Lloyd's Register

TABLE 5.1.b RN College tests
Tests and Numerical Results

MODEL NUMBER	TEST	CAMBRIDGE		MANCHESTER		MONASH		L.R.		PRESENT METHOD	
	Φ	Φ	% ERROR	Φ	% ERROR	Φ	% ERROR	Φ	% ERROR	Φ	% ERROR
P13	0.988	0.900	-8.9	0.473	-55.8	0.856	-13.4	0.948	-4.0	0.962	- 2.6
P14	0.764	0.580	-24.1	0.551	-27.9	0.688	-9.9	0.697	-8.7	0.722	-5.5
P15	0.569	0.581	2.1	0.540	-5.1	0.552	-3.0	0.583	2.5	0.572	0.5
P16	0.506	0.598	18.0	0.475	-6.1	0.468	-7.5	0.538	6.3	0.503	-0.6
P17	0.822	0.723	-12.1	0.440	-46.5	0.819	-0.4	0.880	7.1	0.753	-8.4
P18	0.656	0.525	-20.0	0.467	-28.8	0.693	5.6	0.683	4.1	0.652	-0.6
P19	0.563	0.487	-13.5	0.448	-20.4	0.526	-6.6	0.552	-2.0	0.540	-4.1
P20	0.455	0.501	10.1	0.374	-17.8	0.453	0.4	0.527	15.8	0.459	0.9
P21	0.696	0.455	-34.6	0.322	-53.7	0.477	-31.4	0.495	-28.9	0.471	-32.3
P22	0.515	0.446	-13.4	0.393	-23.7	0.563	9.3	0.573	11.3	0.509	-1.2
P23	0.491	0.373	-24.0	0.364	-25.9	0.425	-15.8	0.465	-5.3	0.446	-9.2
P24	0.384	0.382	-0.5	0.388	-12.0	0.469	22.1	0.446	16.1	0.379	-1.3
		MEAN= -8.34 %		MEAN= -23.2 %		MEAN= -7.2 %		MEAN= -1.2 %		MEAN= -3.7 %	
		S.D = 13.4 %		S.D = 16.5 %		S.D = 11.6 %		S.D = 9.9 %		S.D = 9.4 %	

L.R Lloyd's Register

Φ: Collapse Load

TABLE 5.1.b(Cont'd) RN College tests
Tests and Numerical Results

MODEL NUMBER	TEST	CAMBRIDGE		MANCHESTER		MONASH		L.R.		PRESENT METHOD	
	Φ	Φ	% ERROR	Φ	% ERROR	Φ	% ERROR	Φ	% ERROR	Φ	% ERROR
F1	0.566	0.688	21.5	0.550	-2.8	0.472	-16.6	0.575	1.6	0.575	1.6
F2	0.577	0.625	8.3	0.438	-24.1	0.432	-25.1	0.478	-17.1	0.456	-21.0
F3	0.459	0.543	18.4	0.375	-18.3	0.406	-11.5	0.424	-7.6	0.384	-16.3
F4	0.339	0.444	30.9	0.386	13.9	0.454	33.9	0.446	31.0	0.336	-0.9
FL1	0.779	0.739	-5.1	0.285	-63.4	0.867	11.3	0.747	-4.1	0.780	-0.1
FL1S	0.752	0.739	-1.7	0.285	-62.1	0.867	15.3	0.747	-0.7	0.780	3.7
FL2	0.787	0.776	-1.4	0.379	-51.8	0.799	1.5	0.782	-0.6	0.805	2.3
FL2S	0.723	0.776	7.3	0.379	-47.6	0.799	10.5	0.782	8.0	0.805	11.3
T1	0.390	0.435	11.6	0.394	1.0	0.428	9.7	0.440	12.8	0.448	14.9

L.R : Lloyd's Register

Φ: Collapse Load

TABLE 5.1.b(Cont'd) RN College tests
Tests and Numerical Results

MODEL NUMBER	TEST	CAMBRIDGE		MANCHESTER		MONASH		L.R.		PRESENT METHOD	
	Φ	Φ	% ERROR	Φ	% ERROR	Φ	% ERROR	Φ	% ERROR	Φ	% ERROR
T2	0.352	0.399	13.2	0.312	-11.4	0.378	7.4	0.379	7.7	0.395	12.2
T3	0.416	0.504	21.1	0.407	-2.1	0.407	-2.2	0.442	6.3	0.425	2.2
T4	0.403	0.492	22.1	0.408	-1.2	0.493	22.3	0.430	6.7	0.465	15.4
T5	0.619	0.507	-18.1	0.409	-33.9	0.684	10.5	0.549	-11.3	0.600	-3.1
T7	0.558	0.549	-1.7	0.426	-23.7	0.516	-7.5	0.531	-4.8	0.566	1.4
T8	0.744	0.708	-4.8	0.465	-37.5	0.636	-14.5	0.695	-6.6	0.736	-1.1
T9	0.634	0.619	-2.4	0.475	-25.1	0.573	-9.6	0.602	-5.1	0.633	-0.2
T10	0.879	0.722	-12.1	0.583	-33.7	0.825	-6.1	0.852	-3.1	0.929	5.7
T11	0.820	0.884	7.7	0.636	-22.6	0.935	14.0	0.944	15.1	0.875	6.7
		MEAN= 6.4 %		MEAN= -24.8 %		MEAN= 2.4 %		MEAN= 1.6 %		MEAN= 1.9 %	
		S.D = 13.25 %		S.D = 22.23 %		S.D = 15.16 %		S.D = 11.16 %		S.D = 9.37 %	

L.R : Lloyd's Register

Φ: Collapse Load

TABLE 5.1.b(Cont'd) RN College tests
Tests and Numerical Results

Model Number	b mm	t mm	h_w mm	t_w mm	b_f mm	t_f mm	L mm	MEASURED Δ_0 mm	δ_0
7	457.0	9.5	152.5	16.0	0.0	0.0	1830.0	2.5	1.7
14	457.0	9.5	152.5	16.0	0.0	0.0	1830.0	1.5	6.0
12	457.0	9.5	152.5	16.0	0.0	0.0	1830.0	7.0	2.6
8	457.0	9.5	152.5	16.0	0.0	0.0	1830.0	1.4	0.9
13	457.0	9.5	152.5	16.0	0.0	0.0	1830.0	0.6	5.8
11	457.0	9.5	152.5	16.0	0.0	0.0	1830.0	5.9	1.84
D22	457.0	10.0	80.0	12.0	0.0	0.0	1830.0	1.6	1.2
D21	457.0	10.0	80.0	12.0	0.0	0.0	1830.0	1.4	5.7
D23	457.0	10.0	80.0	12.0	0.0	0.0	1830.0	1.4	1.4
D12	457.0	10.0	80.0	12.0	0.0	0.0	1830.0	2.2	3.1
D11	457.0	10.0	80.0	12.0	0.0	0.0	1830.0	1.4	5.4
E23	457.0	6.5	76.0	12.5	0.0	0.0	1830.0	1.1	2.5
E21	457.0	6.5	76.0	12.5	0.0	0.0	1830.0	1.9	5.6
E22	457.0	6.5	76.0	12.5	0.0	0.0	1830.0	2.7	1.3
E12	457.0	6.5	76.0	12.5	0.0	0.0	1830.0	1.6	1.7
E11	457.0	6.5	76.0	12.5	0.0	0.0	1830.0	1.6	6.3
PF2	200.0	9.7	150.0	15.1	0.0	0.0	2700.0	3.3	0.7
PF5	300.0	10.0	150.0	15.1	0.0	0.0	2700.0	3.5	1.4
PF11	350.0	9.8	150.0	15.1	0.0	0.0	2700.0	3.3	1.6
SW1	480.0	9.7	150.0	15.1	0.0	0.0	2700.0	3.9	1.8
SW3	480.0	9.9	150.0	15.1	0.0	0.0	2700.0	2.7	2.7
SW5	480.0	9.9	150.0	15.1	0.0	0.0	2700.0	2.1	2.0
SW7	480.0	9.7	150.0	15.1	0.0	0.0	2700.0	3.5	1.4
FS9	200.0	9.9	148.0	9.8	0.0	0.0	3000.0	3.2	0.9
FS4	200.0	9.9	148.0	9.8	0.0	0.0	3000.0	2.0	0.5
9	457.0	9.5	152.0	9.5	0.0	0.0	1830.0	2.5	0.7
AS2	200.0	10.4	152.0	6.6	38.0	12.0	3000.0	3.6	1.0
AF2	200.0	10.3	152.0	6.5	76.0	9.8	3000.0	4.0	0.8

TABLE 5.2.a Manchester Tests
Geometrical and material details

MODEL NUMBER	σ_{yp} N/mm ^{2}	σ_{ys} N/mm ^{2}	E N/mm ^{2}	E_c mm	MANCH $ MONASH[1]			L.R.		
					δ_0	Δ_{0+}	Δ_{0-}	δ_0	Δ_{0+}	Δ_{0-}
7	254.7	268.1	204000.0	0.0	1.75	2.0	-2.0	2.33	2.0	-1.5 3
14	254.7	268.1	204000.0	0.0	1.75	2.0	-2.0	2.33	2.0	-1.5 3
12	254.7	268.1	204000.0	0.0	1.75	2.0	-2.0	2.33	2.0	-1.5 3
8	262.1	262.0	204000.0	0.0	1.75	2.0	-2.0	2.36	2.0	-1.5 3
13	275.5	262.0	204000.0	0.0	1.75	2.0	-2.0	2.42	2.0	-1.5 3
11	275.5	262.0	204000.0	0.0	1.75	2.0	-2.0	2.42	2.0	-1.5 3
D22	244.3	287.0	204000.0	0.0	1.75	2.0	-2.0	2.28	2.0	-1.5 3
D21	243.0	256.0	204000.0	0.0	1.75	2.0	-2.0	2.28	2.0	-1.5 3
D23	243.2	289.4	204000.0	8.0	1.75	2.0	-2.0	2.28	2.0	-1.5 3
D12	233.6	252.3	204000.0	0.0	1.75	2.0	-2.0	2.23	2.0	-1.5 3
D11	282.9	290.7	204000.0	0.0	1.75	2.0	-2.0	2.46	2.0	-1.5 3
E23	329.8	369.5	204000.0	0.0	2.65	2.0	-2.0	2.65	2.0	-1.5 3
E21	335.6	353.3	204000.0	0.0	2.65	2.0	-2.0	2.67	2.0	-1.5 3
E22	343.2	389.6	204000.0	8.0	2.65	2.0	-2.0	2.70	2.0	-1.5 3
E12	334.7	377.9	204000.0	0.0	2.65	2.0	-2.0	2.66	2.0	-1.5 3
E11	335.9	374.0	204000.0	0.0	2.65	2.0	-2.0	2.67	2.0	-1.5 3
PF2	356.0	408.0	204000.0	0.0	1.4	3.0	-2.3	1.21	3.0	-2.3
PF5	413.0	416.0	204000.0	0.0	2.1	3.0	-2.3	1.95	3.0	-2.3
PF11	379.0	410.0	204000.0	0.0	2.5	3.0	-2.3	2.18	3.0	-2.3
SW1	382.0	428.0	204000.0	0.0	3.5	3.0	-2.3	3.00	3.0	-2.3
SW3	384.0	422.0	204000.0	0.0	3.5	3.0	-2.3	3.00	3.0	-2.3
SW5	408.0	409.0	204000.0	0.0	3.5	3.0	-2.3	3.10	3.0	-2.3
SW7	418.0	434.0	204000.0	0.0	1.4	3.0	-2.3	3.13	3.0	-2.3
FS9	346.0	410.0	204000.0	-1.0	1.4	3.3	-2.5	1.19	3.3	-2.5
FS4	357.0	410.0	204000.0	-1.0	1.4	3.3	-2.5	1.21	3.3	-2.5
9	262.0	273.0	204000.0	0.0	1.75	2.0	-2.5	2.36	2.0	-1.53
AS2	367.0	410.0	204000.0	-3.0	1.4	3.3	-2.5	1.22	3.3	-2.5
AF2	354.0	410.0	204000.0	-3.0	1.4	3.3	-2.5	1.20	3.3	-2.5

TABLE 5.2.a(Cont'd) Manchester Tests
Geometrical and material details

MODEL NUMBER	TEST	CAMBRIDGE		MANCHESTER		MONASH		L.R.		PRESENT METHOD	
	Φ	Φ	% ERROR	Φ	% ERROR	Φ	% ERROR	Φ	% ERROR	Φ	% ERROR
7	0.790	0.740	-6.3	0.703	-11.0	0.763	-3.4	0.764	-3.3	0.845	6.9
14	0.830	0.740	-10.8	0.703	-15.3	0.763	-8.1	0.764	-7.9	0.849	2.3
12	0.790	0.740	-6.3	0.703	-11.0	0.763	-3.4	0.764	-3.3	0.828	4.8
8	0.850	0.779	-8.4	0.713	-16.1	0.773	-9.1	0.870	2.4	0.844	-0.7
13	0.750	0.766	2.1	0.718	-4.3	0.777	3.6	0.876	16.8	0.835	11.3
11	0.790	0.766	-3.0	0.718	-9.1	0.777	-1.6	0.876	10.9	0.812	2.8
D22	0.600	0.569	-5.2	0.533	-11.2	0.567	-5.5	0.673	12.0	0.594	-1.0
D21	0.570	0.580	1.8	0.509	-10.7	0.544	-4.6	0.689	20.8	0.545	-4.4
D23	0.430	0.567	31.9	0.480	11.6	0.542	26.1	0.433	0.7	0.488	13.5
D12	0.650	0.624	-4.0	0.522	-19.7	0.558	-14.1	0.636	-2.1	0.536	-17.5
D11	0.630	0.560	-11.1	0.476	-24.4	0.506	-19.7	0.569	-9.6	0.511	-18.9
E23	0.450	0.425	-5.6	0.414	-8.0	0.463	2.9	0.456	1.3	0.438	-2.7
E21	0.440	0.423	-3.9	0.417	-5.2	0.465	5.7	0.459	4.3	0.424	-3.6
E22	0.340	0.420	23.5	0.335	-1.5	0.348	2.4	0.428	26.0	0.329	-3.2
E12	0.480	0.437	-8.9	0.410	-14.6	0.458	4.6	0.505	5.2	0.474	-1.3

Φ: Collapse Load L.R : Lloyd's Register

TABLE 5.2.b Manchester tests
Tests and Numerical Results

MODEL NUMBER	TEST	CAMBRIDGE		MANCHESTER		MONASH		L.R.		PRESENT METHOD	
	Φ	Φ	% ERROR	Φ	% ERROR	Φ	% ERROR	Φ	% ERROR	Φ	% ERROR
E11	0.470	0.437	-7.0	0.411	-12.5	0.459	2.3	0.505	7.5	0.426	-9.4
PF2	0.780	0.740	-5.1	0.816	4.6	0.842	7.9	0.857	9.8	0.772	-1.0
PF5	0.790	0.713	-9.8	0.744	-5.8	0.814	3.3	0.822	4.0	0.751	-4.9
PF11	0.720	0.787	9.3	0.696	-3.3	0.767	6.5	0.746	3.6	0.686	-4.7
SW1	0.710	0.570	-19.7	0.560	-21.1	0.634	-10.7	0.689	-2.9	0.656	-7.6
SW3	0.710	0.571	-19.6	0.570	-19.7	0.646	-9.0	0.699	-1.6	0.674	-5.1
SW5	0.640	0.560	-12.5	0.576	-10.0	0.650	1.6	0.622	-2.8	0.672	5.0
SW7	0.690	0.541	-21.6	0.558	-19.1	0.628	-8.9	0.681	-1.3	0.641	-7.1
FS9	0.750	0.731	-2.5	0.569	-24.1	0.824	9.9	0.775	3.3	0.768	2.4
FS4	0.670	0.725	8.2	0.554	-17.3	0.815	-21.6	0.765	14.0	0.727	8.5
9	0.780	0.654	-16.2	0.681	-12.7	0.756	-3.1	0.785	0.6	0.726	-6.9
AS2	0.810	0.812	0.2	0.550	-32.0	0.892	10.1	0.839	3.6	0.781	-3.6
AF2	0.890	0.777	-12.7	0.881	-1.0	0.878	-1.4	0.924	3.8	0.820	-7.8
L.R : Lloyd's Register		MEAN= -4.4 %		MEAN=-11.59 %		MEAN= -1.33 %		MEAN= 4.14 %		MEAN= -1.93 %	
Φ: Collapse Load		S.D = 11.79 %		S.D = 9.28 %		S.D = 9.81 %		S.D = 8.27 %		S.D = 7.45 %	

TABLE 5.2.b(Cont'd) Manchester tests
Tests and Numerical Results

Model Number	b mm	t mm	h_w mm	t_w mm	b_f mm	t_f mm	L mm	MEASURED Δ_0 (mm)	δ_0
1	242.7	4.95	50.8	4.76	15.88	4.76	787.4	----	----
2	242.7	4.88	50.8	4.76	15.88	4.76	787.4	----	----
3	120.7	5.03	50.8	4.76	15.88	4.76	787.4	----	----
4	120.7	5.03	50.8	4.76	15.88	4.76	787.4	----	----
8	120.7	4.72	38.1	6.35	0.0	0.0	1320.8	----	----

Model Number	σ_{yp} N/mm^2	σ_{ys} N/mm^2	E N/mm^2	E_c mm	MANCH & MONASH δ_0	Δ_{0+}	Δ_{0-}	L.R. δ_0	Δ_{0+}	Δ_{0-}
1	247.0	329.0	200720.0	0.0	3.43	2.0	-2.0	1.22	0.87	-0.66
2	298.0	277.0	199945.0	0.0	3.48	2.0	-2.0	1.34	0.87	-0.66
3	221.0	288.0	203036.0	0.0	1.64	2.0	-2.0	0.57	0.87	-0.66
4	221.0	288.0	203036.0	0.0	1.64	2.0	-2.0	0.57	0.87	-0.66
8	277.0	312.0	209212.0	0.0	1.75	2.0	-2.0	0.64	0.47	-1.1

L.R : Lloyd's Register

Φ: Collapse Load

TABLE 5.3.a Imperial College Tests
Geometrical and material details

MODEL NUMBER	TEST	CAMBRIDGE		MANCHESTER		MONASH		L.R.		PRESENT METHOD	
	Φ	Φ	% ERROR	Φ	% ERROR	Φ	% ERROR	Φ	% ERROR	Φ	% ERROR
1	0.758	0.620	-18.2	.546	-27.9	0.675	-10.9	0.708	-6.6	0.795	4.9
2	0.686	0.591	-13.8	0.570	-16.9	0.652	-5.0	0.708	3.2	0.668	-2.6
3	0.957	0.885	-7.5	0.800	-16.4	0.829	-13.4	0.880	-8.0	0.914	-4.5
4	0.920	0.885	-3.8	0.800	-13.0	0.829	-9.9	0.880	-4.3	0.914	-0.7
8	0.544	0.427	-21.5	0.374	-31.3	0.391	-28.1	0.454	-16.5	0.459	-15.6
		MEAN= -12.98 %		MEAN=-21.11 %		MEAN=-13.46 %		MEAN= -6.46 %		MEAN= -3.70 %	
		S.D = 7.33 %		S.D = 7.98 %		S.D = 8.75 %		S.D = 7.11 %		S.D = 7.52 %	

L.R : Lloyd's Register

Φ : Collapse Load

TABLE 5.3.b Imperial College tests
Tests and Numerical Results

Model Number	b mm	t mm	h_w mm	t_w mm	b_f mm	t_f mm	L mm	MEASURED Δ_{0+} mm	Δ_{0-} mm	δ_0
1a	609.6	8.00	139.4	7.21	79.0	14.22	1219.2	0.85	-1.58	3.66
2b	304.8	7.37	104.8	5.38	44.7	9.53	1524.0	1.52	-0.91	1.83
3b	304.8	6.40	70.9	4.65	27.9	6.35	1524.0	2.89	-2.59	4.57
4a	254.0	6.43	70.4	4.85	27.7	6.35	1219.2	2.80	-2.19	2.06
5	609.6	6.43	106.5	5.33	46.2	9.53	1524.0	1.22	-0.31	6.10
6	609.6	6.32	69.8	4.55	27.4	6.35	1219.2	2.44	-1.46	7.62
7	609.6	6.30	105.5	5.15	45.2	9.53	1524.0	1.07	-0.31	5.73

Model Number	σ_r N/mm^2	σ_{yp} N/mm^2	σ_{ys} N/mm^2	E N/mm^2	TEST Φ	PRESENT METHOD Φ	% ERROR
1a	----	253.34	257.98	207000.0	0.752	0.760	1.1
2b	87.54	264.16	279.60	207000.0	0.845	0.876	3.7
3b	110.20	256.43	227.08	207000.0	0.604	0.572	-5.3
4a	100.92	268.79	237.89	207000.0	0.820	0.751	-8.4
5	41.20	251.80	234.80	207000.0	0.708	0.605	-14.6
6	53.55	261.07	245.62	207000.0	0.482	0.459	-4.8
7	24.72	295.05	310.50	207000.0	0.622	0.594	-4.5
						MEAN= -4.68 %	
						S.D = 6.00 %	

TABLE 5.4. Smith Tests

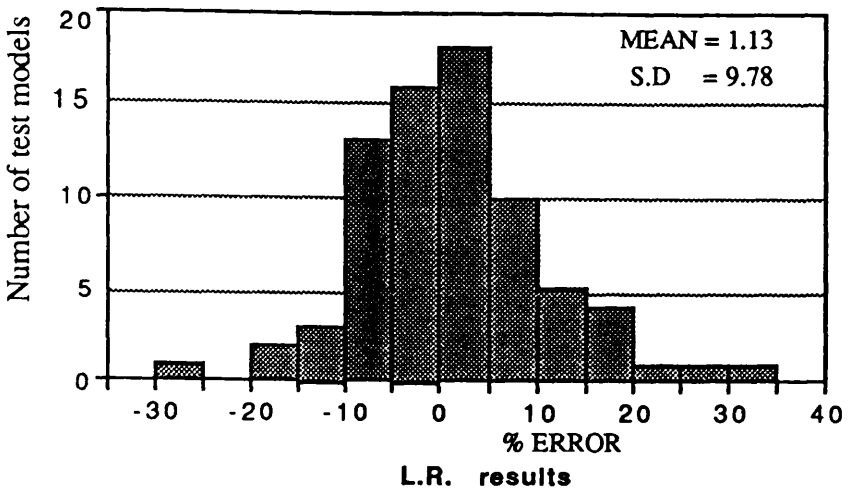

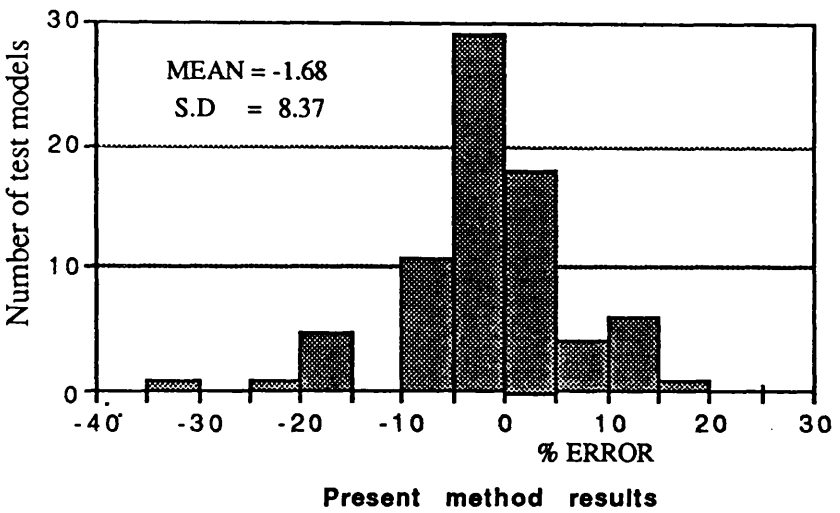

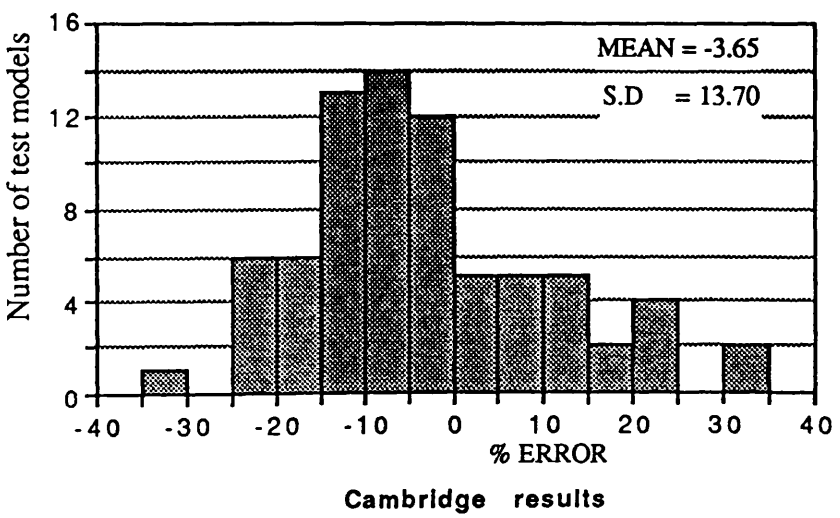

Figure 5.1.a Percentage error of results for 75 tests

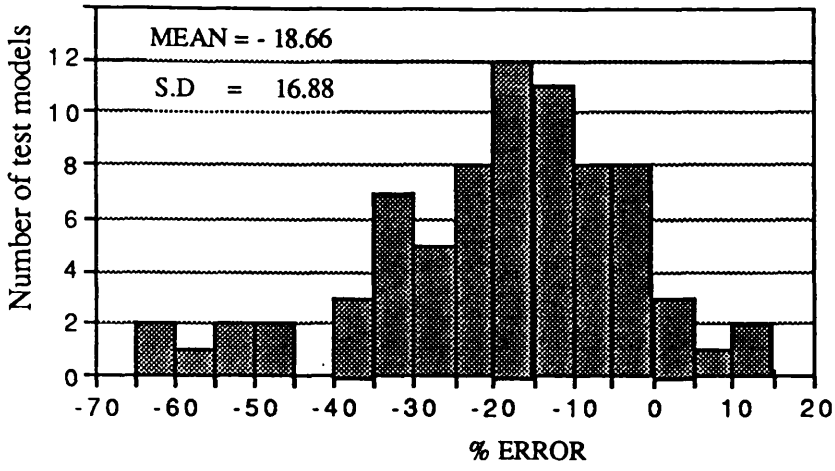

Manchester Results

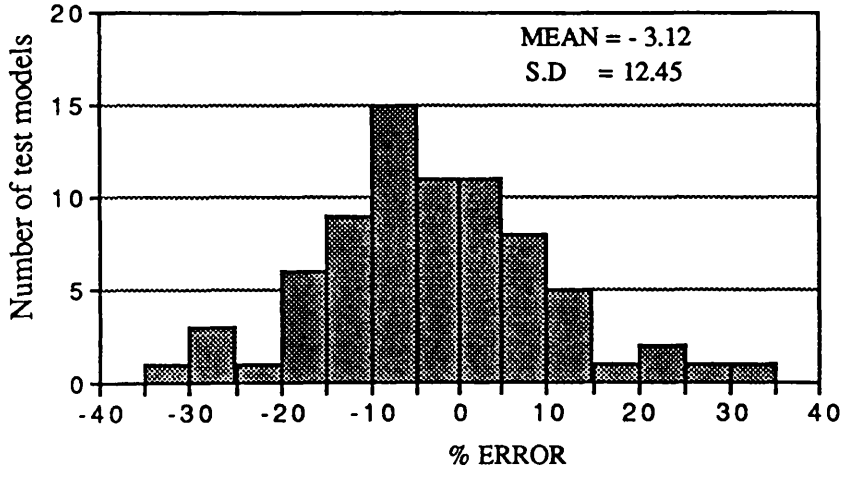

Monash results

Figure 5.1.b **Percentage error of results for 75 tests**

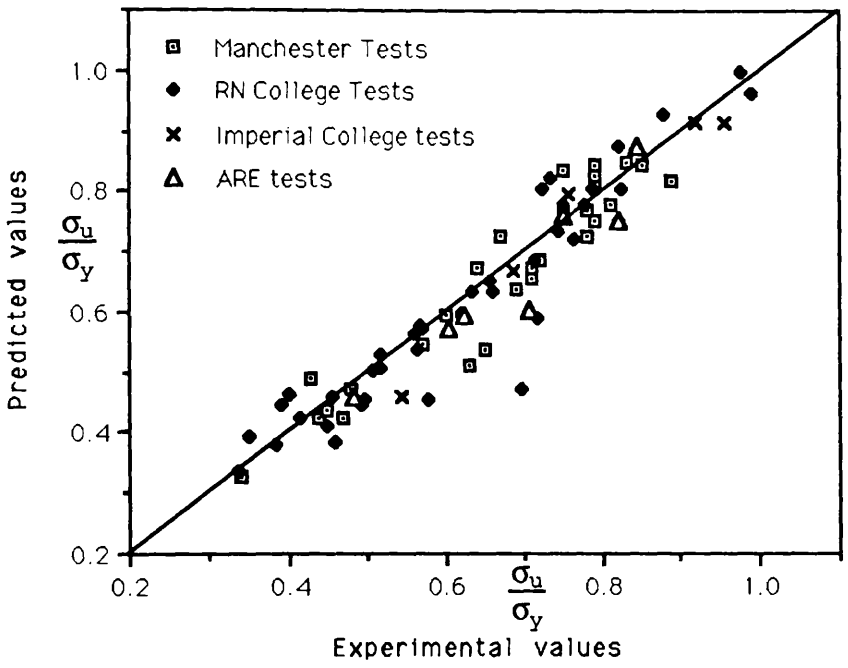

Figure 5.1.c Correlation with test results

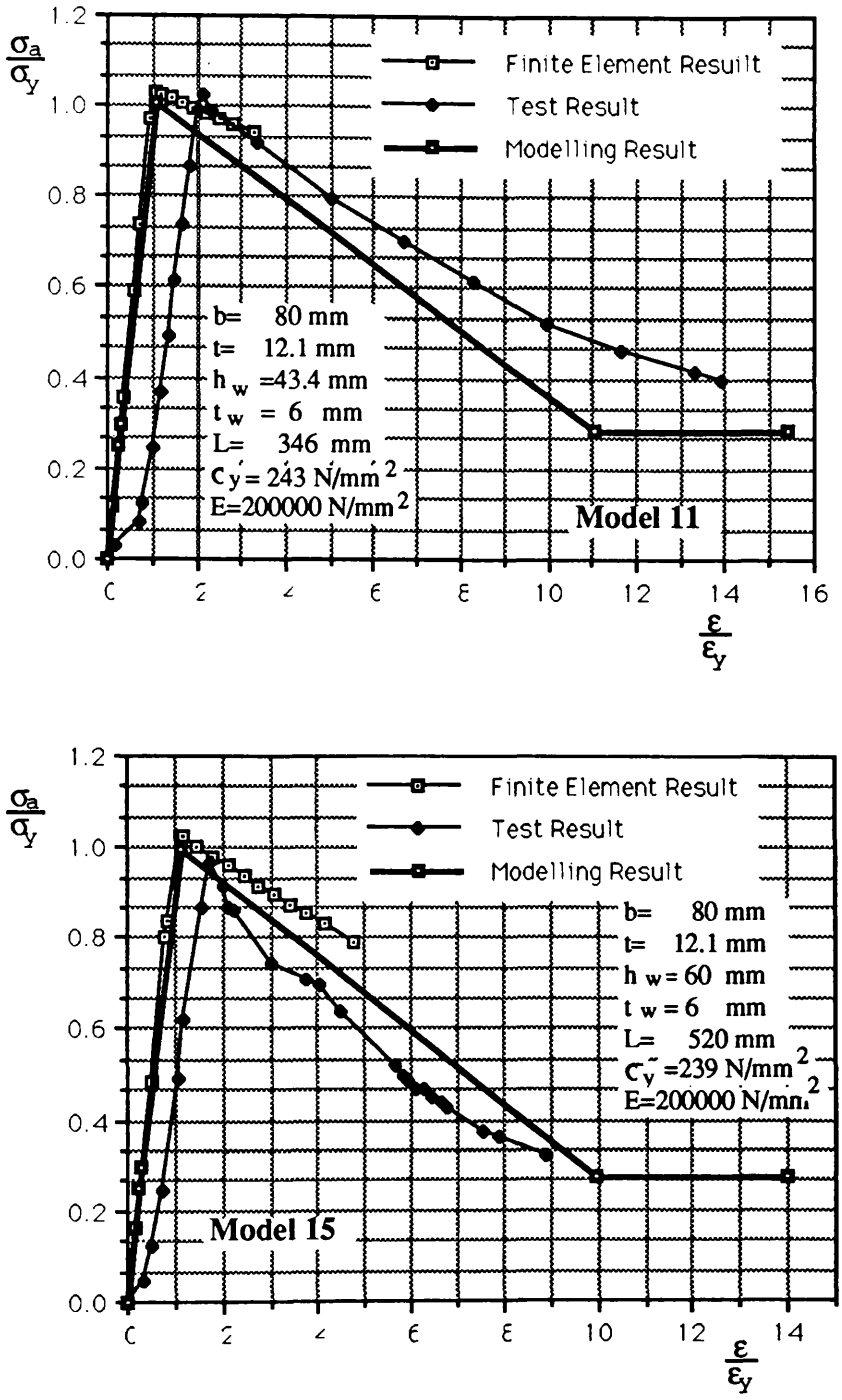

Figure 5.2.a **Unloading curves for test models. Correlation with test results.**

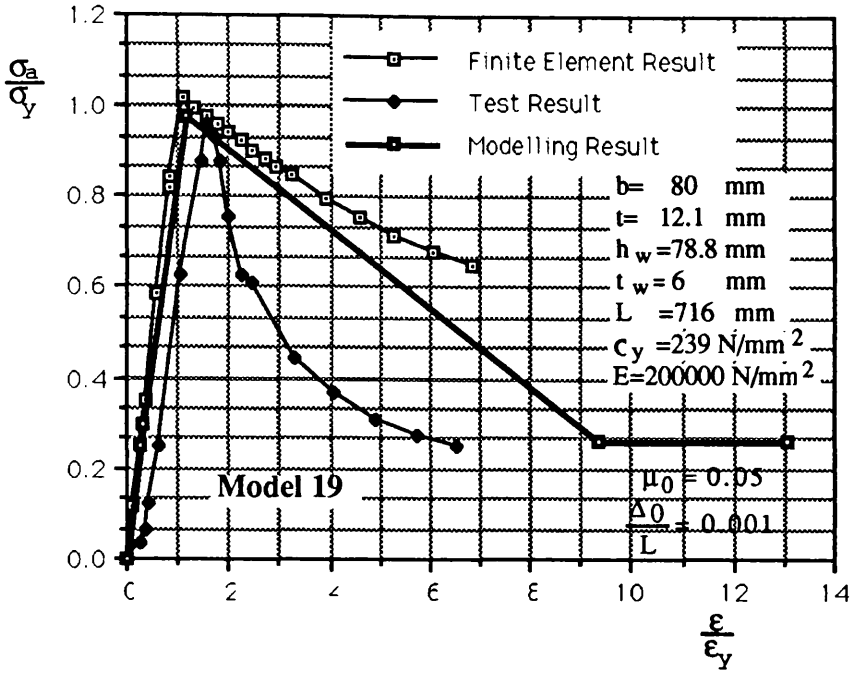

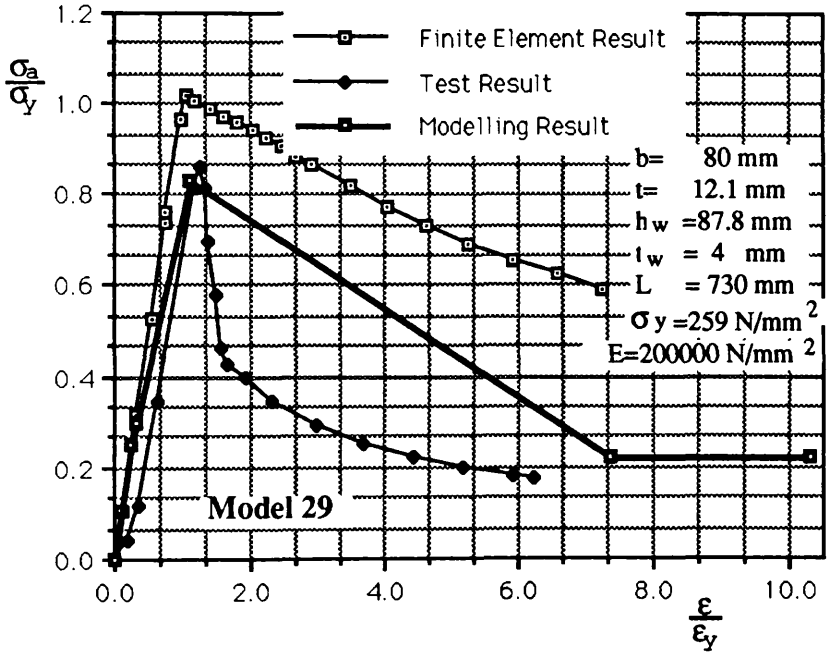

Figure 5.2.b **Unloading curves for test models. Correlation with test results.**

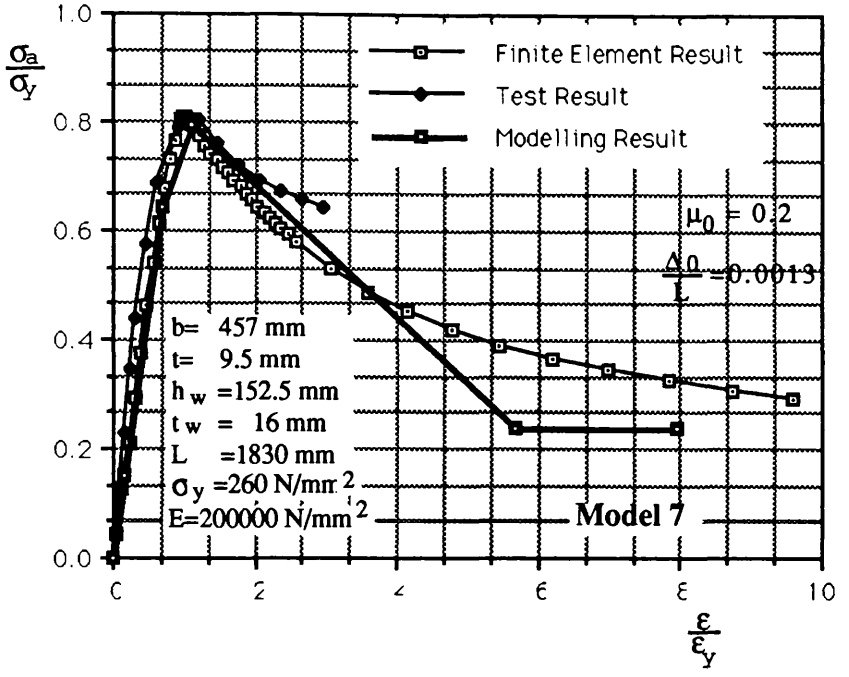

Figure 5.2.c **Unloading curves for test models. Correlation with test results.**

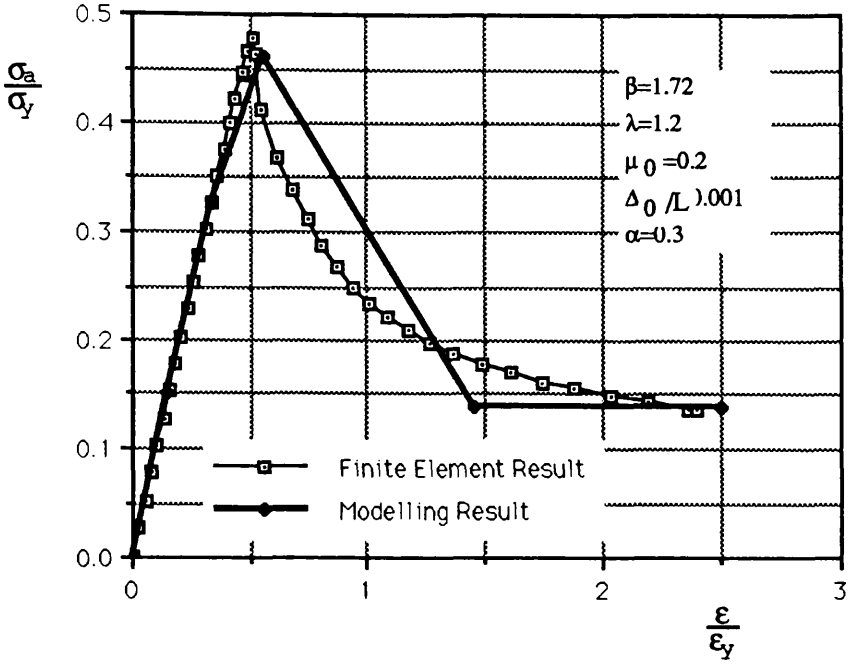

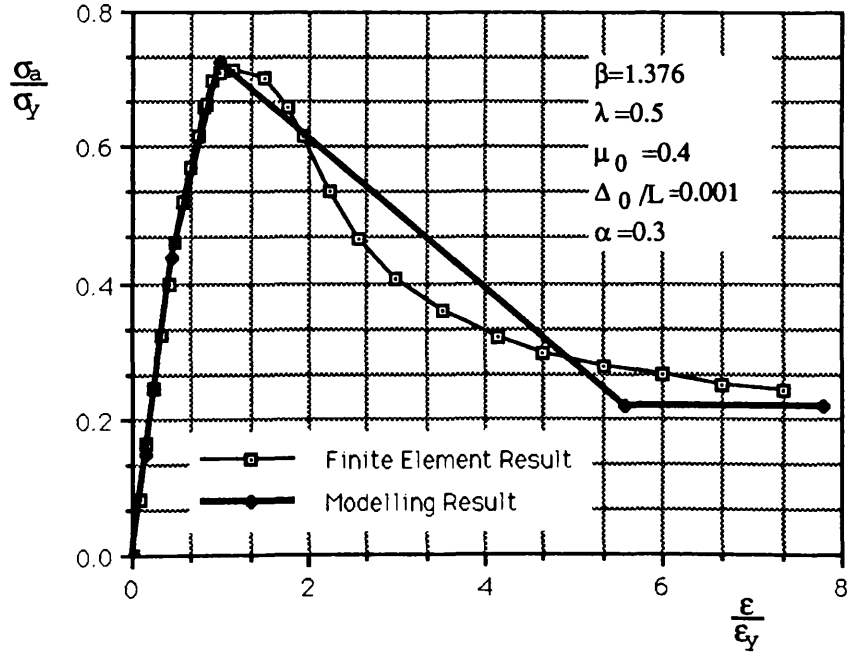

Figure 5.3.a **Unloading curves for stiffened panels. Correlation with numerical results.**

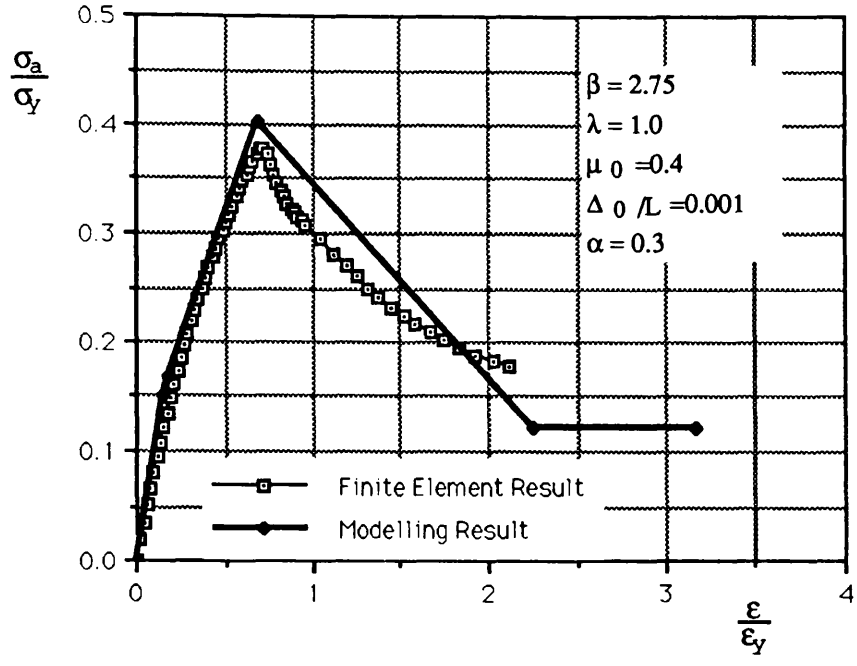

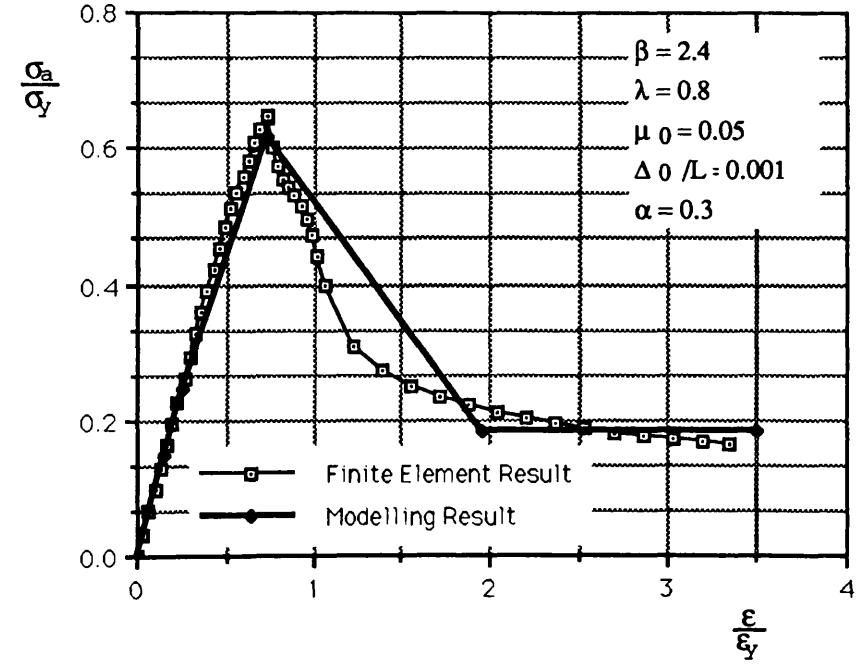

Figure 5.3.b **Unloading curves for stiffened panels. Correlation with numerical results**

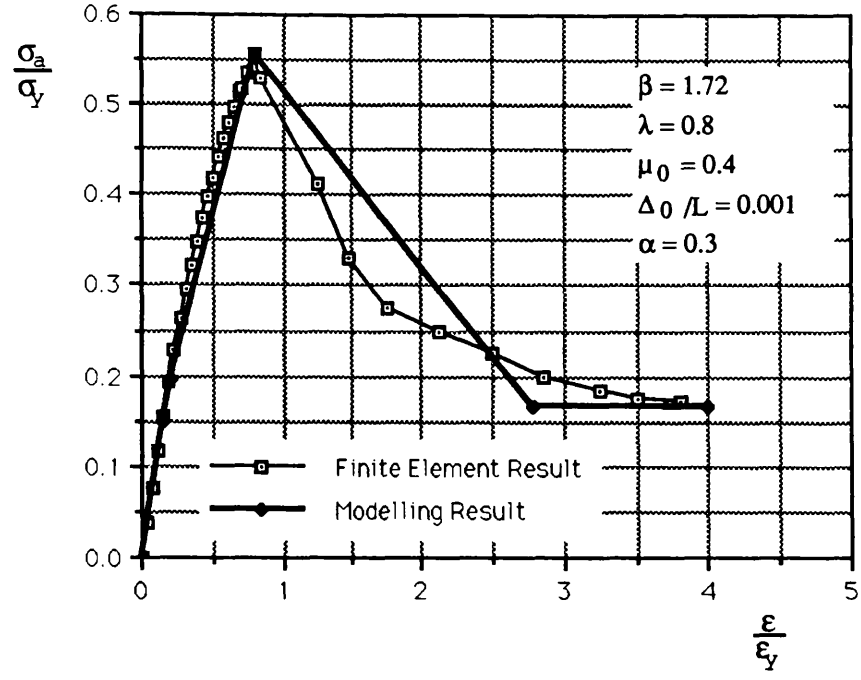

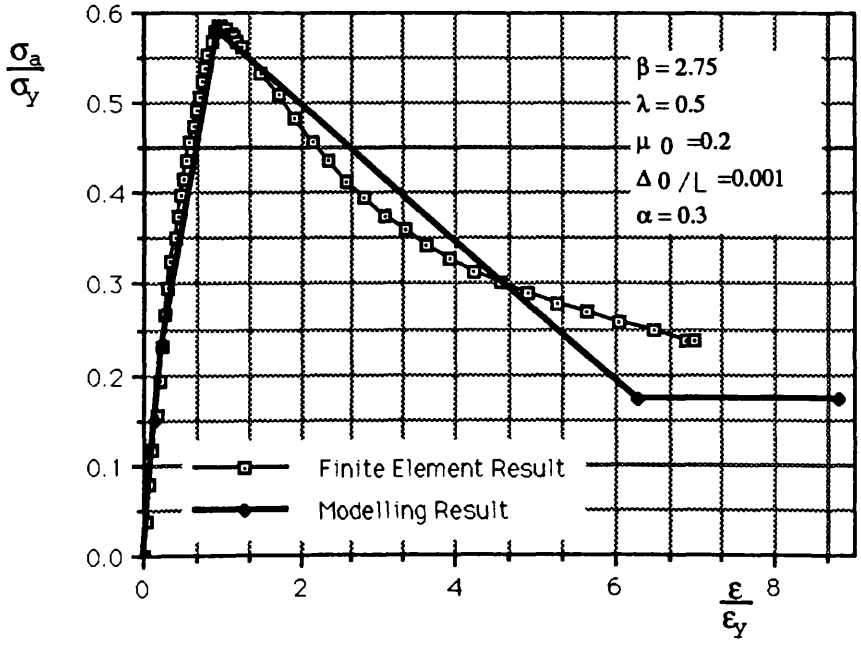

Figure 5.3.c **Unloading curves for stiffened panels. Correlation with numerical results.**

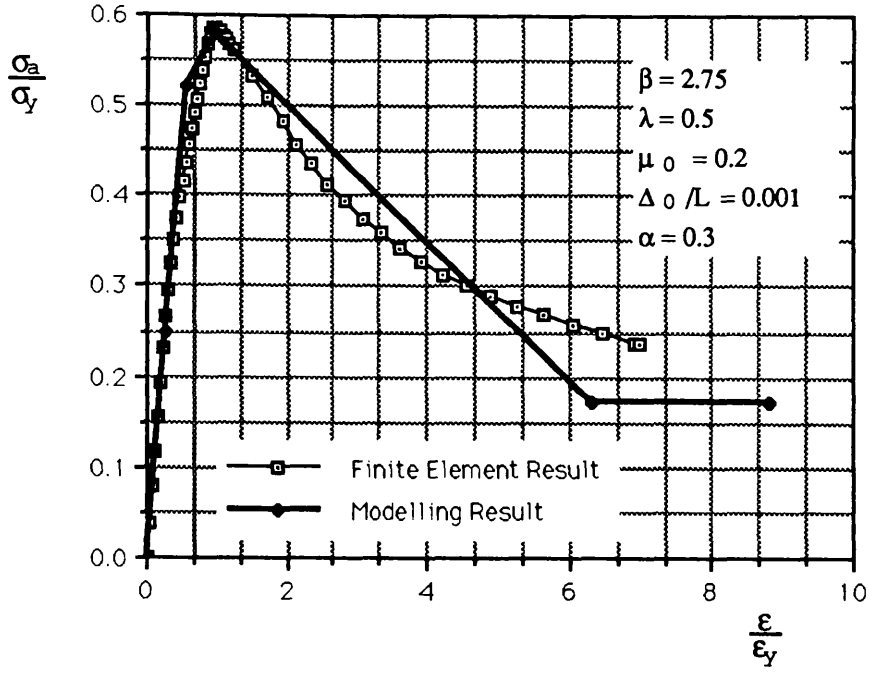

Figure 5.3.d **Unloading curves for stiffened panels. Correlation with numerical results.**

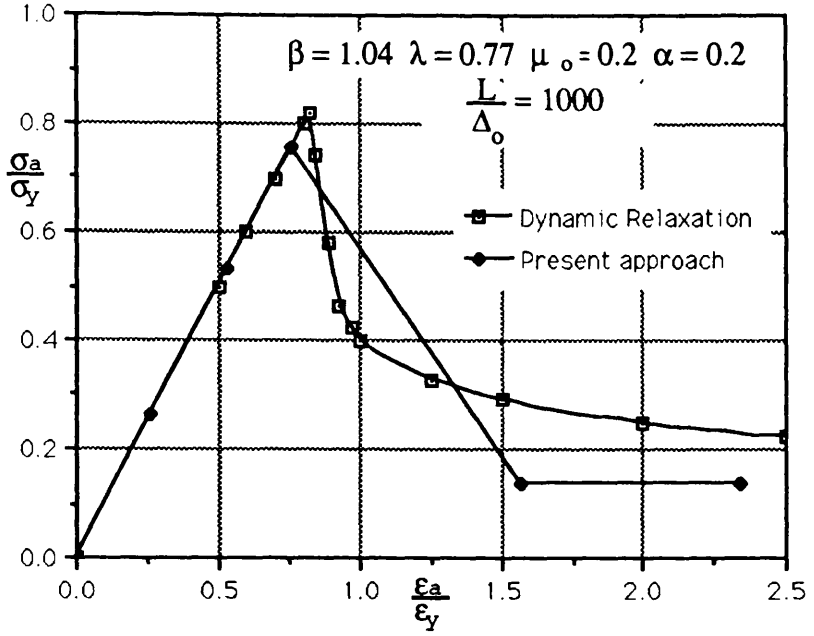

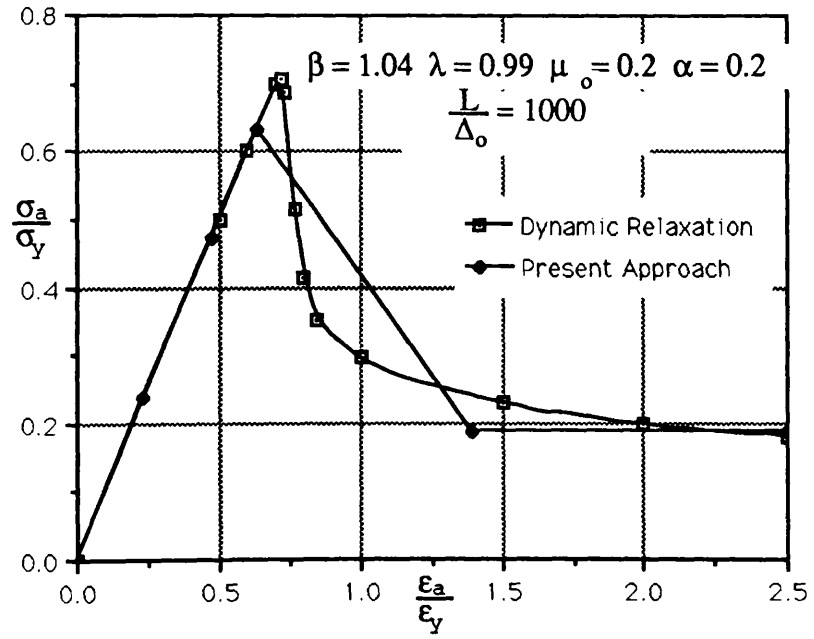

Figure 5.4.a **Stress-strain curves**
Correlation with numerical methods

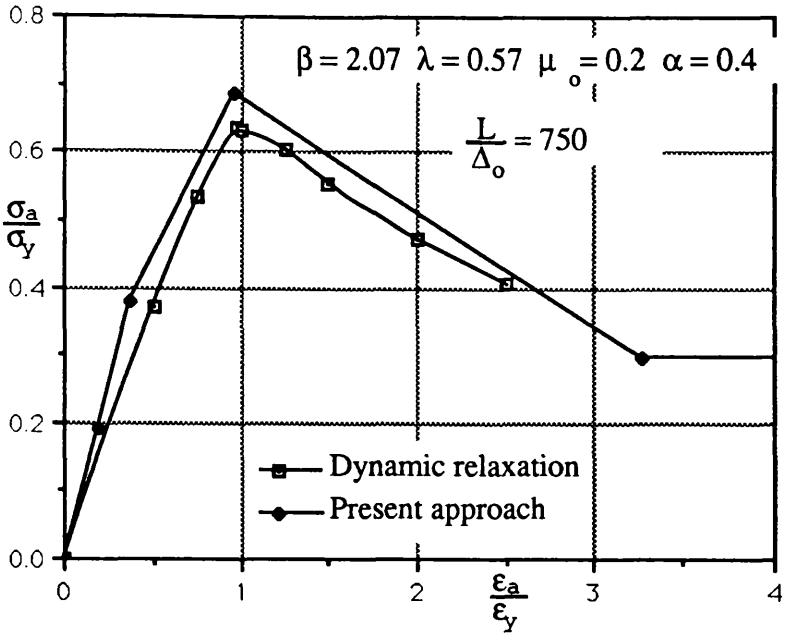

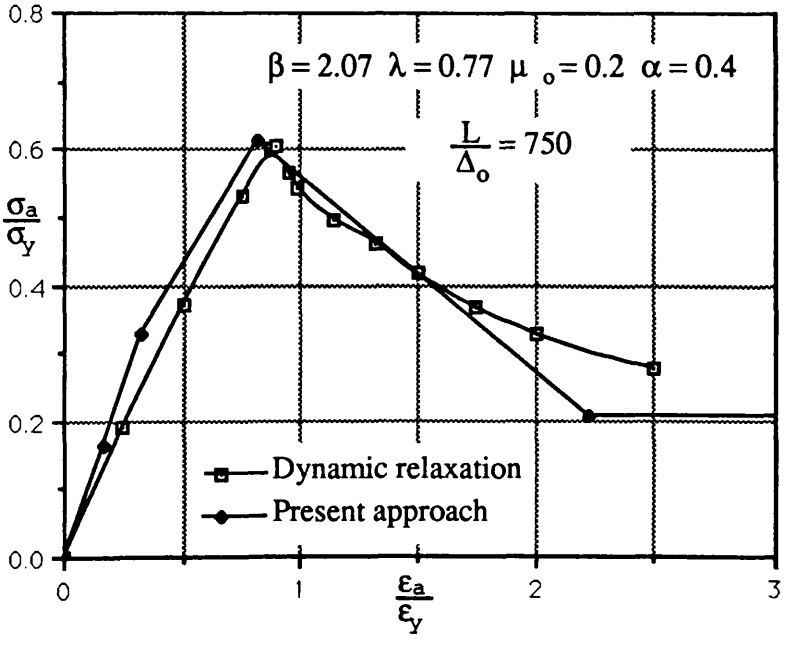

Figure 5.4.b **Stress-strain curves**
Correlation with numerical methods

CHAPTER 6

Hull girder longitudinal strength

6.1 Introduction and review:

The hull girder is a three-dimensional structure. The collapse of such a structure involves various combinations of failure modes. Limit state analysis is more complicated than elastic response due mainly to the non-linear behaviour of the material and structural components. The structure may fail by local plasticity, buckling or fracture. A review of the collapse of the components by buckling and yielding is presented.

Although the finite element method remains the only technique to deal with significant interaction between various local failure modes, researchers have used less rigorous approaches, for economic reasons.

The common approach, which might be called "component approach", in which the ultimate strength of the hull girder is derived by considering failure of the structural components in the the cross-section using step by step failure and post-ultimate behaviour of elements [48], [49], [50], [51].

Caldwell [46] presented a simplified method to evaluate the ultimate longitudinal strength under sagging loading based on the scantlings and material proprieties of its modelled cross-section. The procedure introduced an instability factor for predicting the maximum strength of the components in compression. However the paper did not itself develop the instability ratios needed for deck, side shell, and bottom structures. This was added by Faulkner in the discussion [46]

Stavovy [47] presented a review and discussion of the literature related to work done in predicting ultimate strength of box girders. The report includes strength formula for the elements of hull girders under axial compression.

Other numerical approaches [48], [49], [50], [51] included in the analysis

both pre- and post-buckling ranges. Reference [51] is particularly interesting by its incorporation of horizontal as well as vertical bending and for making predictions on a probability basis for comparison with a historic failure.

In references [53], [54], three dimensional non-linear finite element modelling is used. Initial imperfections were allowed for with the perturbation approach. In addition to the interaction of various failure modes, the dynamic response of the ship hull girder is analysed, which explains more accurately the behaviour of an unstable structure. The method was applied to four different structural arrangements [53]. However it does not include the effect of residual stresses.

6.2 Hull failure versus component failure:

By idealising the geometry of a hull girder, the ultimate strength can be studied. The problem has been the uncertainty regarding the boundary conditions and the interaction of different modes of failure of the components in the cross-section. It has also always been difficult to represent the structure rationally because of the various loadings which the hull girder undergoes and the complexity of the geometry of the structure.

In linear beam theory, although the strain is proportional to the distance from the neutral axis, the stress varies non-linearly due to shear lag and effective width effects. However, it is expected that the girder strain will increase to a stage where either the yield strength of the flange (deck or bottom) is reached or the flange buckles. Initial failure occurs in the weakest component of the ship hull girder. It is therefore important to know the ultimate strength for such elements.

A panel failure mode has to be defined and modelled before being accounted for in the analysis of a hull girder. The results depend on what modelling is used of the panel. For instance, in transversally framed

structures a deck panel modelled as an orthotropic element will have a low buckling stress. However, a typical plate element between transverses will have a relatively higher buckling stress. This modelling would indicate that global grillage buckling could be the dominant failure mode rather than the local buckling of plates between transverses and this in general will not be true. Modelling of "hard spots" formed by the intersection of deck and side panels, bottom and side panels, or bulkheads with either deck or bottom, is important to incorporate into an analysis evaluating the strength of the hull girder. Hard corners modelled either as fully effective or half effective can give a considerable difference in the results of the ultimate moment, especially for transversely framed ships.

When first failure occurs (failure by compression), the panel loses some of its current load-carrying ability. This disturbs the equilibrium of the hull girder which increases its curvature until load redistribution to achieve equilibrium is reached.

It should be noted that the collapse of one panel increases the possibility of collapse of another panel. When a panel collapses in the compression flange of the box girder, the axis of zero strain moves towards the tension flange. This then, decreases the possibility of tensile yielding, while greatly increases the possibility of further panel collapses by compression.

Failure of the cross-section can be achieved by a series of local collapses and collapse of the cross-section progresses as successive components fail. Many structural elements can collapse before the ultimate load of the hull girder is reached.

6.3 Failure modes:

Box girders may fail by yielding, instability or fracture. Instability is an overall behaviour unlike fracture which concentrates on the strength at specified points. Failure by yielding or instability will be described herein:

6.3.1 Plate instability:

Under compressive loading, arising from bending of a ship, the plate elements may buckle between longitudinal girders. This type of failure is characterised by early collapse of the plates before dominant yielding occurs in the stiffeners and hence, the ultimate load of the stiffened panel is reached before stiffener failure occurs.

In this sense, ultimate load of plates is not sufficient and a knowledge of the behaviour of the plate for the entire loading is important for analysing grillage failure. One means of doing this is to describe the behaviour of the plating by stress-strain or load-shortening curves.

Curves of this kind, based upon numerical analyses and experimental results presented in references [28], [30], are reproduced here in Figs. 1.1 and 1.2. These curves show that the post-buckling strength of nearly perfect plates with little residual stress and initial distortions with $b/t \geq 50$, is categorized by a rapid reduction in load. For plates having a considerable residual stress and initial distortion and for nearly perfect plates with $b/t \leq 40$, little, if any, load reduction occurs after maximum load.

In existing grillages which often contain heavy welding, the ultimate load will not normally be reached until the compressive strain is well beyond the yield strain ε_y. At this point extensive yield will normally occur in the stiffeners.

6.3.1 Interframe flexural buckling :

Collapse is a column failure by flexural buckling of stiffeners and plating between transverse girders. This mode of failure is characterised in two types:

(a) Plate induced failure (buckling towards the stiffener)

(b) Stiffener induced failure (buckling towards the plating)

In this kind of behaviour the panel formed by the plate-stiffener

combination is assumed to behave like a beam-column and account taken of reduced plating stiffness and buckling is purely flexural.

The direction of buckling is often influenced by the direction of initial distortion of the stiffeners. Initial distortion will normally induce buckling towards the stiffener. In a few cases, initial distortion may be oriented towards the plating inducing buckling towards this direction. Flexure of the span towards the stiffener in one frame may induce buckling towards the plating in an adjacent span. This arises from structural continuity and carry-over moments.

Numerical analyses show that where buckling occurs towards the plating, the collapse load may be substantially less than where collapse occurs towards the stiffener. This is more pronounced in slender columns. Here is less difference where plating stiffness is reduced by residual stress and buckling effects.

Collapse is influenced by the magnitude and distribution of residual stresses in stiffeners. The panel is affected strongly by the presence of compressive residual stresses in the plating.

Significant coupling may occur between adjacent spans, particularly in a structure with high interframe slenderness. In some cases, in spite of the upward (towards the stiffener) direction of initial deformation in both spans, upward buckling in one half span with large deformation may induce downward (towards the plating) buckling in the adjacent span and hence collapse at a load substantially less than that for upward buckling. More details in the subject can be found in ref. [30].

6.3.3 Stiffener tripping:

This kind of failure may occur in panels with torsionally weak stiffeners (Flat bars or narrow flanges) or stiffeners which are short relative to their depth. Lateral-torsional instability may also occur in connection with flexural buckling where flexure occurs away from the stiffener therefore inducing compression in the outstand. Elastic tripping

can be estimated using folded-plate theory [30], [63] or finite element methods. Faulkner [61] presented a linear elastic formulation for flat and cylindrical shell elements and the report provides an improved understanding of lateral-torsional buckling and of interactive buckling effects in the plating. With the advent of general non-linear finite element analyses, it is now possible to tackle inelastic tripping.

6.3.4 Overall grillage instability :

This kind of failure involves bending of transverses as well as longitudinal stiffeners. This type of failure is more likely to occur in lightly stiffened panels.

Provided that lateral-torsional instability and overall buckling are avoided, the inelastic interframe buckling will be the dominant collapse mode in connection with longitudinal strength of hull girders.

6.4 Numerical procedure:

6.4.1 Introduction:

The numerical procedure presented here is similar to the one in reference [28] but, for the tangential-strain curves accounting for the stability of the components, the modelling presented in chapter 4 is used.

A simple procedure based on cross-section modelling is used to study the ultimate strength of a hull girder. In this approach the collapse of the hull girder is due to failure of local structural elements rather than an overall simultaneous instability. Thus, what is assumed is that there is no significant interaction between various local failure modes.

6.4.2 Modelling of the cross-section:

The cross-section is divided into elements defined by their geometrical and material properties . The approach is based on an incremental iterative procedure.

The failure modes considered are:

(1) Local plate buckling(beyond which the load-shortening behaviour often changes)

(2) Inter-frame flexural buckling of stiffened plates.

(3) Failure by yielding.

The cross-section is divided into relatively small elements defined by their area, distance from centroid of the element to an axis (usually taken as the base of the bottom flange), as illustrated in Fig. 6.1, and a code number related to a certain collapse mode or an effective tangential-strain curve.

The loading is uni-axial compression or tension due to vertical bending moment of the box girder.

6.4.3 Incremental procedure:

In order to follow the moment-curvature relationship, loading is applied incrementally in terms of the curvature (φ) and the procedure follows the steps shown below:

1. Apply load incrementally in terms of curvature $\Delta\varphi_k$
2. Elemental strains are then estimated using a linear beam theory and cumulative values are then estimated:

$$\Delta \varepsilon_{ik} = \Delta \varphi_k (Z_i - Z_{Nk}) \qquad \text{where} \qquad (6.1)$$

Z_i is the distance from element centroid to the base axis.
Z_{Nk} is the distance of theurrent neutralaxis of the cross-sectionto the baseaxis.

3. Elemental stresses for each component are derived using the effective tangent modulus and cumulative values are then calculated:

$\Delta \sigma_{ik} = \Delta \varepsilon_{ik} E_{ik}$ where E_k is the effective tangent modulus of the i^{th} element.

$$\sigma_{ik} = \sigma_{i,k-1} + \Delta \sigma_{ik} \qquad (6.2)$$

The neutral axis of the cross section is calculated during each incremental loading and is used for the next incremental loading. Ignoring the local inertia of the components, the neutral axis is estimated as follows:

$$Z_{N\,k} = \frac{\sum_{i=1}^{i=NE} E_{i\,k}\, A_i\, Z_i}{\sum_{i=1}^{i=NE} E_{i\,k}\, A_i} \qquad (6.3)$$

The instantaneous rigidity of the cross section $(EI)_{Hk}$ is calculated from the equation:

$$(EI)_{H\,k} = \sum_{i=1}^{i=NE} E_{i\,k}\, A_i\, Z_i^2 - Z_{N\,k}^2 \sum_{i=1}^{i=NE} E_{i\,k}\, A_i \qquad (6.4)$$

(4) Incremental moments are estimated, and cumulative values are then derived:

$$\Delta M_k = (EI)_{H\,k}\, \Delta \varphi_k$$

$$M_k = M_{k-1} + \Delta M_k \qquad (6.5)$$

$$\varphi_k = \varphi_{k-1} + \Delta \varphi_k$$

6.5 Results and comparison:

6.5.1 Correlation with test results :

6.5.1.1 Models of Dowling et al:

Two models, numbers 2 and 4, tested by Dowling et al [56], [57] at Imperial College, were chosen for comparison. The models failed by flexural buckling of the stiffened panels in the compression flange.

Model 2:

In the present analysis, model 2 was discretised, as shown in Fig. 6.2. Dimensions and material parameters are listed in Table 6.1. Hard corners formed by the intersection of side shell deck and side shell bottom were assumed to have an elastic-perfectly plastic relationship during compression and tension. Curves representing the stiffened panels were derived using the present modelling, and those for plate panels were derived using the same approach for a value of 0.4 for the column

slenderness. Load-shortening curves representing components of the box-girder are shown in Fig. 6.3.

Results obtained using the present approach in the sagging condition, together with experimental results, are shown in Fig. 6.3. Good agreement can be seen with test results.

Model 4:

Model 4 has the same overall dimensions as model 2, but with closer stiffening. Dimensions and material parameters are listed in Table 6.1. The subdivision of the cross-section into elemental areas is shown in Fig. 6.2.

The experimental results, and those obtained applying the present approach, together with the load-shortening curves of the components, are shown in Fig. 6.4. The results show good agreement.

6.5.1.2 Models of Reckling:

Two of the models tested at the Technical University of Berlin by Reckling [58] were selected for comparison.

Collapse of model 23 occurred by buckling of the plate panel between longitudinal stiffeners in the deck. Model 31 is characterised by an early buckling of the deck panels. However, as noted by Reckling, the collapse was delayed by the restraining effect of the side walls.

Model 23:

Dimensions and material parameters are listed in Table 6.2 and the subdivision of the cross-section into elemental areas is shown in Fig. 6.5. Results for the moment-curvature relationship, together with the test results and load-shortening curves for the components, are illustrated in Fig. 6.6. The results derived using the present approach show a reasonable agreement with the test results.

Model 31:

The descretisation of the model into small elements is shown in Fig. 6.5.

Dimensions and material parameters are summarised in Table 6.2. The predicted results for the ultimate moment and the strength of the components forming part of the cross-section of the model, together with test results, are illustrated in Fig. 6.7. The results give a good correlation with those presented from the test.

6.5.2 Correlation with numerical results:

6.5.2.1 ARE results:

In reference [28], the ultimate strength of a destroyer type vessel is evaluated. For the strength of the components, the authors used load-shortening curves derived using the finite element program [28]. The analysis was conducted for two frame spacings (L=1000 mm and 2000 mm) to show the close correlation that exists between the hull girder failure and that of their components. An attempt is made to compare the results derived using the present method and that presented in reference [28]. The cross section of the destroyer with the subdivision into elements is shown in Fig. 6.8 and dimensions of the components are also presented. All elements have a yield stress of 325 N/mm^2 and a Young's modulus of 207000 N/mm^2. An average magnitude of residual stress and initial distortion was considered and a stiffener initial distortion Δ_0 /L = 0.0013 was assumed. The method shows that failure occurs by buckling of the stiffened panels in the deck under sagging loading. As seen in Fig. 6.9, doubling the frame spacing lead to a reduction in ultimate moment of 30% in the sagging condition and 20% in the hogging condition, and the moment-curvature pattern reveals a close correlation with the load-shortening curves of the components forming part of the upper flange or the bottom flange. The maximum moment occurs at or soon after failure in the deck or bottom components. Results also indicate that the assumption made for the "hard corners" may give rise to a difference in the results, as illustrated in Fig. 6.10, where hard corners were considered to be half effective, during the sagging condition. The results then

decrease by 5 and 1% for the frame spacing L=2000 mm and 1000 mm respectively. During hogging loading the results then, decrease by 4.3 and 3% for the frame spacing L=2000 mm and 1000 mm respectively.

In general, the present approach provides good agreement with ARE results concerning the ultimate moment, a mean error having a value of -5.4% and a standard deviation of 3.8%, the highest error (-10.4%) was experienced for the sagging condition at the frame spacing L=2000 mm, which is due to the difference in the maximum strength of panels forming part of the deck for the the two predicted values (0.79 and 0.74). The discrepancy, however, in the post-ultimate strength is more pronounced, particularly at the lower frame spacing, this is due to the differences in the post-ultimate strength of the components between the two methods (illustrated in Figs. 6.10.b and 6.10.c).

6.5.2.2 USAS finite element program results :

The method is applied to a cross-section of a tanker [53]. USAS [53] is a non-linear finite element program able to model a three-dimensional structure and analyse the dynamic response of the structure. The vessel has full longitudinal framing. The longitudinal girders were treated as beams with bi-linear representation for the average stress-strain being assumed. The stiffened panels consisted of longitudinal stiffeners and an effective width of plating which were treated as a beam-column (the analysis involves only the plating and the longitudinals and not the heavy transverses).

The cross-section of the tanker is presented in Fig. 6.11 and the results are illustrated in Fig. 6.12. The value of M_u/M_P derived using USAS is 0.98 for the sagging condition and the value of M_u/M_P derived using the present approach is 0.96 which shows a good agreement.

The results show the high effectiveness of the structure where the column slenderness varies in the range (0.9 to 2.4) for stocky panels.

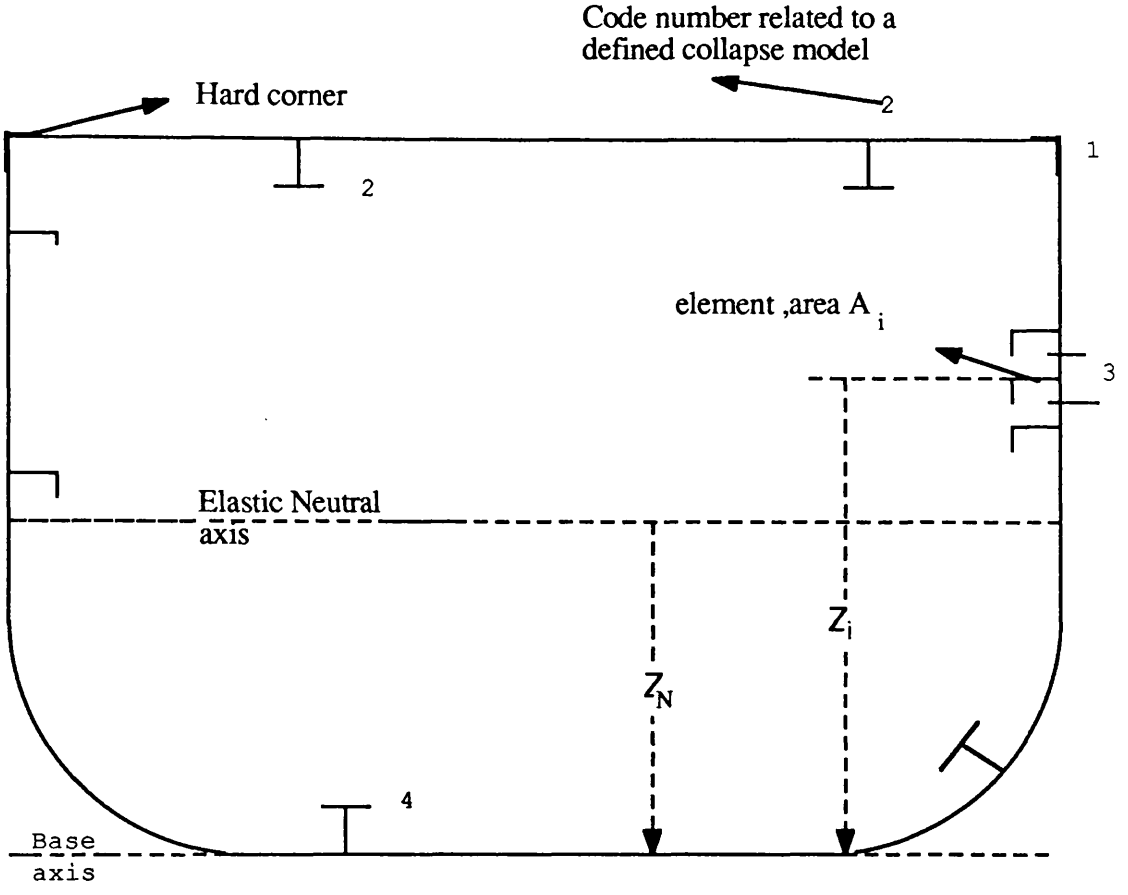

Z_N Distance from The neutral axis of the cross-section to the base axis.

Z_i Distance from element centroid to the base axis.

Figure 6.1 Hull girder subdivision into elements

	Model 2	Model 4
1. Compression flange		
Plate thickness (mm)	4.86	5.02
Stiffener spacing (mm)	241.3	120.65
Plate yield stress (N/mm^2)	297.3	221.0
Plate Young's modulus (N/mm^2)	208500	207000
Stiffener dimensions (mm)	"L" 50.8*4.76 / 15.9*4.76	"L" 50.8*4.76 / 15.9*4.76
Stiffener yield stress (N/mm^2)	276.2	287.9
Stiffener Young's modulus (N/mm^2)	191500	199200
2. Tension Flange		
Plate thickness (mm)	4.86	4.94
Stiffener spacing (mm)	241.3	120.65
Plate yield stress (N/mm^2)	297.3	215.6
Plate Young's modulus (N/mm^2)	208500	208700
Stiffener dimensions (mm)	"L" 50.8*4.76 / 15.9*4.76	"I" 50.8*6.35
Stiffener yield stress (N/mm^2)	276.2	303.8
Stiffener Young's modulus(N/mm^2)	191500	206200
3. Side Flange		
Plate thickness (mm)	3.36	4.94
Stiffener spacing (mm)	273.05	98.425, 114.3, 111.125
Plate yield stress (N/mm^2)	211.9	280.6
Plate Young's modulus (N/mm^2)	216200	214100
Stiffener dimensions (mm)	"L" 50.8*4.76 / 15.9*4.76	"L" 50.8*4.76 / 15.9*4.76
Stiffener yield stress (N/mm^2)	276.2	287.9
Stiffener Young's modulus(N/mm^2)	191500	199200
$\frac{\sigma_r}{\sigma_y}$	0.2	0.2
$\frac{\delta_o}{b}$	1/400	1/800
$\frac{\Delta_o}{L}$	1/1000	1/1000
Experimental ultimate moment (kN.m)	1542.7	2212.4

TABLE 6.1 Models 2 and 4 of Dowling et al.

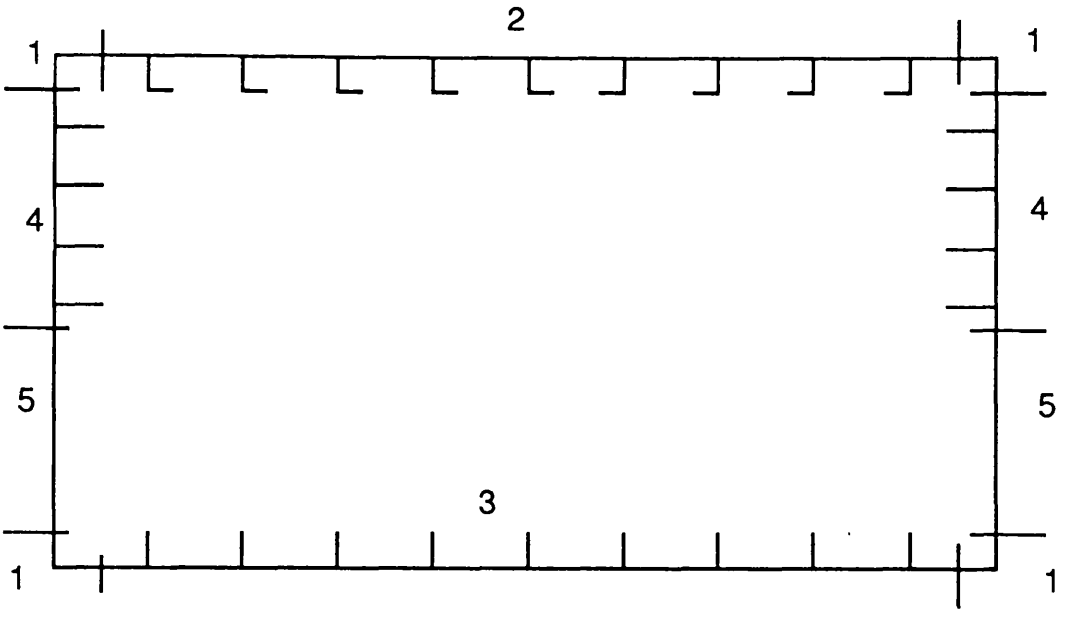

Model 4

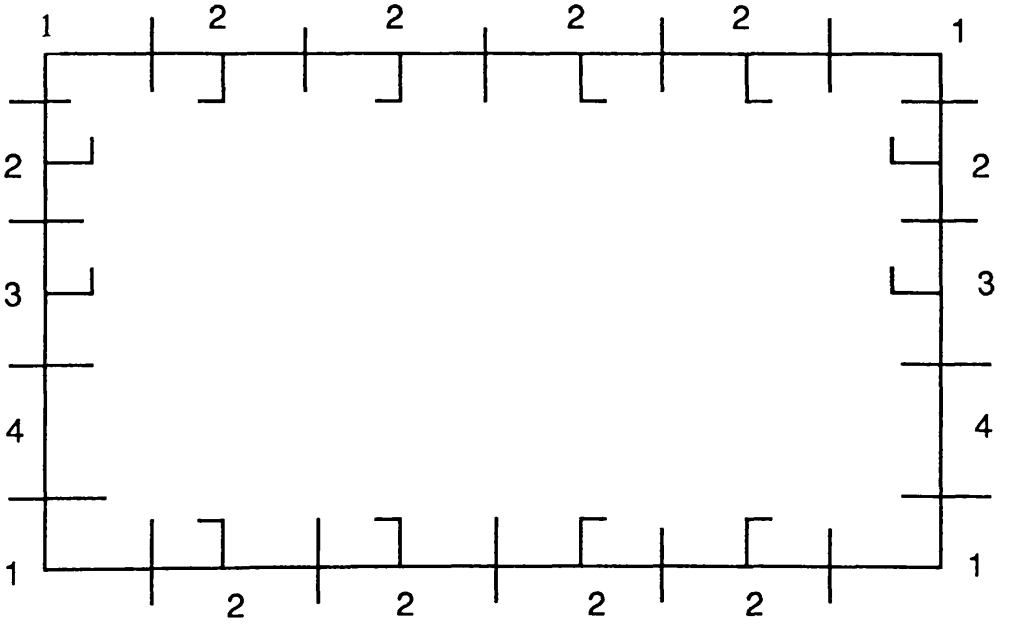

Model 2

Figure 6.2 **Models of Dowling et al.**

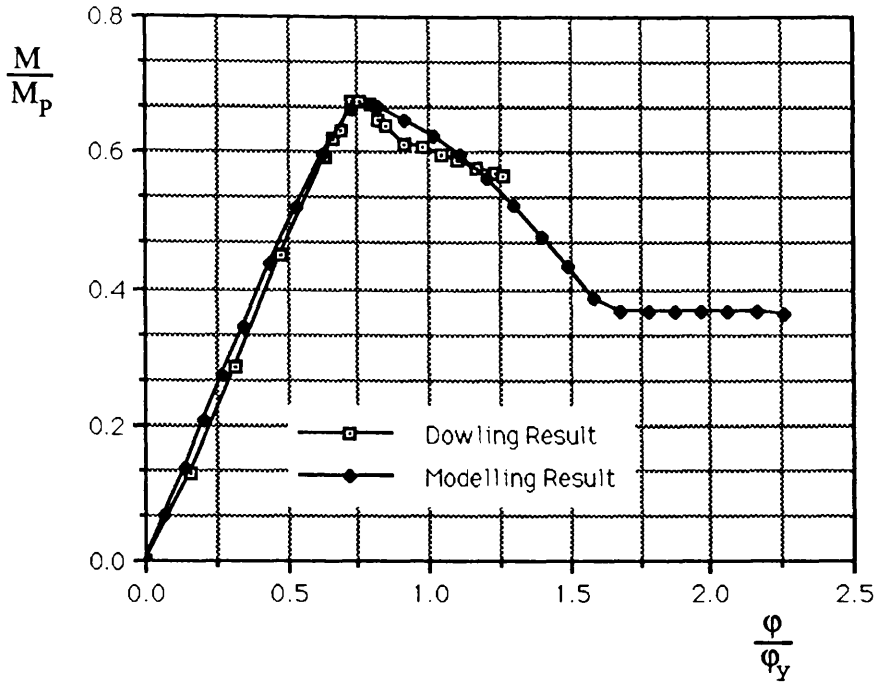

Moment-curvature relationship

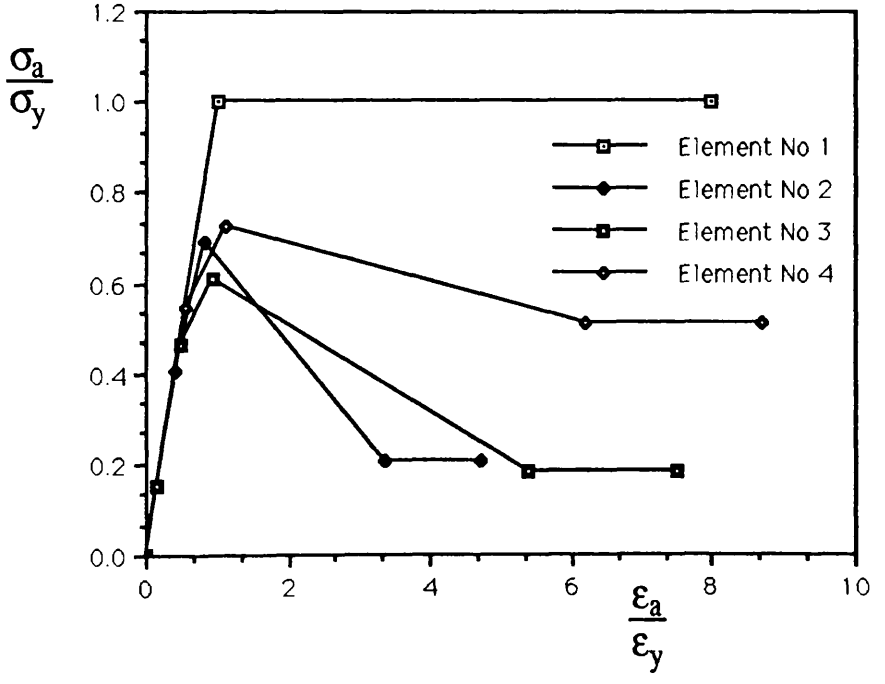

Stress-strain curves for elements of the cross-section

Figure 6.3 Model 2 of Dowling et al

	Model 23	Model 31
1. Compression flange		
Plate thickness (mm)	2.50	2.50
Stiffener spacing (mm)	85.71	120.00
Plate yield stress (N/mm^2)	246.0	246.0
Plate Young's modulus (N/mm^2)	210000	210000
Stiffener dimensions (mm)	"L" 30.0*2.50 / 20.0*2.50	"L" 30.0*2.50 / 20.0*2.50
Stiffener yield stress (N/mm^2)	246.0	246.0
Stiffener Young's modulus(N/mm^2)	210000	210000
2. Tension Flange		
Plate thickness (mm)	2.50	2.50
Stiffener spacing (mm)	85.71	120.0
Plate yield stress (N/mm^2)	246.0	246.0
Plate Young's modulus (N/mm^2)	210000	210000
Stiffener dimensions (mm)	"L" 30.0*2.50 / 20.0*2.50	"L" 30.0*2.50 / 20.0*2.50
Stiffener yield stress (N/mm^2)	246.0	246.0
Stiffener Young's modulus(N/mm^2)	210000	210000
3. Side Flange		
Plate thickness (mm)	2.50	2.50
Stiffener spacing (mm)	100.0	133.33
Plate yield stress (N/mm^2)	246.0	280.6
Plate Young's modulus (N/mm^2)	210000	214100
Stiffener dimensions (mm)	"I" 30.0*2.50	"I" 30.0*2.50
Stiffener yield stress (N/mm^2)	246.0	246.0
Stiffener Young's modulus(N/mm^2)	210000	210000
$\frac{\sigma_r}{\sigma_y}$	0.2	0.2
$\frac{\delta_o}{t_p}$	0.25	0.55
$\frac{\Delta_o}{L}$	1/1000	1/1000
Experimental ultimate moment (KN.m)	249.37	215.9

TABLE 6.2 Models 23 and 31 of Reckling

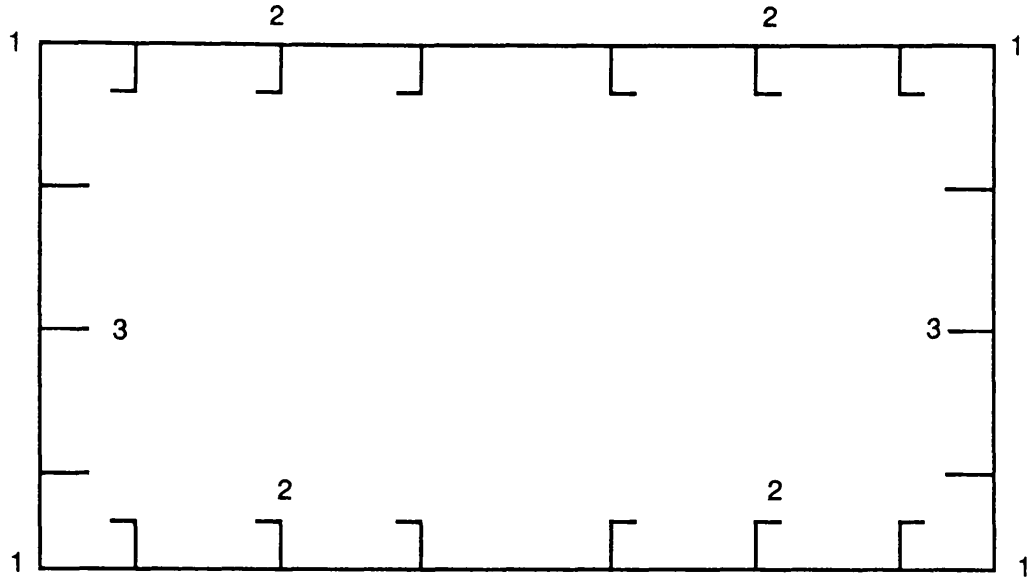

Model 23

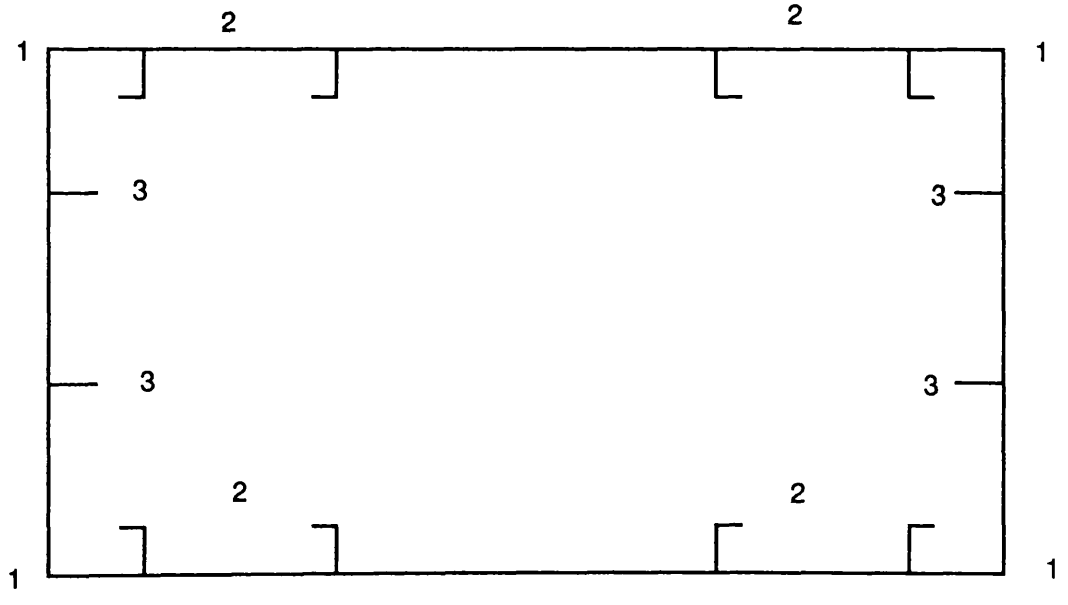

Model 31

Figure 6.5 Models of Reckling

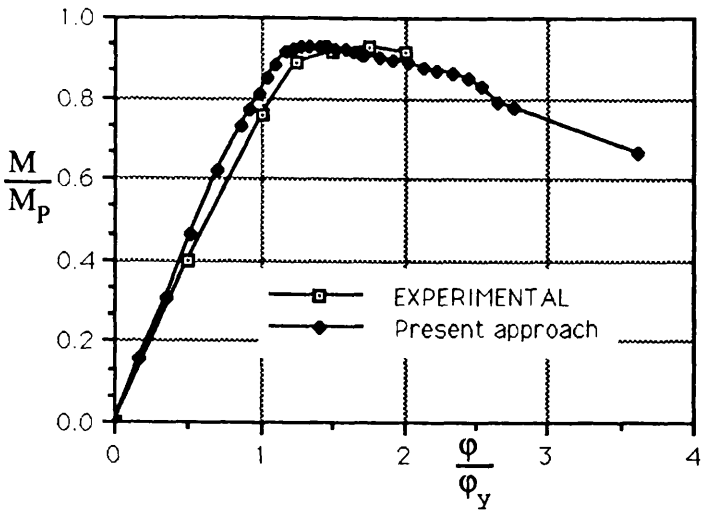

Moment-curvature relationship

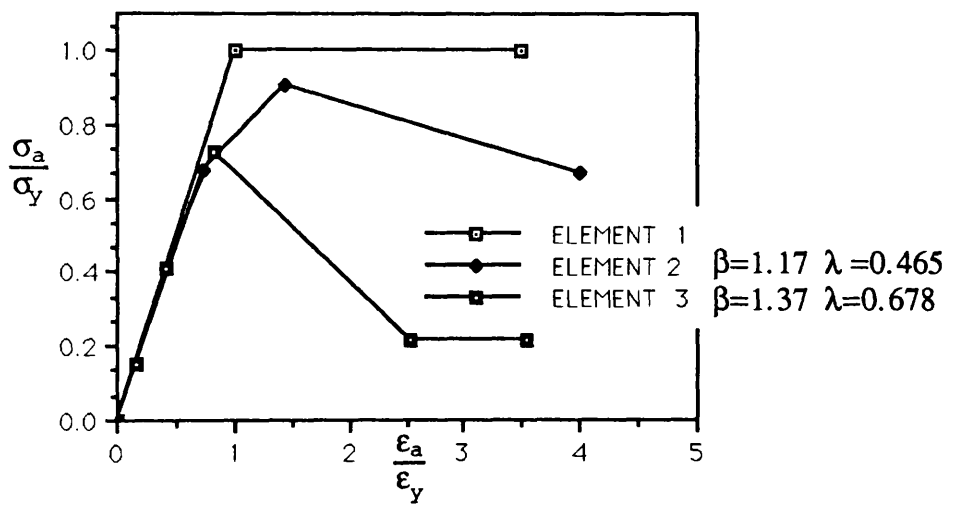

Stress-strain curves for elements of the box girder

Figure 6.6 Model 23 of Reckling

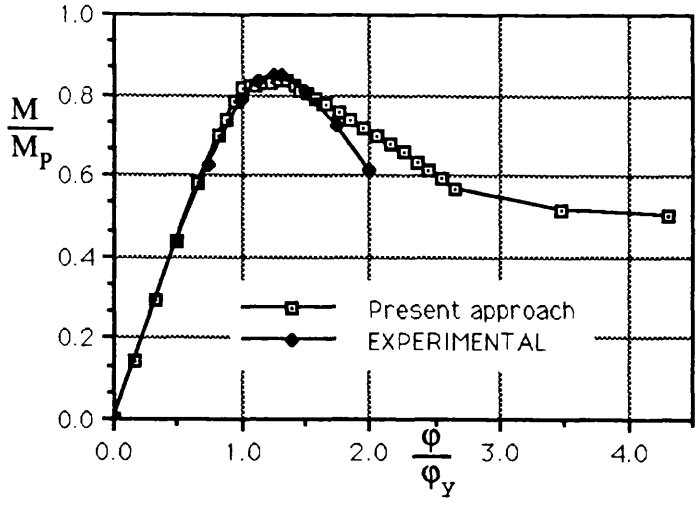

Moment-curvature relationship

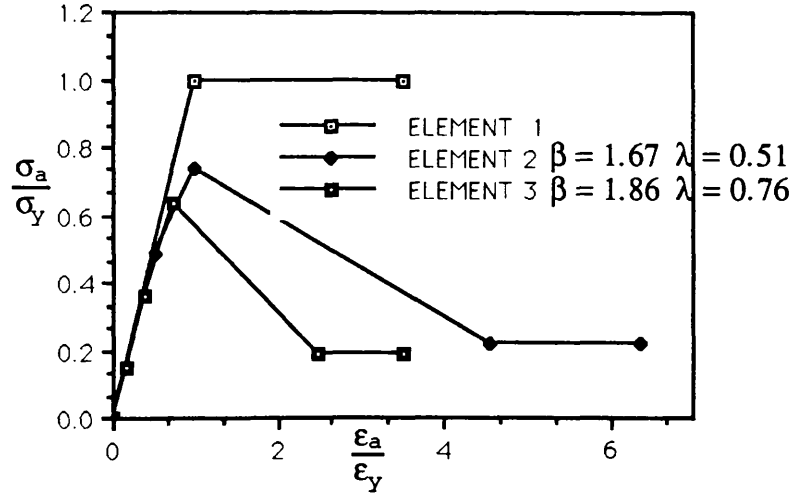

Stress-strain curves for elements of the box girder

Figure 6.7 Model 31 of Reckling

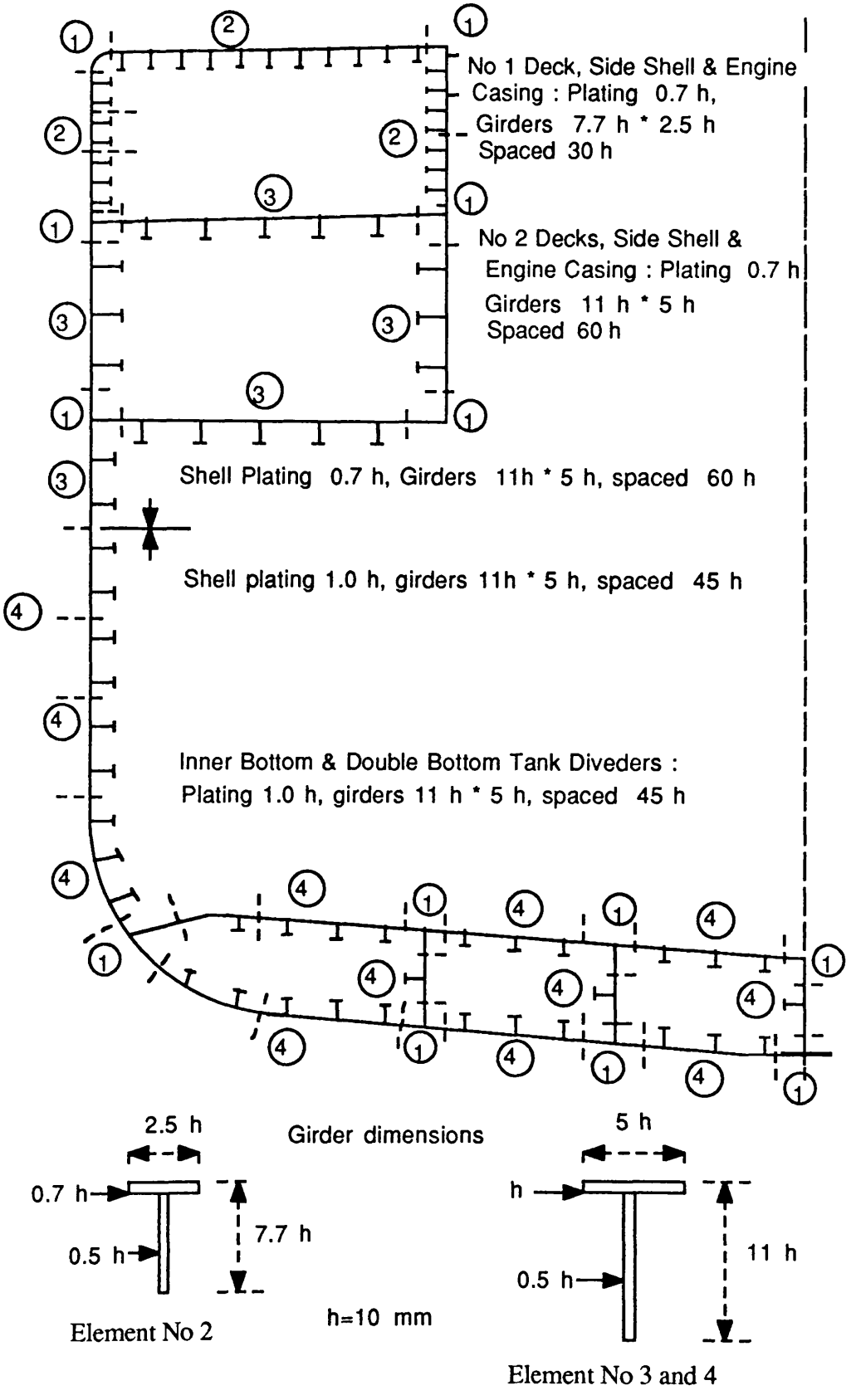

Figure 6.8 Destroyer midship section

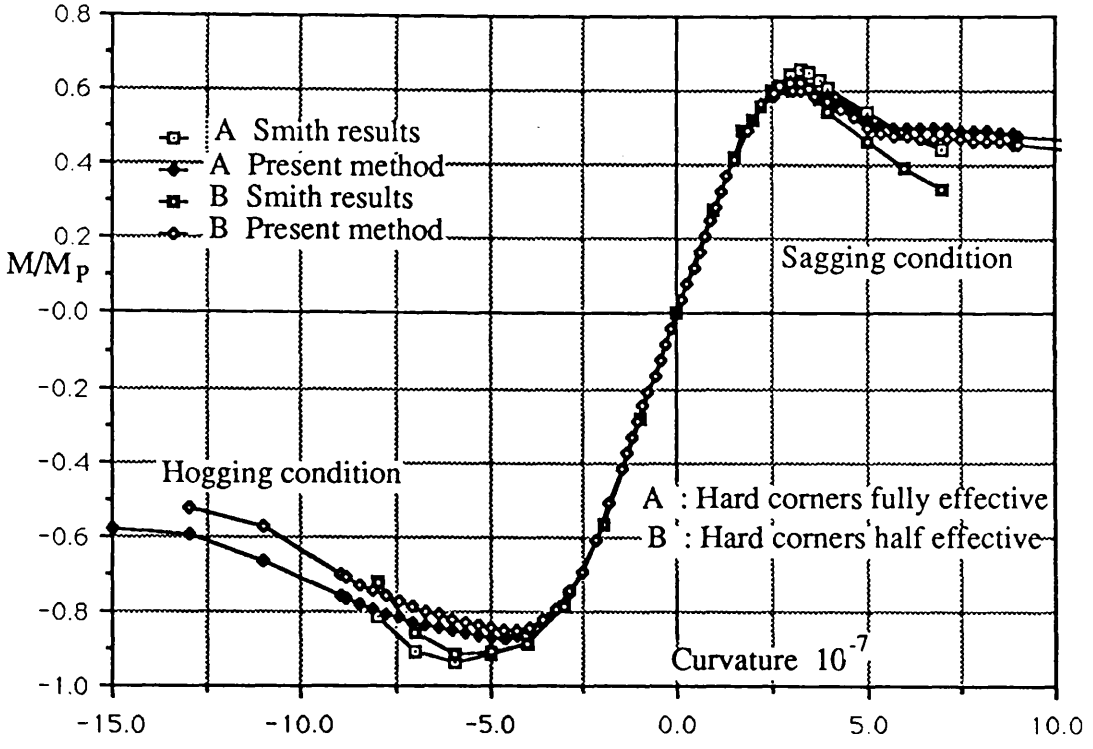

1- Frame spacing= 1000 mm.

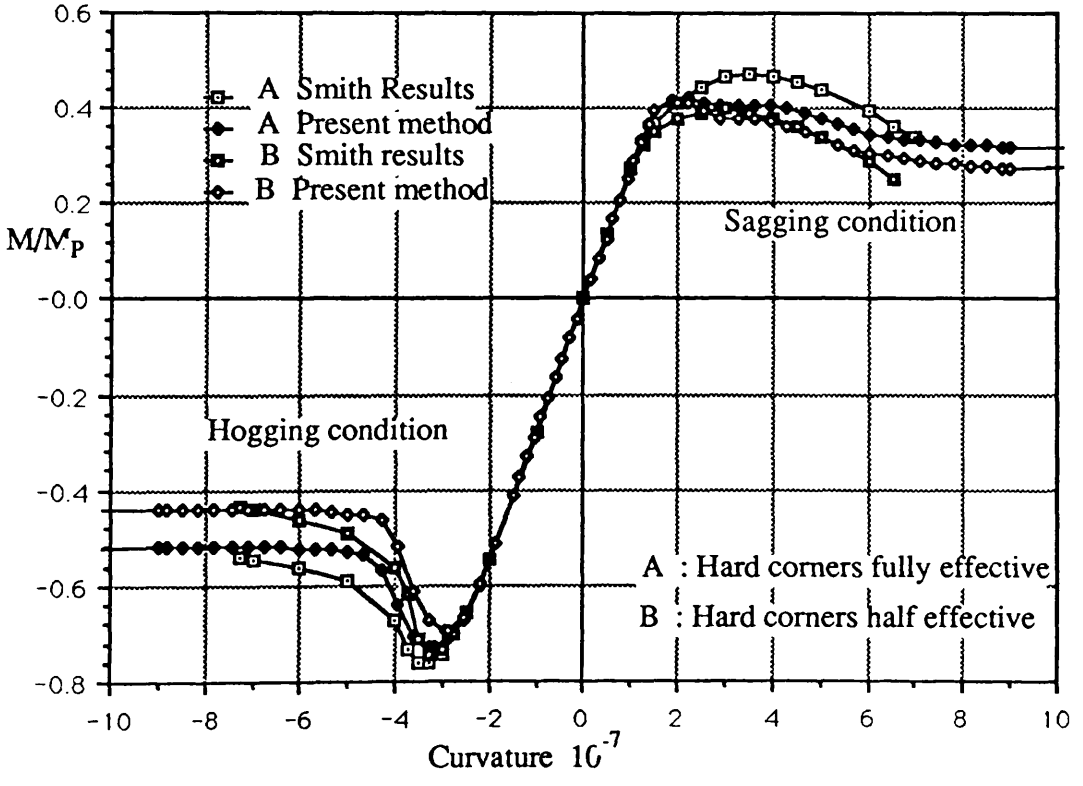

2- Frame spacing=2000 mm.

Figure 6.9 Moment-curvature curves for a destroyer cross-section

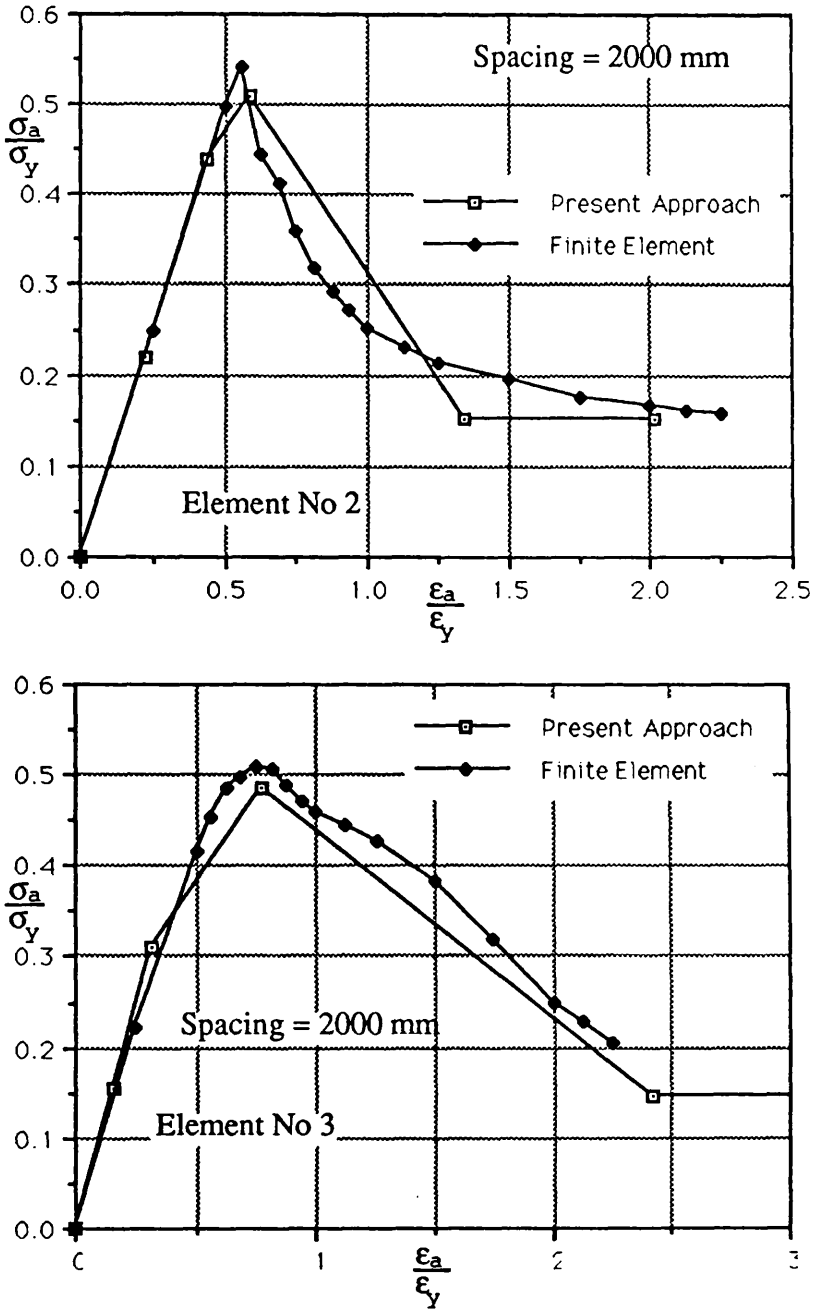

Figure 6.10.a **Stress-strain curves for elements of the destroyer**

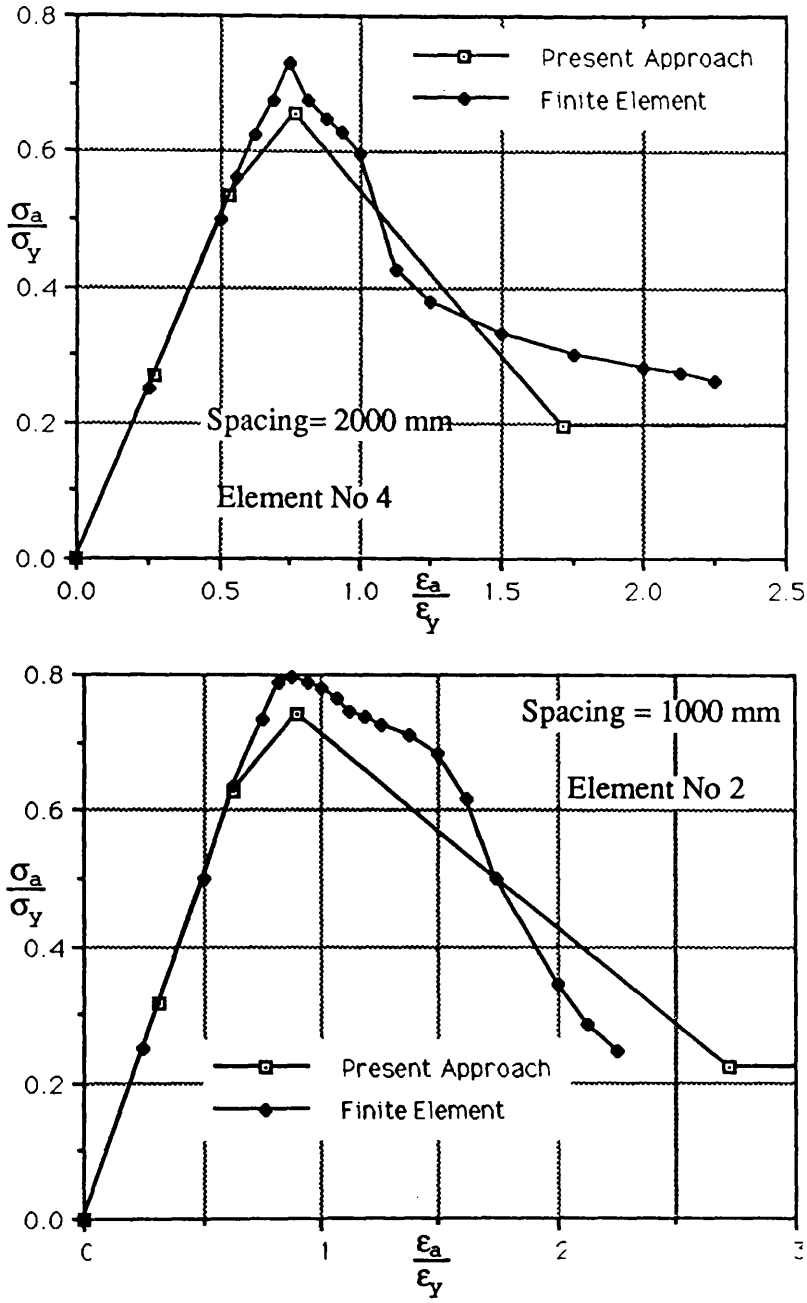

Figure 6.10.b **Stress-strain curves for elements of the destroyer**

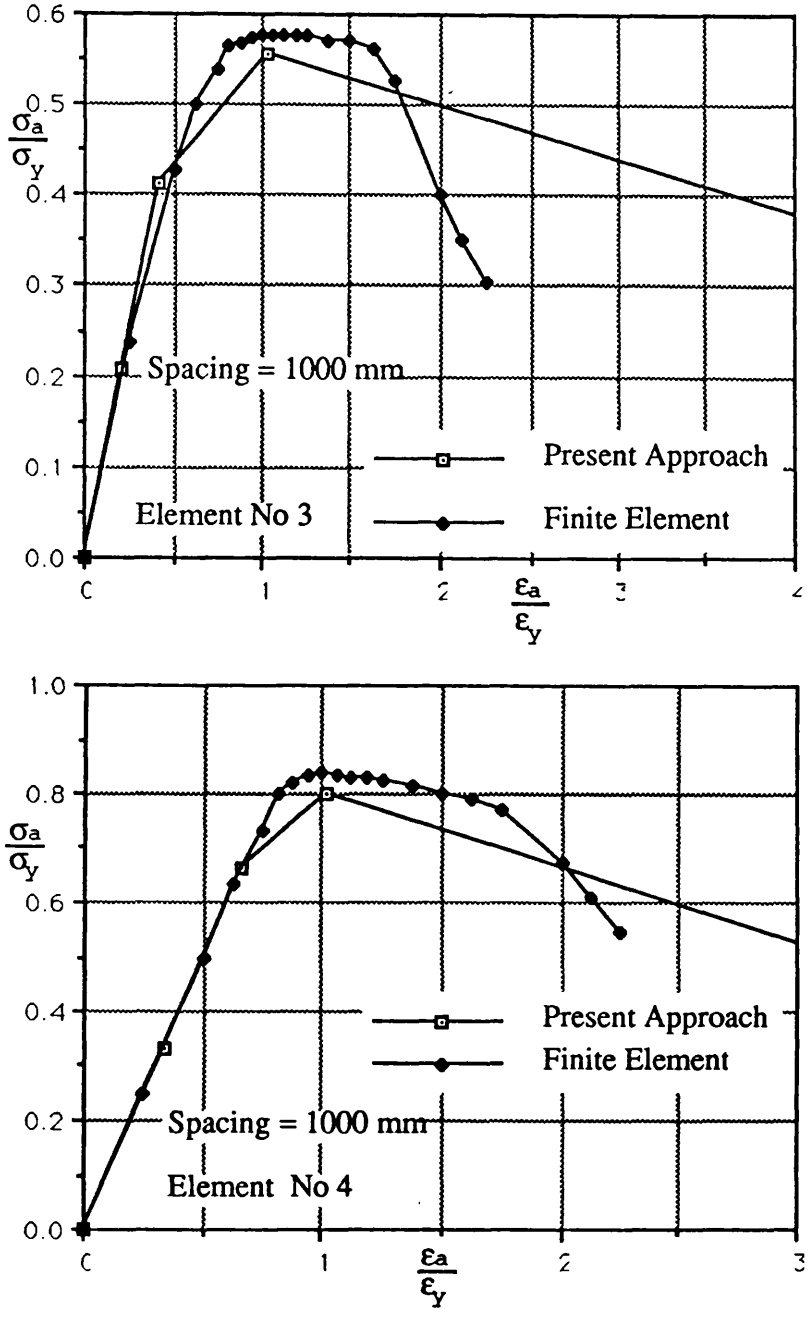

Figure 6.10.c **Stress-strain curves for elements of the destroyer**

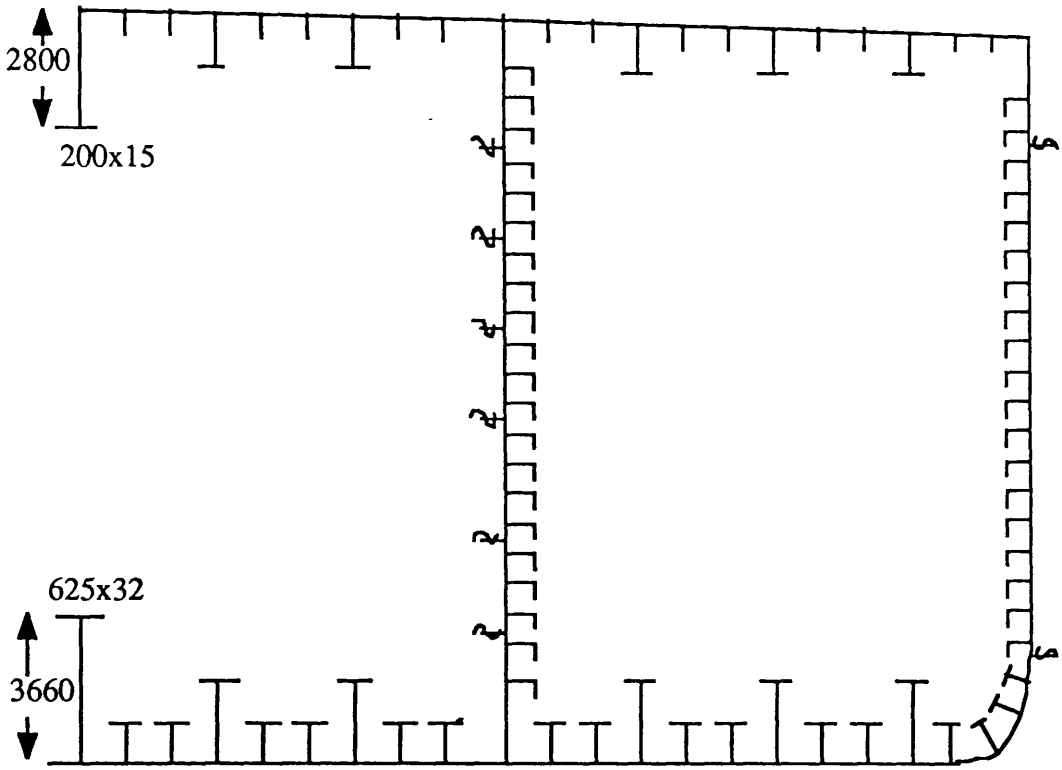

Bottom

Plate thickness 34.0,32.0
Longitudinals 465x18,190x25
Girders 1220x16,350x25
Spacing 910

Deck

Plate thickness 27.0
Longitudinals 450x35
Girders 1000x16/400x16
spaced 910

Side shell

Plate thickness 27.0, 21.5
Longitudinals 190x25/450x16

Longit.Bulkheads

Plate thickness 25.5,12.5,11,12.5,14,14.5,25.5
Longitudinals 190x25/450x16
Spacing 762

(All figures are in mm)

Figure 6.11 Cross-section of Tanker

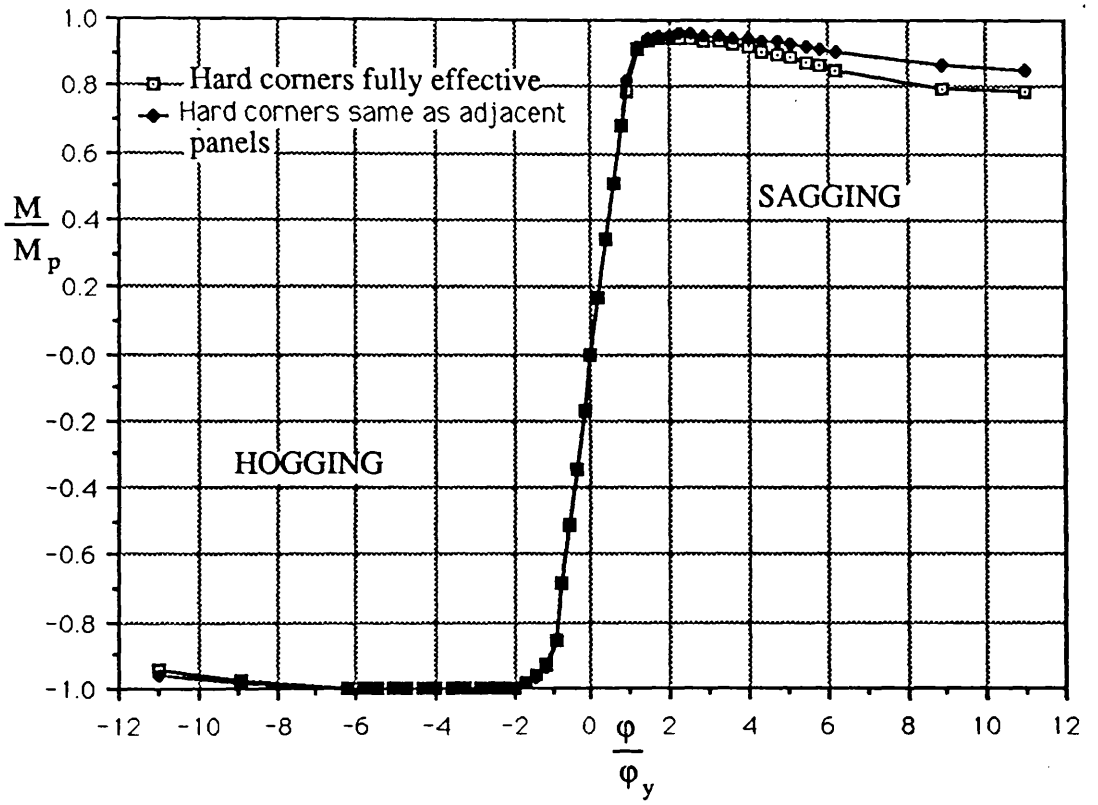

Figure 6.12 Moment-curvature curves for a tanker cross-section

CHAPTER 7

Conclusions

7.1 General discussion and future work:

The aim of the research work outlined in this thesis has been to develop a simplified design approach for the evaluation of strength of longitudinally stiffened panels under compressive loading. Maximum load capacity and post-buckling strength are included. The approach was carried out using a parametric analysis with the aid of a finite element computer program.

A review of the strength of unstiffened and stiffened panels has been presented relating to work done in carrying out such analysis and to test results.

Parameters found to have a significant influence on the behaviour of stiffened plate panel under compressive loads were, plate slenderness, column slenderness, plate residual stress and initial distortions. Of less significance were stiffener to plate area ratio and stiffener residual stress.

The present simplified analytical approach for deriving the ultimate strength of stiffened panels subjected to uni-axial compression and for accounting for a number of geometrical and material parameters effects, including post-ultimate strength, shows a reasonable correlation with test results and rigorous numerical techniques. The importance of the method lies in its simplicity to incorporate in a program analysing the ultimate strength of a box girder.

The effect of initial distortion and residual stress is restricted to three magnitudes (as explained in paragraphs 3.2.3 and 4.4.3) and the adoption of one of these in design level will allow these effects to be incorporated in a more general approach.

It has been noticed (paragraph 3.2.4) that the assumptions of the applied load following the shifting of the neutral axis and that of not

following the shift gives rise to considerable differences in the results. This perhaps suggests the need for more tests in order to recommend the more realistic approach. Meanwhile, adopting the shifting neutral axis approach is recommended.

It has been noticed from the series of the parametric analysis (chapter 3) that stiffener to plate area ratio has a slight effect on the maximum strength which increases with the increase of stiffener to plate area ratio. The effect, however, is very pronounced on post-buckling strength. An increase in the stiffener to plate area ratio improves the load carrying capacity, which is more dominant for low and moderate values of plate slenderness. The stiffened panel behaviour path in the unloading range changes from a sudden sharp pattern to a less severe and gradual process. A realistic representation of such behaviour requires the modelling to include the stiffener to plate area ratio.

It has also been noticed that more complete modelling should take into account all parameters governing the strength and covering the entire loading range. Panels in the unloading range behave differently in a non-linear and complicated pattern and, in order to achieve a more accurate representation of such behaviour the modelling may need more than the present two state modelling for the unloading path. Nevertheless such modelling has recently [67] proved valuable for system strength modelling in TLPs. The present investigation has also been restricted to low and high values of column slenderness.

Achieving an optimum of simplicity and accuracy in a design approach is a state-of-the-art in itself, and an accurate representation of the buckling of stiffened panels in a simple way is still a difficult task. In spite of the reasonable accuracy of the present method, its procedure needs to be further improved and simplified, yet it should retain a reasonable degree of accuracy for design purposes.

From the numerical analysis, non-dimensional design curves have been produced which enable the ultimate load to be determined for various

levels of panel parameters.

Using the proposed modelling, some hull girder configurations have been analysed to determine the moment-curvature relationship. The results show high correlation that exists between hull failure and that of the elements forming part of the compression or the tension flange, as well as the post-ultimate strength. Longitudinally framed vessels show a relatively high residual strength in regard of these of the components.

The work presented here identifies some areas where further studies may advantageously be pursued. These are:

(a) Failure of panels by tripping of the stiffener and coupling of tripping and flexural buckling and the need for more tests and numerical investigation covering the lateral stiffener buckling with interaction from plate instability effects.

(b) Effect of eccentricity of the applied loading on the strength of stiffened panels. This parameter remains an unknown quantity in tests and a small change in the position of the applied loading can influence the direction of buckling.

(c) A design approach must account for residual stresses and initial distortions. In this connection, a survey of initial distortions and measurement of residual stresses during the process of welding is needed in order to adopt reasonable tolerances during design. In particular the use of the present combined parameter requires examining for larger values [68].

(d) During any future tests, grillages of various number of bays should be tested in a realistic approach to the behaviour of actual marine structures by accounting for the interaction of one span with another.

(e) The assumptions made for the hard corners in box girders, and the need for full scale tests on collapse of box girders to determine the effective area of hard corners which resist buckling. The elements formed by the intersection of decks and side shell, bottom with side shell or bulkheads with decks or bottom are termed as "hard corners", and are

generally assumed to be stiff enough to resist buckling. Using the numerical approach for deriving the strength of the box girder, the modelling of these elements can strongly affect the maximum strength of the hull girder. In an extremely flexible design [51] such hard corners provided most of the longitudinal strength.

References:

1. Little, G.H. : "*Rapid analysis of plate collapse by like-energy minimisation*", Jnl. of Mech. Sciences, Vol. 19, 1977.
2. Moxham, K.E. : "*Compression in welded web plates*", Ph.D Thesis, Univ. of Cambridge, June 1970.
3. Crisfield, M.A. : "*Large-deflection elasto-plastic buckling analysis of plates using finite elements*", TRRL Report LR593, 1973.
4. Frieze, P.A. : "*Ultimate load behaviour of steel box girders and their components*", PhD Thesis, Univ. of London, 1975.
5. Harding, J.E., Hobbs, R.E. and Neal, B.G. : "*The elasto-plastic analysis of imperfect square plates under in-plane loading*", Proc. Instn. Civ. Engrs., Part 2, Vol 63, March 1977.
6. Frieze, P.A., Dowling, P.J. and Hobbs, R.E. : "*Parametric study on plates in compression*", Engg. Structures Lab., Civil Engg. Dept., Imperial College, London, CESUC Report BG39, Jan. 1975.
7. Crisfield, M.A. : "*Full range analysis of steel plates and stiffened plating under uniaxial compression*", Proc. Instn. Civ., Engrs, Part 2, Vol 59, 1975.
8. Harding, J.E., Hobbs, R.E. and Neal, B.G. : "*Ultimate load behaviour of plates under combined direct and shear in-plane loading*", Proc. Intl. Conf. on Steel Plated Structures, Imperial College, London, 1976.
9. Crisfield, M.A.: "*A computer program to generate load/shortening relationships for simply supported steel plates*", TRRL Report LR683, 1975.
10. Davidson, H.L.: "*Post-buckling of long rectangular plates*", Fritz Eng. Lab., Report No 248.15, Lehigh University, June 1965.
11. Becker, H.:"*Compressive strength of ship hull girders*", Part 1, Unstiffened Panels, Ship Structures Committee, Report SSC-217, 1970.
12. Dwight, J.B. and Ractliffe, A.T.:"*The strength of thin plates in compression*", Proc. Symposium on Thin-Walled Steel Structures, Swansea, 1967.
13. Moxham, K.E.: "*Buckling tests on individual welded steel plates in compression*", Univ. of Cambridge, Dept. of Engg., Report CUED/C-Struct./TR.3, 1971.
14. Bradfield, C.D.: "*Tests on plates loaded in in-plane compression*", Jnl. of Constructional Steel Research, Vol. 1, No. 1, Sept. 1980.

15. Walker, A.C.: "*The postbuckling behaviour of simply supported square plates.*", Aeronautical Quarterly, 20, 3, Aug. 1969.
16. Dawson, R.G. and Walker, A.C.: "*Postbuckling of geometrically imperfect plates.*", Jnl. of Struct. Div., Proc. A.S.C.E., Jan. 1972, ST1.
17. Yamaki, N.: "*Postbuckling behaviour of rectangular plates with small initial curvature loaded in edge compression*", Jnl. of Applied Mechanics, 26, 3, Sept. 1959.
18. Coan, J.M.: "*Large deflection theory for plates with small initial curvature loaded in edge compression.*", Jnl. of Applied Mechanics, 18, 2, Jun. 1951.
19. Basu, A.K. and Chapman, J.C.: "*Large deflection behaviour of transversally loaded rectangular orthotropic plates.*", Proc. Instn. Civ. Engrs., Vol.35, Sept. 1966.
20. Bhaumik, A.K. and Hanley J.T.: "*Elasto-plastic plate analysis by finite differences.*", Jnl. of Struct. Div., Proc. A.S.C.E., Oct. 1967.
21. Lin, T.H., Lin, S.R. and Mazelsky, B.: "*Elasto-plastic bending of rectangular plates with large deflection.*", Jnl. of Applied Mechanics, Dec. 1972.
22. Alami, B.: "*Large deflection of elastic plates under patch loading.*", Proc. Jnl. of Struct. Div., Proc. A.S.C.E., Vol.98, No ST11, Nov. 1972.
23. Williams, D.G.: "*Some examples of elastic behaviour of initially deformed bridge panels.*", Civ. Engrs. & Pub. Wks. Rev., Oct. 1971.
24. Rushton, K.R.: "*Large deflection of plates with unsupported edges.*", Jnl. of Strain Analysis, Vol. 7, No 1, 1972.
25. Ostapenko, A. and Lee, T.: "*Tests on longitudinally stiffened plate panels subjected to lateral and axial loading*", Lehigh Univ. Pennsylvania, Fritz Eng. Lab. Report, No. 248.4, Aug. 1960.
26. Soreide, T.H., Moan, T. and Nordsve, N.T.: "*On the behaviour and design of stiffened plates in ultimate limit state*", Jnl. of Ship Research, Vol. 22, No. 4, Dec. 1978.
27. Crisfield, M.A.: "*A combined Rayleigh-Ritz/Finite element method for the nonlinear analysis of stiffened plated structures*", Computers & Structures, Vol. 8, 1978.
28. Smith, C.S., Kirkwood, W.C and McKeeman, J.L.: "*Evaluation of ultimate longitudinal strength of a ship's hull*", Admiralty Marine Technology Establishment (Dunfermline), Report No: AMTE(s)/ R671, 1986.

29. Smith, C.S. and Dow, R.S.: "*Ultimate strength of a ship's hull under biaxial bending*". Admiralty Marine Technology Establishment (Dunfermline), Report No: ARE TR 86204, 1986.
30. Smith, C.S.: "*Compressive strength of welded steel ship grillages*", The Royal Institution of Naval Architects, 1975.
31. Faulkner, D.: "*A review of effective plating for use in the analysis of stiffened plating in bending and compression*", J. Ship Research, 19 (1975).
32. Jastrzebski, T. and Kmiecik, M.: "*Statistical investigations of the deformations of ship plates*", Bull. Assoc. Tech. Marit. Aeronaut., 86 (1986).
33. Guedes Soares C.: "*A Code requirement for the compressive strength of plate elements*", Marine Structures 1, Vol. 1, No 1, (1988). See also fuller review by C. Guedes Soares "*Design equation for the compressive strength of unstiffened plate elements with initial distortions*", University of Glasgow Report, NAOE-87-20, June 1987.
34. Rutherford S. E.: "*Stiffened compression panels, the analytical approach*", Lloyd's Register of Shipping, Hull Structures Dept., Report No. HSR 82/26/R1, 1984.
35. Crisfield M. A.: "*Full range analysis of steel plates and stiffened plating under uniaxial compression*", Proc of Intl. Symposium on Steel Plated Structures, Imperial College, London, July 1976.
36. Little G. H.: "*Stiffened steel compression panels, theoretical failure analysis*", The Structural Engineer, Vol 12, Dec 1976.
37. Moolani F.M. and Dowling P.J.: "*Ultimate load behaviour of stiffened plates in compression*", Proc. of Intl. Symposium on Steel Plated Structures, Imperial College, London, July 1976.
38. Soreide T.H., Bergan P.G and Moan T.: "*Ultimate collapse behaviour of stiffened plate using alternative finite element formulations*", Proc. of Intl. Symposium on Steel Plated Structures, Imperial College, London, July 1976.
39. Frieze, P.A.: "*Ultimate load behaviour of steel box girders and their components*", PhD. Thesis, University of London, 1975.
40. 'Merrison Rules: Part IV : Materials and workmanship', U.K, 1973.
41. 'BS5400 Steel, Concrete and composite bridges - Draft', U.K, 1979.
42. 'European Recommendations for steel construction', ECCS, 1978.

43. Massonnet, Ch. and Janss, J.: "*A state of art report on tolerances in steel plated structures*", The Design of Steel Bridges, Editors: Rockey, K.C and Evans, H.R., Granada Publishing, 1980.

44. Somerville, W.L., Swan, J.W. and Clark, J.D.: "*Measurment of residual stresses and distortions in stiffened panels*". Jnl. of Strain Analysis, Vol. 12, No 2, 1977.

45. Antoniou, A.C.: "*On the maximum deflection of plating in newly built ships*", Jnl. of Ship Research, Vol. 24, No 1, March 1980.

46. Caldwell, J.B.: "*Ultimate Longitudinal Strength*", R.I.N.A., Vol. 107, Jul. 1965.

47. Stavovy, A.B.: "*Ultimate Longitudinal Strength Of Ships*", Washington, D.C 20007, N.S.R and D.C., Report 3270 , Jan. 1970.

48. Billingsley, D.W.: "*Hull Girder Response To Extreme Bending Moments*", Proceedings, SNAME/Star Symposium, Coronado, California, 1980.

49. Dow, R.S., Hugill, R.C., Clark, J.D. and Smith, C.S.: "*Evaluation of Ultimate Ship Hull Strength*", Proceedings, Extreme Loads Response Symposium, Arlington, 1981.

50. Ostapenko, A.: "*Strength Of Ship Hull Girder Under Moments Shear and Torque*", Proceedings, Extreme Loads Response Symposium, Arlington, 1981.

51. Faulkner, J.A., Clark, J.D., Smith, C.S. and Faulkner, D.: "*The Loss Of HMS COBRA*", The RINA, 1984.

52. Lin, Y.T.:"*Ship Longitudinal Strength Modelling*", Ph.D Thesis, Univ. of Glasgow, 1983.

53. Lembit, M.K., Christopher, M.P., Yung-Kuang, C. and Donald, L.: "*Evaluation of the Longitudinal Ultimate Strength of Various Ship Hull Configurations*", SNAME Transactions, Vol. 93, 1985.

54. Yung-Kuang, C., Lembit M.K., Christoher M.P. and Maciej, P.B.: "*Ultimate Srength of Ship tructure*", SNAME Transactions, Vol. 91, 1983.

55. Dowling, P.G., Chatterjee, S., Frieze, P.A. and Moolani, F.M.: "*Experimental and Predicted Collapse Behaviour of Rectangular Steel Box Girders.*", Intl. Conf. On Steel Box Girder Bridges, London, February 1973.

56. Dowling, P.J., Chtterjee, S., Frieze, P.A and Moolani, F.M.: "*Experimental and predicted collapse behaviour of rectangular steel box girders*" Proc. Intl. Conference on Steel Box Girders Bridges, Instn. of Civ. Engrs., London, Feb. 73.

57. Dowling, P.G., Moolani, F.M. and Frieze, P.A.: "*The effect of shear lag on the ultimate strength of box girders*", Intl. Conference on Steel Structures, Imperial College, London, 1976.

58. "Report on Comittee II.2 on non-linear structural response", Proc., 7th Intl. Ship Structures Congress, Paris, 1979.

59. Horne, M.R., Montague, P. and Narayanan, R.: "*Influence on strength of compression panels of stiffener section, spacing and weld connection*". Proc. Instn. Civ. Engrs., Part 2, March 1977, Vol. 63.

60. Horne, M.R. and Narayanan, R.: "*Ultimate capacity of longitudinally stiffened plates used in box girders*". Proc. Instn. Civ. Engrs., Part 2, June 1976, Vol. 61.

61. Faulkner, D.: "*Towards a better understanding of compression induced stiffener tripping*", Intl. Conf. Steel and Aluminium Structures, Cardiff, July 1987.

62. Jackson, R.L. and Frieze, P.A.: "*Design of deck structures under wheel loads*", Trans. RINA, Vol. 122, 1980.

63. Smith, C.S.: "*Bending, buckling and vibration of orthotropic plate-beam structures*", Jnl. of Ship Research, Vol. 12, Dec. 1968.

64. Faulkner, D.: "*Effects of residual stresses on ductile strength of plane welded grillages and ring stiffened cylinders,*", Jnl. of Strain Analysis, Vol. 12, No 2, I Mech. E., 1977.

65. Faulkner, D.: "*Compression tests on welded eccentrically stiffened plate panels*", Steel Plated Structures, ed. by P.J, Dowling et al, Crosby Lockwood Staples, 1977, pp. 581-617.

66. Guedes Soares, C.: "*Survey of methods of prediction of the compressive strength of stiffened plates*", Report No MK/R57, Div. of Marine Structures, NIT, Trondheim, August 1981.

67. Lee, J-S. and Faulkner, D.: "*System design of floating offshore structures*", Paper No 8, RINA Spring Meeting, London, April 1989.

68. Guedes Soares, C. and Faulkner, D.: "*Probalistic modelling of the effect of initial imperfections on the compressive strength of rectangular plates*", PRADS'87 Conf., Trondheim, June 1987.